Alma Mater Studiorum · University of Bologna

School of Science
Department of Physics and Astronomy
Master Degree in Physics

Black to White Hole Transition in Covariant Loop Quantum Gravity

Supervisor:
Prof. Roberto Balbinot

Co-supervisor:
Prof. Pietro Donà

Submitted by:
Jacopo Taddei

Academic Year 2023/2024

To my beloved Pippi.

Contents

Introduction

One of the major unsolved problems in theoretical physics is the unification of gravity with the principles of quantum mechanics. Gravity, as described by Albert Einstein's theory of General Relativity (GR), is extremely accurate in explaining the behavior of objects at large scales, such as planets, stars, and galaxies. Additionally, General Relativity has allowed for understanding phenomena such as the universe's expansion, gravitational waves, and black holes. However, the real revolution of this theory is the profound modification of the very concepts of space and time. The theory links the presence of any form of energy and matter to the curvature of a continuous entity called spacetime. Space-time emerges for the first time as a dynamic field and no longer as a fixed stage on which the rest "happens." This theory clarifies the bizarre nature of inertial reference frames, which remained preferred systems from the birth of theoretical physics. General Relativity declares the equivalence of the laws of physics for each reference system. In fact, by construction, general relativity completely disengages itself from the notion of an observer, being completely independent of the choice of coordinates. General relativity's conceptual and practical revolutions are profound, and the experimental validations are countless. However, despite the huge success, it still needs to be completed. When the energy scale becomes very high, divergences appear, indicating an attempt to apply the theory outside its validity ranges. Furthermore, the equations of General Relativity are classical and incompatible with the mathematical framework of quantum mechanics.
On the other side is quantum mechanics. The latter, along with GR, represents the watershed of classical physics. Quantum mechanics is the most accurate theory for describing interactions at the atomic and subatomic scales. It, too, turns out to be a profound revolution in understanding nature. The description that emerges from this theory is that of an inherently indeterminate world. Quantum mechanics presents an ontological unknowability, unlike classical physics and general relativity, which must be taken into account and encoded in a particular mathematical formalism. The success of this theory is immeasurable, and its developments, such as quantum field theory, have turned out to be the most experimentally precise theories ever written in the history of physics. What is more, the field of application of quantum mechanics is vast and enjoys the highest experimental confidence. Another key feature of this theory is a form of granularity at the fundamental level. The world at microscopic scales is no longer

continuous but quantized. The framework of quantum mechanics perfectly describes all the fundamental forces, strong and weak nuclear and electromagnetic, except for one: gravity. However, quantizing gravity with the typical procedures used for other interactions turned out to be impossible.
Thus, there is a tension: general relativity and quantum mechanics seem incompatible. This tension is called Quantum Gravity. Quantum gravity represents the branch of theoretical physics that seeks to incorporate General Relativity into the framework of quantum mechanics. The necessity of quantum gravity is evident, and as such, a theory should be able to describe gravity not only as a deformation of space-time on large scales but also as a quantized force that interacts with subatomic particles. The absence of a quantum theory of gravity leaves a gap in the comprehension of the physical world.

The history of quantum gravity spans almost one hundred years. The first attempts to quantize gravity date back to the 1930s. The initial approach followed the path of canonical quantization, which was successful in the context of QED. However, these attempts quickly encountered problems related to the theory's non-renormalizability. The resulting equations contained infinities that couldn't be removed using standard techniques.
In the '60s and '70s, the development of quantum field theory led to new approaches based on fundamental covariant properties of gravity. However, these approaches couldn't solve problems related to renormalizability.
All these attempts suggested the need for a radical change in standard methods for quantization. Since the 1980s, various approaches have taken steps forward, the two main ones being Loop Quantum Gravity and String Theory.
String Theory completely changed the way quantization was approached by introducing the concept of a one-dimensional closed loop, known as a string, with various vibration modes. This theory has many advantages, including being renormalizable, and has led to significant theoretical developments, such as extra dimensions and dualities between gauge theories and gravity. However, it relies on several unverified assumptions and has yet to be confirmed through experiments.
On the other hand, Loop Quantum Gravity does not introduce new concepts but creates a purely geometric picture of quantum spacetime through a series of mathematical procedures. This is the main topic of this work.

Loop Quantum Gravity (LQG) is one of the most promising tentative theories of quantum gravity. LQG represents an innovative approach that quantizes space and time directly without introducing extra dimensions or hypothetical particles. This approach maintains the fundamental property inherited from General Relativity, which is being background-independent. As a quantum theory, it is also non-perturbative. These two properties are essential and directly derived from a deep comprehension of the structure of spacetime that comes from General Relativity.

Loop Quantum Gravity's most striking result is the picture of a spacetime that is not continuous but discrete at the Planck scale. This unifies the geometrical picture from GR with the natural discretization coming from QM. Indeed, it is motivated by the fundamental lessons taught by quantum mechanics that every dynamic field should be quantized, united by the discovery of general relativity, which states that the metric is not a background structure but a dynamic field.
The core components of Loop Quantum Gravity consist of canonical variables like the spin connection and the densitized triad. These variables undergo quantization using canonical quantization techniques, resulting in the creation of quantum operators. These operators function within a well-defined Hilbert space that exists on abstract graphs. By incorporating geometric operators such as area and volume, we can perceive spacetime as quantized chunks of volume interacting with quantized areas. These quantum states of space, the spin networks, allow us to describe the behavior of quantum geometries. LQG also describes the dynamics of these quantum states, and this work centers on the theory's covariant formalism. Covariant Loop Quantum Gravity incorporates the dynamics as a path integral sum over histories.
The theory not only offers a way to associate a quantum behaviour to space and time but also to obtain a well-defined quantum theory of gravity without introducing new ingredients, just combining GR and QM.

The primary objective of this thesis is to develop a comprehensive model that explains the transition process between black holes and white holes, a phenomenon of significant interest and importance in the field of quantum gravity. The work on this starts from the original research [1], and [2]. In the latter, it was possible to write a classical metric capable of satisfying Einstein's equations everywhere except in a purely quantum zone. This metric connects a black hole space-time with a white hole space-time through a genuine quantum process, imaginable as a bounce. The fate of matter subjected to extreme gravitational collapse is thus not to end up in a catastrophic singularity but to reach a level of pressure such that there is a rebound. In Fireworks' spacetime [1], this results in a white-hole quantum transition. Interest in this kind of process is central to the quantum gravity community. These, in fact, lend themselves to finding traces of quantum gravity. One possible and most credited scenario is tunneling, a prototype of a purely quantum effect that has been theoretically well-studied. Loop Quantum Gravity is well-suited for studying this system, as it is capable of computing quantum transitions between space-like hypersurfaces. By enclosing the Fireworks spacetime's quantum zone within two such hypersurfaces, it becomes possible to calculate the transition amplitude of the process. A four-dimensional model of the transition can be found in the literature [3]; however, it is complex and requires strong approximations. In this thesis its three-dimensional analogue will be constructed, with a strong focus on the mathematical details of the calculation and concentrating on its fundamental aspects.

The discussion will be divided into four chapters. The first three will be used to acquire the tools needed to understand the calculation of the probability amplitude for the black hole and white hole transition in three dimensions, which is the last part.
The first chapter (1) will introduce Loop Quantum Gravity, particularly in its covariant formulation. The discussion is divided into kinematics and dynamics. In the former (1.1), the Hilbert space of the theory will be studied, and the main operators defined. With the introduction of the Area operator and the Volume operator, spin network states, namely the states of the gravitational field used in LQG, will be defined. A more detailed analysis will be devoted to 3D kinematics (1.2), preparing the ground for the black hole-white hole transition model. The same reasoning will then be applied to the dynamics. The first part will study how to implement a path integral formulation in Loop Quantum Gravity (1.3). This will result in the definition of spin foams, mathematical objects that describe the sum over geometries à la Feynman. Also this time, a part of the discussion will be devoted to three-dimensional dynamics through the famous Ponzano Regge model (1.4).
The second chapter is devoted to the study of coherent states (2). The latter are a fundamental tool for studying quantum mechanics in the semiclassical limit. These states are crucial for the black-to-white hole transition, and in the second chapter, they will be constructed step by step. To do so, the complexifier method will be studied, first applied to the free particle case and then arriving at constructing a coherent spin network (2.2.2). Finally, a convenient parameterization of Loop Quantum Gravity variables will be discussed at the end of this chapter. In particular, techniques typical of twisted geometries will be used (2.3).
The third chapter combines the previous two, introducing a semiclassical study of the problem's dynamics (3). In this chapter, a standard technique for semiclassical calculation, the saddle point approximation, will be reviewed. Once the general method has been studied, it will be applied to calculate the transition amplitude combined with the structure of coherent states. Moreover, this approximation will also be applied in a novel way to calculate amplitudes in Loop Quantum Gravity (3.3.3).
The last chapter results from combining all the previous chapters. The latter emerges as the true three-dimensional transition model between a black hole and a white hole (4). In addition to the model's definition and motivation, special attention will be paid to the meaning of tunneling between geometries (4.2). In this part, all the previously introduced techniques will be used to write the first analytical form of transition amplitude with all approximations under control. Among the main results obtained, the structure of coherent states in quantum processes will be discussed in detail, and the transmission coefficient for the black hole-white hole transition will be studied. Regarding the first result, the interesting novelty will be the breaking of the coherent states in purely quantum regions. Concerning the transmission coefficient, the result of this work will be different from those found in previous calculations and will offer new insights for the future study of the process in four dimensions.

The Ultimate Limit of Space-Time

Before introducing the theory of Loop Quantum Gravity, the following semiclassical argument illuminates the nature of quantum gravity itself. This is an elementary example [4] of how combining the typical indeterminacy of quantum mechanics with General Relativity requires giving up the very idea of space and time as a continuum.
Consider the famous relationship between position and momentum dispersion in quantum mechanics,

$$\Delta x \Delta p > \hbar. \tag{1}$$

Imagine that a region of space of dimension $\Delta x = L$ should be studied experimentally by sending photons. Considering then that the momentum dispersion is always smaller than its modulus then,

$$|p| > \frac{\hbar}{L}. \tag{2}$$

Using the relation between energy and momentum given by special relativity, in particular in the ultra-relativistic limit, it is true that $E = c|p|$. Now General Relativity comes into play. Every source of energy gravitates, and consequently bends space around itself, effectively it acts like a gravitational mass $M \propto E/c^2$. Moreover, for any mass, it is possible to define its Schwartzchild radius, which is the radius beyond which a black hole is created. The latter corresponds to $R_s = GM/c^2$, where G is Newton's gravitational constant, and thus, the minimum length that is explorable without creating a mini-horizon hiding the space-time region inside corresponds to the value $L = R$. Combining the above information, minimal length results:

$$L = \frac{GM}{c^2} = \frac{GE}{c^4} = \frac{|p|G}{c^3} = \frac{\hbar G}{Lc^3} \quad \longrightarrow \quad L := l_p = \sqrt{\frac{\hbar G}{c^3}} \approx 10^{-33} cm. \tag{3}$$

The latter is called the Planck length. It is the minimum fundamental scale beyond which the very definition of distance loses its meaning. This simple argument intuitively explains why continuous space-time, as commonly imagined, turns out to be an approximation of a granular structure.
This derivation is genuinely semiclassical. The result, however, illuminates the spirit behind a quantum gravity theory. Since the gravitational field coincides with geometry, one must resort to a theory of quantum geometry.

Chapter 1

Loop Quantum Gravity

In this chapter, Loop Quantum Gravity is introduced. The theory will not be derived from the classical GR. A few remarks about the link with GR can be found in the Appendix A. Here, it is adopted a more modern approach, and the theory is introduced operatively, defining from the beginning the Hilbert space and the main operators without a formal derivation. However, the historical path to Loop Quantum Gravity is long and well-structured. For interested readers, the journey to this construction is summarized and extensively presented in [5],[6].
A quantum theory can generally be defined with a triplet $(\mathcal{H}, \mathcal{A}, W)$. The Hilbert space of the theory $\mathcal{H}$ is the complex space containing the quantum states of the system. The algebra of operators $\mathcal{A}$ is really the core of the quantum theory. It contains operators describing the properties of the quantum system. These two together form the kinematics of a theory, analyzed first in this chapter. The last element W that completes the quantum theory should encode the dynamics, providing the evolution of the states that constitute the kinematics. This object can be a Hamiltonian or, as in this case, transition amplitudes between states derived from a path integral.

1.1 Kinematics

Usually, quantum mechanics requires the definition of a preferred time variable. However, when formulating a theory of quantum gravity, as learned from GR, this preferred time variable does not exist. Thus, it requires formulating a quantum theory that, as much as possible, does not rely on this concept. In the following, a formalism developed by Oeckl called the *positive formalism* [7] will be used. This is a way of encoding quantum theories in the general boundary formulation (GBF), in which all of the variables live on the boundary of a system.
In the context of LQG, it is studied a four-dimensional region $\mathcal{R}$ of spacetime, and the variables (metric and its derivatives, for example) sit on the boundary. The dynamics will

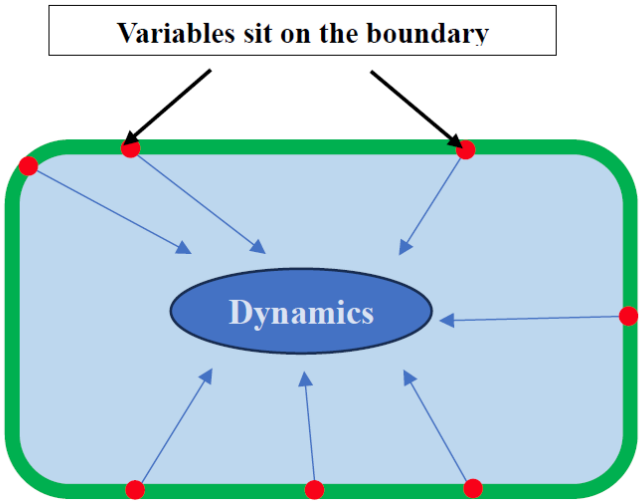

represent the differences between the variables without specifying what state comes first and what next, being all included in a single boundary state. Loop Quantum Gravity, in particular, concerns the study of spacelike boundaries (see Appendix A). It is possible, therefore, to study a region of space enclosed between spacelike hypersurfaces.

1.1.1 Hilbert space of LQG

LQG is a field theory, even if not in the traditional sense, meaning that the theory has infinite degrees of freedom. This is the case in all quantum field theories, and the Hilbert spaces are always built by truncating the number of degrees of freedom and then taking a well-defined formal limit. For example, for QED, the starting point consists of defining the Hilbert space of one particle. One of two particles, and then three, and so on, and the complete Fock space of the theory is the tensor product of an infinite number of the fixed particle Hilbert spaces. In lattice QCD, the Hilbert space is defined on a lattice, and the formal physical space is the one for which the so-called lattice spacing is set to zero. So this is a usual procedure in quantum mechanics, and there is a similar situation in LQG.

The LQG full Hilbert space $\mathcal{H}$ is constructed using the truncated Hilbert space $\mathcal{H}_\Gamma$ where Γ is a *graph*. A graph is defined as a couple $(N, \mathcal{L})$: respectively a finite set of n elements called nodes and a collection of links, ordered couples l of elements of N, for example, $l_{42} = (n_4, n_2)$. A graph is a set of nodes that are connected by ordered links. Since the links are oriented, we can refer to the starting node as the *source* of the link and the one at the end as its *target*. In the following chapters, we will also use the notion of the valence of a node, which is simply the number of links attached to it.

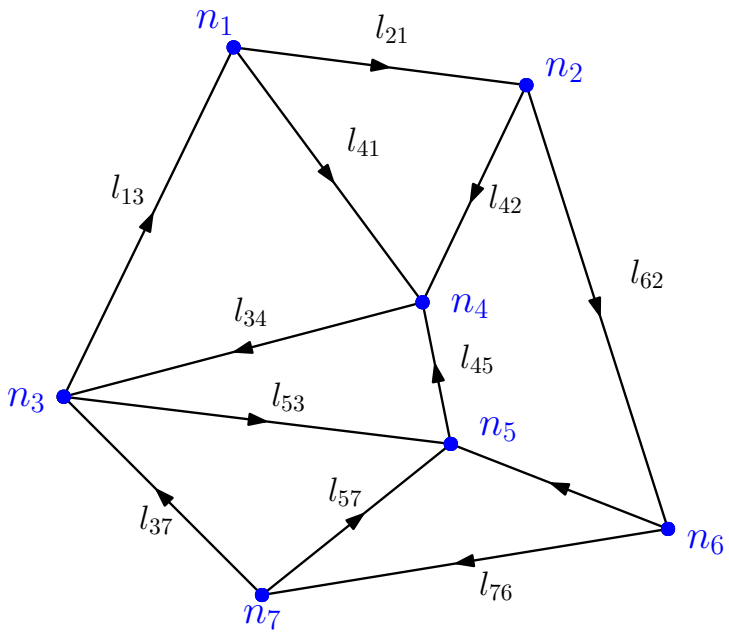

Figure 1.1: Simple example of a graph Γ, with $(n_1, ..., n_7) \in N$ and $(l_{13}, ..., l_{76}) \in \mathcal{L}$.

The Hilbert space $\mathcal{H}$ of LQG is defined as the projective limit [8]:

$$\mathcal{H} = \lim_{\Gamma \to \infty} \mathcal{H}_\Gamma. \tag{1.1}$$

The meaning of the above limit corresponds to the "infinitely refined graph". Roughly speaking meaning that every finite graph is a sub-graph of the infinitely refined one. The limit is well defined [8] and coincides with $L^2(\mathcal{A}, \delta\mu_{AL})$ where $\mathcal{A}$ denotes the space of connections and $\delta\mu_{AL}$ is the (unique) Ashtekar-Lewandowski measure. Pragmatically, we will always work with the truncation of the Hilbert space (as in QFT, we always compute Feynman diagrams with a finite number of particles), but the limit (1.1) ensures the consistency of the theory.

On the graph, we define a state playing the wave function role in LQG. We associate an $SU(2)$ element h_l to each link, representing the parallel transport between two nodes of the graph. The reasons behind this are briefly summarized in Appendix A, but for further details see [9][4]. We consider functions of these elements $\psi(h_l)$ and define the Hilbert space $\tilde{H}_\Gamma$ as the set of squared integrable functions with respect to the Haar measure, namely:

$$\tilde{H}_\Gamma = L_2[SU(2)^L], \tag{1.2}$$

where $SU(2)^L$ indicates L copies of $SU(2)$ where L is the number of links.

The Hilbert space $\mathcal{H}_\Gamma$ in the gauge invariant subspace of (1.2). Precisely, the gauge

freedom is represented by an independent transformation $g_n \in SU(2)$ at each node:

$$h_l \quad \longrightarrow \quad g_{t_l}^{-1} h_l g_{s_l} \ . \tag{1.3}$$

This gauge freedom is equivalent to the invariance of choosing some particular orthonormal frames at the graph's nodes. Gauge invariant wavefunctions satisfy:

$$\psi(h_l) = \psi(g_{t_l}^{-1} h_l g_{s_l}) \ . \tag{1.4}$$

The set of these functions forms $\mathcal{H}_\Gamma$, and since we are dividing by the freedom to choose an element of $SU(2)$ in each node, if we imagine having N nodes then the Hilbert space (1.1) can be written as:

$$\mathcal{H}_\Gamma = L_2[SU(2)^L / SU(2)^N] \subset \tilde{H}_\Gamma \ . \tag{1.5}$$

Now that we have defined what is the wavefunction, we will introduce the LQG operators.

1.1.2 LQG Algebra

The algebra of a Hilbert space studies the properties and operations of operators acting on this space, providing a rigorous framework for dealing with concepts such as quantum states and observables. In one-dimensional quantum mechanics, given a wave function $\psi(x)$, it is possible to define the action of the position $\hat{x}$ and momentum $\hat{p}$ operators:

$$\begin{aligned} \hat{x}\psi(x) &= x\psi(x), \\ \hat{p}\psi(x) &= -i\hbar \frac{d}{dx}\psi(x). \end{aligned} \tag{1.6}$$

In LQG the role of the position variables is played by the elements h_l of $SU(2)$ that act in a similar fashion,

$$\hat{h}_l \psi(h_l) = h_l \psi(h_l). \tag{1.7}$$

Despite the formal similarity with the position operator of (1.6), remember that h_l is a group element; therefore, the previous equation is a matricial one.
Finding a momentum operator requires a notion of derivative inside the $SU(2)$ group. We introduce the left-invariant operator, which is fundamental in LQG. To grasp its definition, remember that the algebra can be seen as the tangent space to the manifold. Within the algebra, every element corresponds to a direction. We define as L^i, acting on the functions of $SU(2)$, $\psi(h)$, the following operator:

$$L^i \psi(h) = (-i) \lim_{t \to 0} \frac{1}{t} [\psi(h e^{t J_i}) - \psi(h)]. \tag{1.8}$$

This is called the *left invariant operator* being invariant under the multiplication of group elements on the left. The form of (1.8) is transparent considering that $J_i \equiv -\frac{i}{2}\sigma_i$ is the

generator of $SU(2)$ and that the exponential map $\exp[tJ_i]$ is the one that allows to pass from the Lie group to its algebra. Therefore, the above limit is the usual incremental ratio used in the definition of derivative; the difference is the noncommutativity of the space. A right invariant operator also exists, just for completeness, but it is not important in this context.

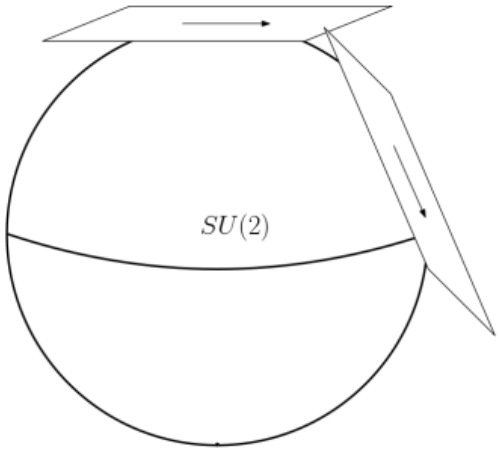

Figure 1.2: $SU(2)$ is diffeomorphic to the 3-sphere; if we represent it in one dimension less, we can imagine visualizing every element of its algebra as a point on the sphere. It can be viewed as an arrow on the tangent plane to the group, defined on every point (every element h_l). Image taken from [10]

The commutation relations of L_l^i are,

$$[L_l^i, L_{l'}^j] = \epsilon_k^{ij} L^k \delta_{l,l'}, \tag{1.9}$$

which is exactly the angular momentum operator's algebra in quantum mechanics. The generators of $SU(2)$ are proportional to the Pauli matrices $\vec{\sigma}$, therefore $L^i = (L_x, L_y, L_z)$. Notably, these operators are not gauge invariant because they carry an index of $SU(2)$. Therefore, they are not defined in the Hilbert space $\mathcal{H}_\Gamma$ but just in $\tilde{\mathcal{H}}_\Gamma$.

A fundamental property of $\vec{L}_l$ is the closure condition, which can be written as:

$$\sum_{l \in n_i} \vec{L}_l \psi(h_l) = 0 \ , \tag{1.10}$$

where $\psi(h_l)$ is gauge invariant. The operators $\vec{L}$ act on the left of h_l on one of the, let's say, four links coming out from a node by turning it in one direction of the algebra. The combined action $(\vec{L}_1 + \vec{L}_2 + \vec{L}_3 + \vec{L}_4)$ performs the same rotation to all links, not changing the overall configuration. This condition is sometimes called also gauge constraint or Gauss constraint.

The algebra of the theory is described by the commutation relations,

$$[h_l, L^i_{l'}] = i\gamma(8\pi\hbar G)\delta_{ll'}h_l\tau^i. \tag{1.11}$$

The proportionality constant is strictly related to the physical interpretation of the theory. This will become clear in the next section, discussing the geometric operators.

1.1.3 Geometric Operators

The algebra of gauge-invariant operators on the LQG Hilbert space includes *Geometric Operators*, operators derived from geometric quantities of General Relativity. One such operator is the **Area Operator**, which quantizes the area of 2-dimensional surfaces. For more details, see the original work by C. Rovelli and L. Smolin [11]. This operator acts locally on the links of the spin network graph, which is a fundamental structure in LQG representing quantum states of the gravitational field.
The area operator $\hat{A}$ is defined through its action on a given link l of the graph. Mathematically, it is expressed as:

$$\hat{A}^2_l = (8\pi\gamma\hbar G)^2 \ \vec{L}_l \cdot \vec{L}_l, \tag{1.12}$$

where $\vec{L}_l$ are the generators of the SU(2) algebra associated with the link l. The prefactor $l_p^2 = 8\pi\hbar G$ is proportional to the Planck area (length squared), which is the natural quantum of area in this theory. The parameter γ is known as the Barbero-Immirzi parameter and it plays a crucial role in the formulation of LQG.
The area operator has a discrete spectrum, which is a distinctive feature of LQG. The eigenvalues of the area operator are given by:

$$a_l = 8\pi\gamma\hbar G\sqrt{j_l(j_l+1)}, \tag{1.13}$$

where j_l is a quantum number that labels the SU(2) representation associated with the link l. According to the representation theory of SU(2), j_l can take values such as $j_l = \frac{1}{2}, 1, \frac{3}{2}, \ldots$, indicating that the physical area can only take on these discrete values.
One of the significant predictions of LQG is the existence of a minimal non-zero area. The smallest possible eigenvalue of the area operator is:

$$\delta_\gamma = 4\pi\gamma\hbar G\sqrt{3}, \tag{1.14}$$

which corresponds to the case when $j_l = \frac{1}{2}$. This minimal area value highlights the granular structure of space at the quantum level predicted by LQG and provides a physical interpretation of the Barbero-Immirzi parameter as δ_γ (it is equivalent to), the area gap of the theory.
In summary, in LQG, areas are represented by operators with a discrete spectrum. Quantum states of the gravitational field are described by spin networks, which are graphs with links carrying quanta of area.

In addition to the Area Operator, another fundamental operator is the **Volume Operator**, which quantizes the volume of 3-dimensional regions. This operator acts on the nodes of the graph and has a complicated expression. For simplicity we report here the formula of the volume squared operator restricted to the case of 4-valent nodes

$$\hat{V}_n^2 = (\gamma\hbar G)^3 \vec{L}_{l1} \cdot \vec{L}_{l2} \times \vec{L}_{l3} \ . \tag{1.15}$$

The expression depends on three links l_1, l_2, l_3 of the node n. Even if not manifestly, the definition is independent of the choice of the three links thanks to the closure condition (1.10). If we use the fourth link l_4 instead of one of the other three, we can rewrite $\vec{L}_{l4}$ as the sum of the other. The properties of the triple product ensure that $\hat{V}_n^2$ is independent of the choice of the triple of links, and thus, it depends only on the node.
The spectrum of the volume operator is again discrete, with a minimal excitation proportional to the Planck Volume (length cube). The explicit formula for the eigenvalues is much more complicated than that of the area and cannot be written in closed form. We refer the interested reader to the literature for the exact calculation of all the eigenvalues [12].
Angles are also geometric operators. The Angle Operator measures the dihedral angle between intersecting surfaces. It also acts on nodes (where surfaces meet) and has discrete spectra. The eigenvectors are related to the recoupling basis of the intertwiners spaces.
The discrete spectrum of the geometric operators suggests a very enticing geometrical picture for the LQG states. A graph labels states, providing a notion of adjacencies between nodes. Quanta of volume are associated with the graph nodes, suggesting a structure of space made of quantized chunks of space. Quanta of areas are associated with the graph's links. The interface's area separating two nodes (chunks of space) is quantized. Similarly, the angles between these interfaces are quantized. We can interpret LQG states as describing quantum space formed of chunks with discrete volumes separated by interface surfaces with discrete areas with discrete dihedral angles between them and with adjacency relations given by a graph. This geometrical interpretation is one of the foundations of the theory and guided its development in modern ages. The next section will further clarify this picture by introducing the Spin Network basis.
It is essential to distinguish between the discreteness of geometry and the graph structure in loop quantum gravity. The former is **not** a consequence of the latter. Discreteness is a fundamental prediction of the theory derived from the spectrum of the geometric operators. Conversely, the graph serves as a tool to truncate the gravitational degrees of freedom and should be viewed as a regulator within the theory. Recent studies [13] have demonstrated that the discreteness of geometry can be derived independently of the graph structure. Therefore, it persists even after taking the projective limit (1.1).

1.1.4 Spin-network basis

The Area Operator and Volume Operator $(\hat{A}_l, \hat{V}_n)$ form a maximally commutative set in the gauge invariant Hilbert space $\mathcal{H}_\Gamma$. The simultaneous diagonalization of the two forms a complete orthonormal basis of (1.5). This basis is the *Spin Network Basis* $|\Gamma, j_l, i_n\rangle$ where j_l are the representations associated with the links of the graph and i_n are the intertwiners related to the nodes. This basis concretely realizes the geometrical interpretation of LQG states. The spin network states are, therefore, characterized by:

- A set of nodes labeled with intertwiners i_n. The intertwiners are associated with the eigenvalues of the volume operator. This provides a natural interpretation of chunks of space featuring a discrete volume.
- A graph Γ containing the notion of adjacency of these chunks of space.
- A set of spins j_l on each link. In light of (1.13), the spins offer the transparent interpretation of discretized interface area between the portions of space.

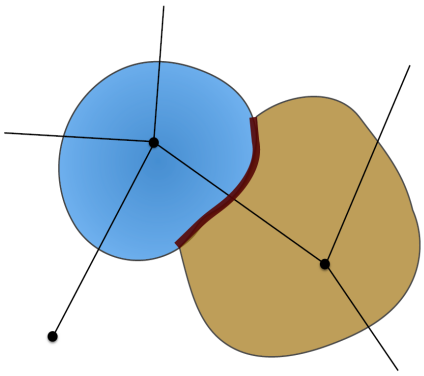

Figure 1.3: Physical interpretation of a spin network. Chunks of space with discrete volume that are in contact by interface quantized area (in red). Image taken from [4].

It is then possible to decompose a generic function $\phi(h)$ in the spin network basis. The Hilbert space of a single link is $L_2[SU(2)]$. A generic square-integrable function $\phi(h)$ can be expanded in the Fourier modes. The decomposition uses (unitary) irreducible representations of $SU(2)$, which are labeled by a spin j (half-integer). The spin j representation is $2j+1$ dimensional, and states are labeled by the magnetic number m that takes values between $-j$ and j. The elementary basis functions of $SU(2)$ are the Wigner matrix elements:

$$D^j_{mn}(h) = \langle h|j,m,n\rangle = \langle jm|\, h\, |jn\rangle \quad . \tag{1.16}$$

In terms of Fourier coefficients f^j_{mn} we can decompose

$$\phi(h) = \sum_{j,m,n} f^j_{mn} D^j_{mn}(h) \ . \tag{1.17}$$

This decomposition is often referred to as the Peter-Weyl theorem. Wigner matrices are also eigenvectors of the area operator (1.12),

$$\hat{A} D^j_{mn}(h) = 8\pi\gamma\hbar G\sqrt{j(j+1)} D^j_{mn}(h) \ . \tag{1.18}$$

This description is still in the non-gauge invariant Hilbert space $\tilde{\mathcal{H}}_\Gamma$; the links labeled by different representations do not know how to combine with the others. It is necessary to connect the links invariantly to implement the information about adjacency in the graph.

Here enters into play the intertwiners. Suppose having a four-valent node. An intertwiner $i^{n_1 n_2 n_3 n_4}$ is an operator acting on the spin network node gluing the links together. The Hilbert spaces of different links, labeled by the four j_i irreducible representations, met in that node. Usually, the tensor product of irreducible representations is not irreducible anymore and can be decomposed. If the spins satisfy the Clebsh-Gordan conditions, an invariant subspace exists. An intertwiner $i^{n_1 n_2 n_3 n_4}$ acts as a projector into

$$\mathcal{H}^0 = \mathrm{Inv}_{SU(2)}(\mathcal{H}^{j_1} \otimes \mathcal{H}^{j_2} \otimes \mathcal{H}^{j_3} \otimes \mathcal{H}^{j_4}). \tag{1.19}$$

For details see Appendix B.
The fundamental remark is that the volume eigenvalues are linear combinations of intertwiners. Therefore, labeling the node with $i^{n_1 n_2 n_3 n_4}$ carries the information about the volume of the chunk of space dual to that node.

A gauge invariant function $\phi(h)$ is thus decomposed in the following way,

$$\phi(h_l) = \sum_{j_\ell, i_n} f^{j_\ell, i_n} \otimes_n i^n \otimes D^{j_l}(h_l), \tag{1.20}$$

magnetic indices are omitted for simplicity and contracted with the intertwiners following the graph connectivity. This form is intuitive: $D^{j_l}(h)$ represent the base of $\tilde{\mathcal{H}}_\Gamma$, i^n act as projectors on the gauge invariant $\mathcal{H}_\Gamma$ and at the end f^{j_l, i^n} are just the Fourier coefficients.

These mathematical concepts clarify the meaning of the spin network basis $|\Gamma, j_l, i_n\rangle$. The spin networks offer a clear geometric picture of quantum spacetime, manifesting the discreteness and fuzziness usual in quantum mechanics, united with the typical

non-commutativity. An arbitrary linear combination of $|j_l, i_n\rangle$ represents the possible geometry states.

This geometrical interpretation also clearly hints at the node's valence choice. Remember that the spin networks describe spacelike hypersurfaces. In three dimensions, they represent a 2D surface. A 2D surface is naturally discretized with triangles in contact by three interface sides. A three-valent node is, therefore, dual to a triangle. On the other hand, a three-dimensional portion of space is discretized with tetrahedra in contact with four triangles. A four-valent node is thus dual to a tetrahedron. The representations j carried by the link represent the length of the sides in the former case and the area of the triangles in the other. The following picture clarifies this interpretation.

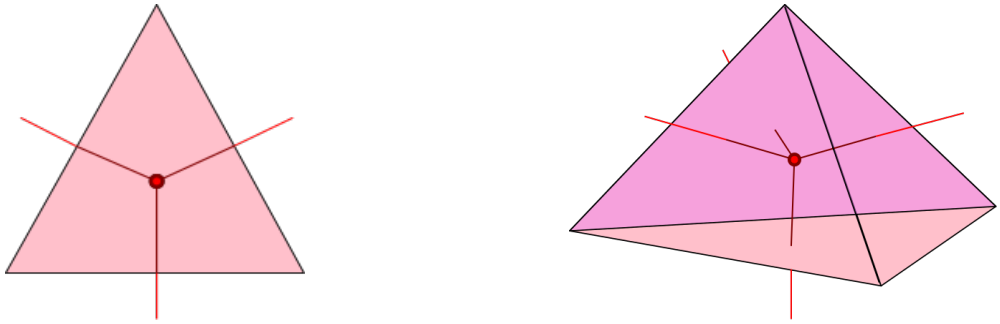

Figure 1.4: Geometrical interpretation of a three-valent node (left) and of a four-valent node (right).

1.2 Kinematics 3D

Since this work aims to create a three-dimensional model for the black-to-white hole transition, it is worth expanding the discussion on the three-dimensional case. Consider a three-valent graph Γ. We seek out a realization of the algebra

$$[h_l, L^i_{l'}] = i(8\pi\hbar G)\delta_{ll'} h_l \tau^i, \tag{1.21}$$

on the Hilbert space $\tilde{\mathcal{H}}_\Gamma$. An important remark is on the dimensions of the proportionality constant in this commutator. From the Einstein Hilbert action in d dimensions, it is clear that $\hbar G = [L^{d-2}]$. Therefore, when considering the four-dimensional case, $d = 4$ and therefore $\hbar G$ is an area, while in this context, $d = 3$ and consequently $\hbar G$ have the units of a length.
The gauge invariant Hilbert space is again the space of square-integrable functions of $SU(2)$,

$$\mathcal{H}_\Gamma = L_2[SU(2)^L/SU(2)^N]. \tag{1.22}$$

Seeking for gauge invariant wave functions correspond to considering functions $\psi(h_l)$ such that,

$$\psi(h_l) = \psi(g_{t_l}^{-1} h_l g_{s_l}), \quad \text{where} \quad g_n \in SU(2). \tag{1.23}$$

This procedure is the usual group averaging technique. Equivalently, $\psi(h_l)$ must respect the three-dimensional closure condition (1.10),

$$\vec{C}_n = \vec{L}_{l_1} + \vec{L}_{l_2} + \vec{L}_{l_3} = 0, \tag{1.24}$$

where l_i are the links coming out of a node.
The Peter Weyl theorem provides a notion of a Fourier transform on the group, and, as discussed in the previous section, the functions can be decomposed on a Wigner matrix basis. A state is a function of L group elements and therefore we can write $\psi(h_l)$ as,

$$\psi(h_l) = \sum_{j_l m_l n_l} C_{j_1 \dots j_l m_1 \dots m_l n_1 \dots n_l} D^{j_1}_{m_1 n_1}(h_{l_1}) \dots D^{j_l}_{m_l n_l}(h_{l_L}). \tag{1.25}$$

These states are eigenfunctions of the Lenght Operator, the three-dimensional version of the Area Operator (1.12),

$$\vec{J}_l \psi_{j_l}(h_l) = J_{j_l} \psi_{j_l}. \tag{1.26}$$

As before, the links need to be connected invariantly on the nodes to gain the information contained in Γ. The intertwiners are required.
Consider the tensor product of the three Hilbert spaces meeting at a node,

$$\mathcal{H} = \mathcal{H}^{j_1} \otimes \mathcal{H}^{j_2} \otimes \mathcal{H}^{j_3}. \tag{1.27}$$

Imagine that the spins satisfy the Clebsh-Gordan conditions. Namely, their sum is an integer, and the triangular inequality

$$|j_1 - j_2| < j_3 < j_1 + j_2, \tag{1.28}$$

is respected.
In that case, there exists an invariant subspace

$$\mathcal{H}^0 = \mathrm{Inv}_{SU(2)}(H_{j_1} \otimes H_{j_2} \otimes H_{j_3}) \in \mathcal{H}. \tag{1.29}$$

In 3D, the dimension of this subspace is equal to one. There exists just one invariant object living in it. This is the three-dimensional intertwiner,

$$i^{m_1 m_2 m_3} = \begin{pmatrix} j_1 & j_2 & j_3 \\ m_1 & m_2 & m_3 \end{pmatrix}. \tag{1.30}$$

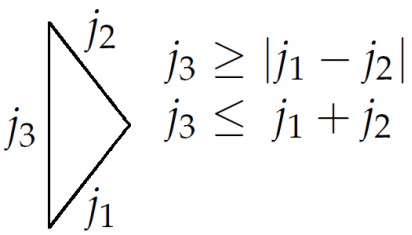

Figure 1.5: The existence of the space $\mathrm{Inv}_{SU(2)}(H_{j_1} \otimes H_{j_2} \otimes H_{j_3})$ is strictly linked to the usual triangular inequalities. Image taken from [4].

Therefore, the gauge-invariant states must have the form,

$$\psi(h_l) = \sum_{j_l m_l n_l} C_{j_1 \dots j_l} i_1^{m_1 m_2 m_3} \dots i_N^{m_{L-2} m_{L-1} m_L} D^{j_1}_{m_1 n_1}(h_{l_1}) \dots D^{j_l}_{m_l n_l}(h_{l_L}). \tag{1.31}$$

In compact notation, the gauge-invariant wave function is,

$$\psi_{j_l}(h_l) = \langle h_l | j_l \rangle = \bigotimes_n i^n \bigoplus_l D^{j_l}(h_l). \tag{1.32}$$

This completes the simple structure of the kinematics of Loop Quantum Gravity in three dimensions.

1.3 Dynamics

Quantum mechanics admits two possible formulations: the canonical and the path integral. The first one is based on Hilbert spaces and operators and implements evolution through unitary operators. The second is manifestly covariant and realizes the sum-over-paths, implementing evolution by assigning transition amplitudes to states. In this work, the dynamic is introduced à la Feynman, and in the context of LQG, the sum-over-paths become sum-over-geometries. This formalism aims to define transition amplitudes, which are the basic objects in which the dynamic is encoded.
In this section, the spin-foam formalism is introduced. The first part analyzes how to construct a spin-foam and the definition of spin-foam models, starting from an action of a general BF theory. In the second, the Ponzano-Regge model is studied. The Ponzano-Regge model is well established as a sum over geometries in 3D and is the basic model utilized to compute the analog of the black-to-white hole transition amplitude in three dimensions.

1.3.1 Spin-foam Models

For a detailed discussion on this topic, see [4][9][14]. We start considering a simple BF theory (for details, see Appendix (A)) whose action is,

$$S[e, w] = \frac{1}{2}\int B \wedge F. \tag{1.33}$$

The dynamical variables are the 2-form B and the connection ω appearing in the action through its field strength F. General Relativity can be recast through a change of variables into a constrained BF theory (which is a topological quantum field theory). The quantization is rather simple in the path integral approach. The partition function is

$$Z = \int \mathcal{D}B\mathcal{D}w e^{\frac{i}{\hbar}\int B\wedge F}. \tag{1.34}$$

The usual path integration is based on breaking down trajectories into small parts and using the resolution of the identity at each step. When this process is taken to the limit, it becomes the path integral.
In the context of Loop Quantum Gravity, we perform a sum of quantum geometries over a 4D region of space-time. The first step is to discretize the region. Since the objective is to have a background-independent theory, it is necessary to triangularize the 4D region in a covariant manner without relying on a background metric. There is some flexibility in triangulating a region of spacetime. The simplest option is to use 4-simplices.
A 4-simplex is the higher-dimensional generalization of a tetrahedron. Each 4-simplex is bounded by five tetrahedra, similar to how a tetrahedron is bounded by four triangles and a triangle is bounded by three lines. It can be imagined as a tetrahedron with an additional point at which spacetime shrinks.
Dealing directly with a triangulation is rather nontrivial. It is easier to encode the information into a 2-complex Γ. A 2-complex is a set of vertices, edges, and faces organized to form a two-dimensional complex structure.
To build Γ from the original triangulation, it is sufficient to follow a systematic procedure, summarized in the following associations:

- **4-Simplex $\longrightarrow$ Vertex**
  Associate a vertex of the 2-complex Γ in the center of each 4-simplex of the original triangulation.

- **3-Simplex (Tetrahedron) $\longrightarrow$ Edge**
  Associate a one-dimensional edge in the dual graph to each tetrahedron bounding the 4-simplex (to each triangle bounding a tetrahedron in 3D).

- **2-Simplex (Triangle) $\longrightarrow$ Face**
  Surrounding each edge, associate as many faces as the number of triangles bounding

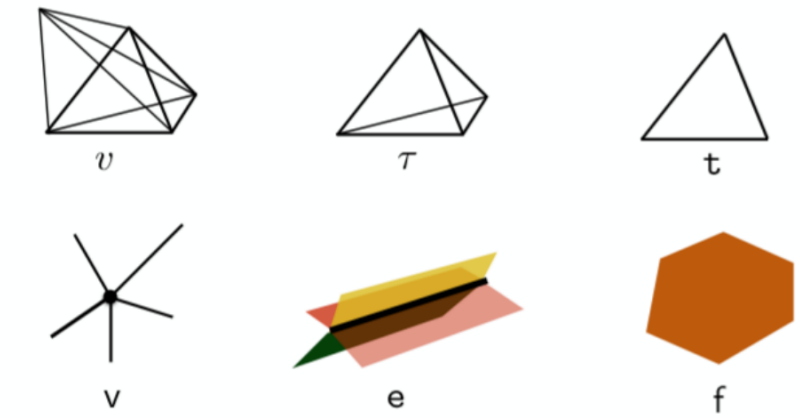

Figure 1.6: Correspondence between the elements of a triangulation and the 2-complex structure. From left to right, at each 4-simplex is associated a vertex, to each tetrahedron an edge, and to each triangle a face. Image taken from [4].

each tetrahedron. In 4D, therefore, each edge is shared by four faces of the 2-complex. (In 3D, instead, associate three faces around the edge, i.e., the number of sides bounding each of the triangles).

The 2-complex is a way of discretizing and regularizing the spacetime enclosed within the boundary hypersurfaces. Discretizing the spacetime, the field theory becomes truncated. Adding more vertices to Γ involves more degrees of freedom in the evolution. It is now possible to discretize the partition function that was written before.

In equation (1.34), the B is a 2-forms field. It is, therefore, natural to integrate it over the faces of the 2-complex and discretize it. Then, $B_f = \int_{\text{faces}} B$ takes values in the algebra of the group. On the other hand, the connection w that defines the F field (Appendix A) is a 1-form, naturally integrated and along paths; however, in Loop Quantum Gravity, the connection is never involved directly; instead, the focus is on its exponentiation. We can, therefore, associate a group element $g_e \sim \exp[\int_{\text{edge}} w]$ to each line.

Performing the previous substitutions inside (1.34) results in a well-defined path integral of discrete quantities on the 2-complex. The partition function becomes,

$$Z = \int \mathcal{D}B_f \int_G \mathcal{D}g_e e^{\frac{i}{\hbar}\sum_f \mathrm{Tr}[B_f \prod_{e\in f} g_e]} \,. \tag{1.35}$$

The curvature has been discretized by using the connection defined on the edges. The $\prod_{e\in f} g_e$ at the exponent is the product of group elements sitting on the edges around a dual face, which measures the curvature.

This path integral can be formally solved by integrating out the fields B_f, transforming it in

$$Z = \int_G dg_e \prod_f \delta(g_{e_1} ... g_{e_n}). \tag{1.36}$$

The group elements g_{e_i} inside the delta distribution are those surrounding a dual face, and the integration is performed over a copy of the group G for each edge. Z is a number and depends only on the topology of the manifold $\mathcal{M}$. This can be taken as a definition of the path integral.

Therefore, the spacetime structure is not only encoded in the combinatorial structure Γ but also in its coloring. Upon closer examination, neither a spin network is defined solely by its graph but also by the coloring of the links (representations j_l) and nodes (intertwiners i_n). Accordingly, a spin-foam is obtained by coloring the 2-complex Γ with the values of the representations j_f on the faces and the intertwining operators i_e along the edges.

A spin-foam σ is the triplet $\sigma = (\Gamma, j_f, i_e)$. Spin foams emerge, therefore, as combinatorial objects, independent of any background space. In this construction, as in the spin networks, there is no notion of metric. These structures *represent* themselves the spacetime. As a spin network manifestly models the quantum space, the spin foam itself represents the quantum spacetime. Moreover, the evolution encoded in a spin foam does not require a time variable. Given a boundary geometry (a spin network), a transition amplitude can be computed with the desired truncation of degrees of freedom.
The amplitude (1.36) can be recast in different equivalent ways. Expanded in the complete form (for details on this construction [4] [9] [14]), it reads,

$$Z_{SF} = \sum_{j_f, i_e} \prod_f (2j_f + 1) \prod_e A_e(j_f, i_e) \prod_v A_v(j_f, i_e). \tag{1.37}$$

This is a general expression that we take as the definition of the spin foam formalism.
A choice of:

(i) A 2-complex Γ that represents a regularization of a region of spacetime,

(ii) A set of representations and intertwiners j_f and i_e that color respectively faces and edges of Γ,

(iii) A vertex $A_v(j_f, i_e)$ and edge $A_e(j_f, i_e)$ amplitudes,

defines a spin foam model.
This definition of a spin foam model can be considered the general QFT theory. Specifying a particular form of the vertex and the edge amplitude is akin to selecting a specific

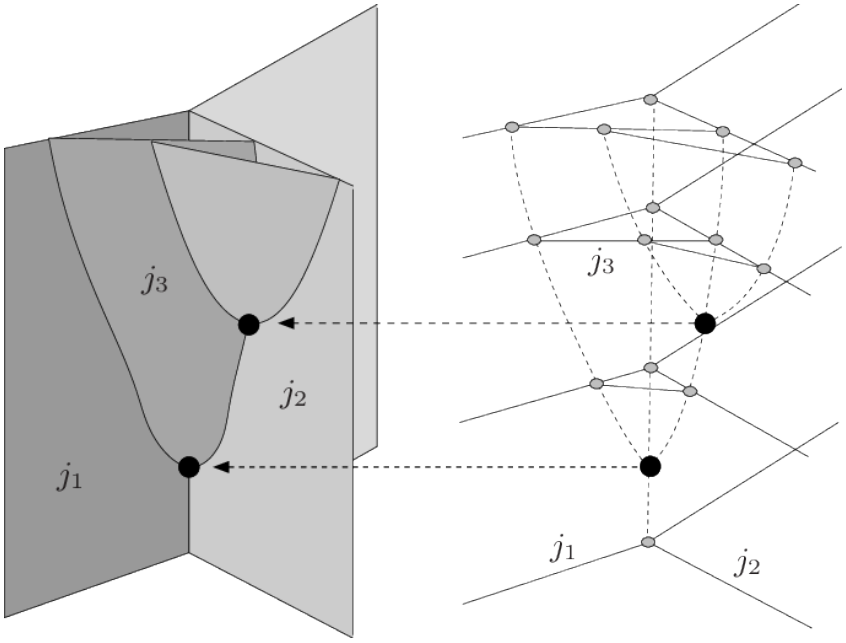

Figure 1.7: A spin foam is composed by a 2-complex Γ dual to a simplicial triangulation with faces colored with representations j_f and where the edges carry the intertwiners operators i_e. To define a precise spin-foam model, a prescription of a definition of the partition function is needed. Image taken from [14]

lagrangian for the system.
Currently, the best spin-foam model for the complete 4-dimensional theory is the EPRL model [15][16]. For the purposes of this work, we work with a simpler model and we introduce the three-dimensional Euclidean Ponzano-Regge model.

1.4 Dynamics in 3D - Ponzano Regge model

The Ponzano-Regge model is a quantization of Euclidean gravity in 3D. The sum over three-dimensional geometries naturally takes the form of a spin foam model. General Relativity in three dimensions does not contain local degrees of freedom, and it is a purely topological theory. Therefore, the dynamics of this theory become an evolution of global variables.
Let's build the model. Define a triangulation and its dual Δ of a region of spacetime with 3-simplices, i.e., tetrahedra in contact with triangular faces. The set of vertices, edges, and faces of the dual triangulation Δ is precisely the 2-complex Γ. We associate a group element $g_e \in SU(2)$ to each edge of Δ, and we color each face with a representation j_f. In three dimensions, the edges are surrounded by three faces, representing the link

length corresponding to those faces in the boundary spin network. The action (1.34), when it is written in terms of the classical variables of the 3D theory and quantized (for details, see [4]), becomes

$$S = \frac{1}{8\pi G}\sum_f \mathrm{Tr}[L_f g_f], \quad \text{where:} \;\; g_f = g_{e_1}....g_{e_n}, \tag{1.38}$$

where L_f are $su(2)$ algebra elements. The g_f are interpreted as the holonomies of gravitational connection along the edges, while L_f as the line integral of the triad (Appendix A) along the segment dual to the face f. Varying the action with respect to L_f results in the equation of motion $g_f = 1$, which is precisely the condition encoded in the delta function in (1.36). This communicates that the lattice connection is flat; roughly speaking, circumnavigating an edge of the spin foam, the sum of the angles gives 2π. Considering this and varying the action in the group elements g_f leads to the closure condition (1.10) in three dimensions.
The amplitude A_Δ can be written as the path integral (1.35) for this action

$$\mathcal{A}_\Delta = \mathcal{N}\int dg_e \int dL_f \; e^{\frac{i}{8\pi\hbar G}\sum_f Tr[L_f g_f]} \;, \tag{1.39}$$

where $\mathcal{N}$ is a normalization constant. Integrating out the L_f gives rise to the form (1.36),

$$\mathcal{A}_\Delta = \mathcal{N}\int dg_e \prod_f \delta(g_f), \tag{1.40}$$

where the delta function is on the group $SU(2)$.
To compute this integral, we expand the delta function in irreducible representations of the group. This is exactly the same procedure as considering a $U(1)$ delta function $\delta(\phi)$ and decompose it as the sum over n of plane waves $e^{in\phi}$. The $SU(2)$ irreducible representations in the same way are decomposed with the Wigner-matrices:

$$\delta(g) = \sum_j (2j+1) Tr[D^j(g)], \tag{1.41}$$

equivalently written as the character $\chi^j(g)$. Performing this decomposition and using the integration properties of Wigner matrices (Appendix B), the integral becomes a bunch of $3j$-symbols contracted one each other. The integrals take the form,

$$\int dg \; D^{j_1}_{m_1 n_1}(g) D^{j_2}_{m_2 n_2}(g) D^{j_3}_{m_3 n_3}(g) = \begin{pmatrix} j_1 & j_2 & j_3 \\ m_1 & m_2 & m_3 \end{pmatrix} \begin{pmatrix} j_1 & j_2 & j_3 \\ n_1 & n_2 & n_3 \end{pmatrix}. \tag{1.42}$$

Indeed, each edge produces two intertwiners: $i^{m_1 m_2 m_3}$ and $i^{n_1 n_2 n_3}$. They can be visualized as "located" at the two ends of the edge, gluing covariantly each magnetic index

related to the three faces surrounding it. In bulk, the vertices are four-valent, being dual to a triangulation of a 3D space with tetrahedra; therefore, we need to contract four intertwiners at each of them in a covariant manner. Without going into details (see [17]) the result is a $\{6j\}$-symbol,

$$\{6j\} = \begin{Bmatrix} j_1 & j_2 & j_3 \\ j_4 & j_5 & j_6 \end{Bmatrix} = \sum_{m_a,n_a} \prod_{a=1}^{6} \delta_{m_a,-n_a} (-1)^{j_a - m_a} \begin{pmatrix} j_1 & j_2 & j_3 \\ m_1 & m_2 & m_3 \end{pmatrix} \times \begin{pmatrix} j_1 & j_4 & j_5 \\ n_1 & m_4 & m_5 \end{pmatrix} \begin{pmatrix} j_2 & j_4 & j_6 \\ n_2 & n_4 & m_6 \end{pmatrix} \begin{pmatrix} j_3 & j_5 & j_6 \\ n_3 & n_5 & n_6 \end{pmatrix}. \tag{1.43}$$

This is a basic object in the representation theory of $SU(2)$, but it emerges naturally from the action (1.38). It is interesting to note that the path of contraction of this $\{6j\}$ reproduces the structure of a tetrahedron. Here, we are not talking about a tetrahedron of the triangulation, but its dual, still a tetrahedron.

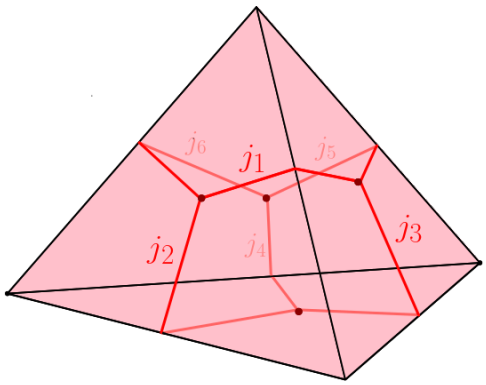

Figure 1.8: A tetrahedron of the triangulation (pink), and its dual associated to the $\{6j\}$-symbol (red)

.

To see the tetrahedron structure, it is sufficient to think of the first triplet of spins in the symbol (1.43) as the length of a triangle that closes. Consequently, the other three connect in the vertices that are not contained in the first triangle. The column (j_1, j_4),(j_2, j_5) and (j_3, j_6) instead represent the links that are not in contact.

The $\{6j\}$ object represents the vertex amplitude A_v in (1.37). The edge amplitude A_e is related to the dimension of the intertwiner space, but the latter is equal to one in three dimensions. The final amplitude form of the Poznano Regge model is,

$$\mathcal{A}_\Delta = \mathcal{N} \prod_f (2j_f + 1) \prod_v (-1)^{\sum_e j_e} \begin{Bmatrix} j_1 & j_2 & j_3 \\ j_4 & j_5 & j_6 \end{Bmatrix}_v, \tag{1.44}$$

in which the f index refers to the internal faces and v to the vertices.

Equivalence of Z and Fundamental cycles 3d

Another form of the transition amplitude is derived in this section, which will be used in the following sections. Consider the form of the amplitude (1.40),

$$\mathcal{A} = \int dg_e \prod_f \delta(g_f), \tag{1.45}$$

and considered a single-spin foam vertex in 3D. The delta functions inside the integration impose the local flatness on the faces of the bulk.

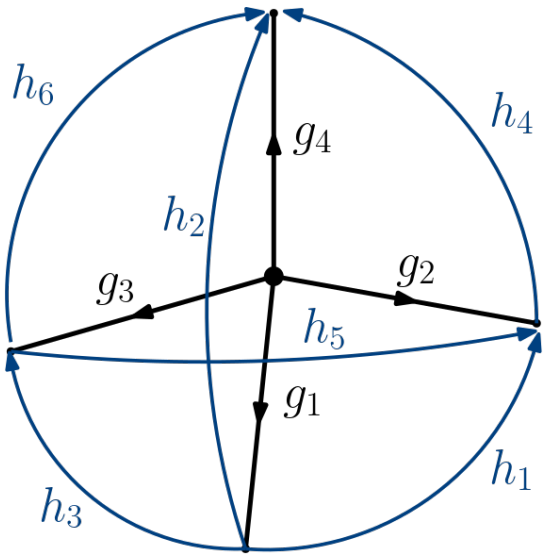

Figure 1.9: A bulk node closed with the boundary's wedge (two half-edge holonomies) holonomies. The blue graph represents the boundary graph of a single node.

The integration in the group elements g becomes over the six faces in figure (1.9). The δ functions represent mathematically the fact that there is no curvature. The explicit amplitude becomes

$$\begin{aligned}\mathcal{A} = \int dg_1 \cdots dg_4 \; & \delta(g_1 h_1 g_2^{-1})\delta(g_1 h_2 g_4^{-1})\delta(g_1 h_3 g_3^{-1}) \\ & \cdot \delta(g_3 h_5 g_2^{-1})\delta(g_3 h_6 g_4^{-1})\delta(g_2 h_4 g_4^{-1}).\end{aligned} \tag{1.46}$$

The delta functions are integrated straightforwardly; for example, $\delta(g_1 h_1 g_2^{-1})$ when resolved gives the condition $g_1 = g_2 h_1^{-1}$ and so on. Of the four integrations, one is redundant, and at the end, the result is

$$\mathcal{A} = \delta(h_2^{-1} h_1 h_4)\delta(h_1^{-1} h_3 h_5)\delta(h_6^{-1} h_5 h_4). \tag{1.47}$$

This is the amplitude expressed in terms of the *fundamental cycles*. A cycle in graph theory is defined as a path that starts from a node and returns to that node, crossing the others just once. The fundamentals are the independent cycles of a graph. Here, the amplitude reduces to the three cycles of the node's boundary graph and involves a combination of boundary holonomies. This condition is gauge invariant and imposes local flatness.

1.4.1 Regge calculs 3D

Regge calculus is a covariant discretization of General Relativity introduced by Tullio Regge in the 1961 [18]. The Ponzano-Regge model represents a quantum version of classical Regge calculus. In three dimensions, a Regge space $(\mathcal{M}, L_s)$ is a metric space obtained by gluing 3-simplices, i.e., tetrahedra, along matching boundary triangles. The triangles, in turn, met at segments, which met at points. This process is called triangulation. Usually, the triangulation is oriented, so each segment has a direction. This simplifies the notation and construction.

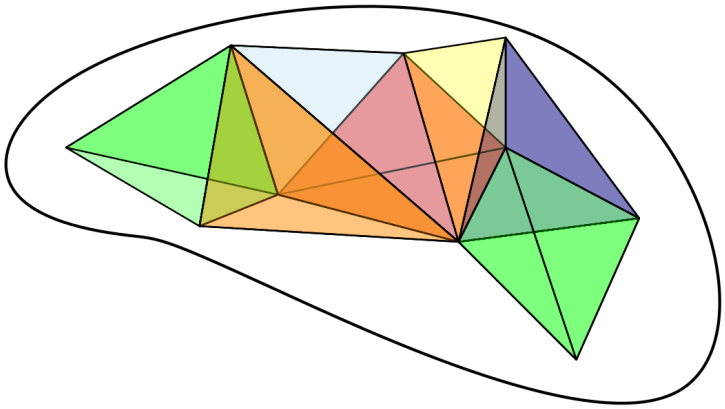

Figure 1.10: Pictorial representation of a three-dimensional space triangulated with tetrahedra.

Gluing flat tetrahedra can generate curvature on the segments (also called hinges). The resulting manifold will be flat everywhere except at these segments. In that way, the metric of the resulting space is uniquely determined by the lengths L_s; this follows from the fact that the shape of a general n-simplex is determined solely by the lengths of its sides.

For any Riemannian manifold $(\mathcal{M}, g)$ and a small parameter ϵ, there exists a Regge manifold $(\mathcal{M}, L_s)$ with sufficiently many simplices, such that the difference between the Riemannian and the Regge distance among any two points P_1 and P_2 in $\mathcal{M}$ is less than ϵ.

The curvature in the Regge calculus is encoded in the deficit angle, defined as:

$$\delta_l(L_s) = 2\pi - \sum_t \theta_t(L_s). \tag{1.48}$$

On the side l, a certain number of tetrahedra in three dimensions met. The deficit angle is 2π minus the sum of the dihedral angles formed by the triangles around it.

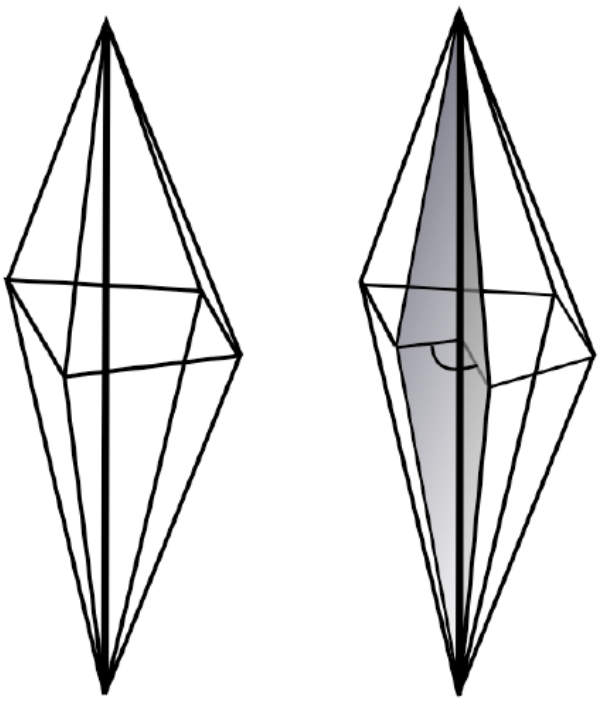

Figure 1.11: Graphical representation of a deficit angle in three dimensions. The black heavy line is the segment l considered. On the left, there is a case in which the deficit angle $\delta_l(L_s) = 0$. On the right, the deficit angle $\delta_l(L_s) \neq 0$ is depicted in gray. Image taken from [4].

The geometric interpretation of the deficit angle is that if we parallel transport a vector in a loop around the segment, the vector gets back-rotated by the deficit angle. Regge defined the action to be, in general n-dimensions,

$$S_M(L_s) = \sum_h A_h(L_s)\delta_h(L_s), \tag{1.49}$$

where the sum is over $(n-2)$-simplices (hinges) and $A_h(L_s)$ is the $(n-2)-$dimensional

volume of the hinge. The equations of motion are obtained by varying this action concerning the lengths L_s. The general variation is,

$$\sum_h \frac{\partial A_h}{\partial L_s}\delta_h(L_s) + A_h \frac{\partial \delta_h(L_s)}{\partial L_s} = 0 \tag{1.50}$$

The second term always vanishes algebraically (the Schläfli Identity). This equation is the equivalent of the vanishing variation of the Riemann tensor in the Einstein-Hilbert action.

In three dimensions, the term $A_h(L_s)$ coincides with the lengths themselves. The Regge action reduces to

$$\sum_l \delta_l(L_s) = 0. \tag{1.51}$$

That is flatness. This is coherent with the continuous case. The Regge calculus reduces to the correct version of GR in three dimensions, and the equations of motion force space to be flat (since the theory is topological).

The Ponzano-Regge model described in the previous section is no longer based on the triangulation itself but on the dual one and, through the introduction of the spin foam methods, realizes the idea of a quantum version of the Regge calculus implementing a path integral formulation of it.

Chapter 2

Coherent States

Coherent states are purely quantum states that resemble the dynamics of a classical system. They are the main tool to perform semi-classical analysis in quantum mechanics. The fundamental feature of these states is that they can be peaked on desired classical values of the variables. More precisely, that means that the expectation values of the quantum operators are given by construction by the classical values of the precise phase space cell on which they are peaked. In general, finding a systematic way of building coherent states is challenging. However, T. Thiemann defined an elegant guideline to generalize this procedure. This chapter will briefly analyze the so-called *Complexifier method*. For details, see [19, 20]. This chapter aims to create the coherent spin-network states [3] that will later be tools for studying the black-to-white hole transition in three dimensions.

2.1 Complexifier method

The definition of a coherent state and a method introduced by T. Thiemann to systematically build such states will be explored (see [20, 19]).

- **Coherent states**

Let $\hat{\mathcal{A}}$ be an algebra of linear operators on the Hilbert space $\mathcal{H}$ and $\mathcal{P}$ a phase space. A set of states $\{\psi_{q,p}\}_{(q,p)\in\mathcal{P}} \in \mathcal{H}$ is said to be coherent if the following properties are satisfied:

(i) *Annihilation operator property*
There exist elementary operators $\hat{g}$ such that $\hat{g}\ \psi_{q,p} = g(q,p)\psi_{q,p}$;

(ii) *Peakedness property*
For any point $(q,p) \in \mathcal{P}$, the overlap function $(q',p') \to |\langle\psi_{q,p}|\psi_{q',p'}\rangle|^2$ is peaked on a phase space cell of Liouville volume $\frac{1}{2}|\langle\psi_{q,p}|[\hat{q},\hat{p}]|\psi_{q,p}\rangle|$;

(iii) *Minimal uncertainty property*
The Heisenberg uncertainty relation is saturated, namely $\Delta q \Delta p = \frac{1}{2} |\langle \psi_{q,p}| [\hat{q}, \hat{p}] |\psi_{q,p}\rangle|^2$;

(iv) *Overcompleteness property*
There exist a resolution of the identity $\mathbb{I}_{\mathcal{H}} = \int_{\mathcal{P}} d\mu(q,p)\ \psi_{q,p} \langle \psi_{q,p}| \cdot \rangle_{\text{kin}}$ for some measure $d\mu$ in the phase space $\mathcal{P}$.

In the context of usual quantum mechanics, the coherent states are described as superpositions of energy eigenstates that satisfy the condition of being eigenvectors of the annihilation operator. This method requires a preferred Hamiltonian for the system, and if we are dealing with nonlinear systems, the construction of an annihilation operator is not trivial. The Complexifier method is an extension that does not require any of these ingredients. Let's see how it works, starting from the definition of the *Complexifier*.

- **Complexifier**

A complexifier is a positive definite function $C : \mathcal{P} \longrightarrow \mathbb{R}$ on the phase space $\mathcal{P}$ which is smooth almost everywhere and whose Hamiltonian vector field χ_C is nowhere vanishing on the configuration space $\mathcal{C}$. Moreover for each point $q \in \mathcal{C}$ the function $p \to C_q(p) := C(q,p)$ grows faster than linearly with $||p||_q$ where p is a local momentum coordinate and $||\cdot||_q$ is a suitable norm on the cotangent bundle $\mathcal{T}_q^*\mathcal{C}$ of the symplectic manifold $(\mathcal{P}, \Omega)$ with a strong symplectic structure Ω.

The complexifier has two main functions. It acts as a smoothing operator and it also complexifies our variables. First, let's consider a delta distribution $\delta(x)_q$ concerning some measure μ, and with support on $x = q$. In other words, $\int f(x)\delta_q(x) = f(q)d\mu$. These types of distributions are not part of the kinematical Hilbert space $\mathcal{H}$, but they reflect the intuitive idea of a particle being localized.
Now consider a complexifier function C. Being positive definite by construction, we can promote it to a self-adjoint operator $\hat{C}$ on $\mathcal{H}$. We also introduce a parameter $t > 0$ that we will call *semi-classicality parameter* that will allow us to control the spread in the coordinates Δx and on the momenta Δp. This parameter is just multiplied by the function that we choose as our complexifier $C(q,p)$:

$$C(q,p) \longrightarrow \tilde{C}(q,p) = tC(q,p). \tag{2.1}$$

From now on, to simplify the notation, we will refer to $\tilde{C}$ as C, while keeping in mind that the t parameter is still a part of the definition of the complexifier. This parameter is handy for controlling the spread of uncertainty in coherent states. However, we anticipate that we will consider $t = 1$ in the next sections.

Now, starting from the state $\psi_q(x) = \delta_q(x)$ we use C promoted to an operator to

smoothen the delta distribution:

$$\psi_q^t(x) = e^{-\frac{\hat{C}}{\hbar}}\delta_q(x). \tag{2.2}$$

The second role of the complexifier is to map our coordinate q into a complex value z, i.e., to perform $q \longrightarrow z \in \mathbb{C}$. The following series defines the correct z

$$z(q,p) = \sum_{n=0}^{\infty} \frac{i^n}{n!}\{q, C(q,p)\}_n, \tag{2.3}$$

where the n-th order Poisson bracket is defined recursively as

$$\{q, C\}_{n+1} = \{\{q, C\}_n, C\}, \qquad \text{with:} \qquad \{q, C\}_0 := q. \tag{2.4}$$

This shift defines local complex coordinates on the extended $\mathcal{P}$, provided $z(q,p)$ and $\bar{z}(q,p)$ are invertible. Locally, this invertibility is guaranteed by the conditions imposed on C.
Then, it is sufficient to perform this complexification in the state $\psi_q^t(x)$

$$\psi_{qp}^t := \left[\psi_q^t(x)\right]_{q\longrightarrow z(q,p)} = \left[e^{-\frac{\hat{C}}{\hbar}}\delta_q(x)\right]_{q\longrightarrow z(q,p)}. \tag{2.5}$$

Besides, the transition to quantum theory is performed as usual, promoting the variables to operators and the Poisson brackets to commutators. It is straightforward to show that $\hat{z}$ as an operator is given by

$$\hat{z} = e^{-\frac{\hat{C}}{\hbar}}\hat{q}e^{+\frac{\hat{C}}{\hbar}}, \tag{2.6}$$

and that given the definition (2.5), ψ_{qp}^t is an eigenstate of $\hat{z}$ with eigenvalue $z(q,p)$,

$$\hat{z}\psi_{qp}^t = \left[e^{-\frac{\hat{C}}{\hbar}}\hat{q}e^{+\frac{\hat{C}}{\hbar}}e^{-\frac{\hat{C}}{\hbar}}\delta_q(x)\right]_{q\longrightarrow z(q,p)} = \left[qe^{-\frac{\hat{C}}{\hbar}}\delta_q(x)\right]_{q\longrightarrow z(q,p)} = z(q,p)\psi_{q,p}^t(x). \tag{2.7}$$

By construction, the annihilation operator property is satisfied.
Starting from $\hat{z}$ we define ladder operators and effectively prove that the coherent states minimize the spread of uncertainties. Indeed, writing in general two operators $\hat{x}$ and $\hat{y}$,

$$\hat{x} := \frac{1}{2}(\hat{z} + \hat{z}^\dagger)\ , \qquad \hat{y} := \frac{1}{2i}(\hat{z} - \hat{z}^\dagger). \tag{2.8}$$

If the coherent states are properly normalized, the expectation value of these last are

$$\langle\hat{x}\rangle = \frac{1}{2}(z(q,p) + \bar{z}(q,p)) = \text{Re } z(p,q)\ , \quad \langle\hat{y}\rangle = \frac{1}{2i}(z(q,p) - \bar{z}(q,p)) = \text{Im } z(q,p). \tag{2.9}$$

Finally, we can check that these states saturate the Heisenberg uncertainty principle:

$$\Delta x \Delta y = \frac{1}{2}|\langle[\hat{x}, \hat{y}]\rangle| = \frac{\hbar}{2}. \tag{2.10}$$

These are excellent coherent state candidates, and the systematic construction performed above is entirely independent of the quantum mechanical system. Indeed, we have not specified it in any way. The standard coherent states minimize Δx^2 and Δy^2 at the same time, indeed

$$\Delta x^2 = \frac{\hbar}{2}t, \qquad \Delta y^2 = \frac{\hbar}{2t}. \tag{2.11}$$

The minimum for both is reached for $t = 1$, corresponding to the standard coherent state definitions in most physical systems under study. To make this construction more tangible, let's apply it to the simple case of the free particle, verifying that the coherent states obtained using this method correspond to the well-known wave packets used in quantum mechanics.

2.1.1 Free Particle

Let us apply the complexifier method to the simple case of a free particle. The first step is to define the complexifier; this can be done easily by choosing the kinetic term for the particle (which is also the only term in the Hamiltonian) which is proportional to k^2, such that the summation (2.3) is truncated at the second order.

$$C = t\frac{k^2}{2}. \tag{2.12}$$

First, we start from the delta distribution, which, as already mentioned, expresses the intuitive notion of a particle being localized and represents a generalized eigenstate of the position operator. We thus start from the simple $\psi_q(x) = \delta(x - q)$. The first step is to smoothen this function with the complexifier promoted to an operator

$$\begin{aligned}
\psi_q^t(x) = e^{-\frac{\hat{C}}{\hbar}}\psi_q(x) &= e^{-\frac{t}{2\hbar}\hat{k}^2}\left\langle x|q\right\rangle, \\
&= e^{-\frac{t}{2\hbar}\hat{k}^2}\int d^n k \left\langle x|k\right\rangle \left\langle k|q\right\rangle, \\
&= N\int d^n k\; e^{-\frac{t}{2\hbar}k^2}e^{\frac{i}{\hbar}k(x-q)}, \\
&= Ne^{-\frac{1}{2\hbar t}(x-q)^2}.
\end{aligned} \tag{2.13}$$

Where N is a constant, it is not essential in that precise step because we will normalize the final coherent state directly. The next step involves using the complexifier to shift the coordinate variable in the complex plane.

$$\{q, C\}_0 := q, \qquad \{q, C\}_1 = tp, \qquad \{q, C\}_{n>1} = 0. \tag{2.14}$$

The notation has been changed to distinguish between the momentum variable k and the classical label of the coherent state p, representing two different things. Consequently

considering the definition (2.3), the complexified variable z is defined as,

$$z = q + itp. \tag{2.15}$$

Complexifing the variable inside $\psi_q^t(x)$, the candidate coherent state $\psi_{q,p}^t(x)$ is obtained. Normalizing it to one, the final result is

$$\psi_{q,p}^t(x) = \left(\frac{1}{\pi\hbar t}\right)^{\frac{n}{4}} e^{\frac{-(x-q)^2}{2\hbar t}} e^{i\frac{p}{\hbar}(x-q)}. \tag{2.16}$$

This represents the typical structure of a wave packet. That is a Gaussian centered at the classical value q and a phase that includes the classical momentum p. Performing the Fourier transform, the state in the momentum space is

$$\tilde{\psi}_{q,p}^t(k) = \left(\frac{t\hbar}{\pi}\right)^{\frac{n}{4}} e^{\frac{-t(k-p)^2}{2\hbar}} e^{i\frac{k}{\hbar}q}. \tag{2.17}$$

Naturally, when a Gaussian is transformed, the result is still a Gaussian but centered around the classical momenta. Note this slight asymmetry between the two states. The phase term with $i\frac{k}{\hbar}q$ can be transformed in $i\frac{q}{\hbar}(k-p)$ with the addition of an irrelevant phase term absorbable in the normalization constant. In that case, performing the inverse Fourier transform, the phase term of the state $\psi_{q,p}(x)$ will become $i\frac{p}{\hbar}x$. This is an interesting detail related to the symplectic structure of the phase space, and later on, this change will be performed.
The expectation values of the coordinate and momenta operators are

$$\begin{aligned} \left\langle \psi_{q,p}^t \right| \hat{x} \left| \psi_{q,p}^t \right\rangle &= q, \\ \left\langle \psi_{q,p}^t \right| \hat{p} \left| \psi_{q,p}^t \right\rangle &= p. \end{aligned} \tag{2.18}$$

This tells us that in the phase space, these states are peaked on the classical values (q, p) as desired.
Computing the spread of these states leads to a very interesting result that clarifies the role of the semi-classicality parameter t, namely

$$\begin{aligned} \Delta x^2 &= \left\langle \psi_{q,p}^t(x) \right| \hat{x}^2 \left| \psi_{q,p}^t(x) \right\rangle - \left\langle \psi_{q,p}^t(x) \right| \hat{x} \left| \psi_{q,p}^t(x) \right\rangle^2 = \frac{\hbar}{2}\, t. \\ \Delta p^2 &= \left\langle \psi_{q,p}^t(x) \right| \hat{p}^2 \left| \psi_{q,p}^t(x) \right\rangle - \left\langle \psi_{q,p}^t(x) \right| \hat{p} \left| \psi_{q,p}^t(x) \right\rangle^2 = \frac{\hbar}{2}\, t^{-1}. \end{aligned} \tag{2.19}$$

Consider the limit as t approaches 0, then the position spread becomes zero, and the momentum spread becomes infinite. In this limit, the complexifier behaves no more like a smoothing operator and becomes equivalent to the identity, leaving the initial delta function in the position. On the other hand, when t approaches infinity, the result is a momentum eigenstate with an infinite spread in the position variable.

2.2 Coherent Spin Network States

The goal is to build a semiclassical state of the gravitational field, namely a coherent spin network. This is motivated by the works [1][2]. In [1], a classical metric describing the black-white hole spacetime has been found. The model suggests some precise features of the intrinsic and extrinsic curvature. Therefore, it is necessary to build states that are peaked on precise classical values. This is the usual construction of coherent states in Loop Quantum Gravity. It is worth anticipating, however, that this work also analyzes the limits of this construction. It will become clear that in a non-classically allowed transition, such as in a tunneling process, the structure of a coherent state breaks down.

2.2.1 Coherent Link

The complexifier procedure is now applied to states $\psi(g) \in \tilde{\mathcal{H}} = L_2[SU(2)]$. The method consists of applying the complexifier to a position's eigenstate, in this case, a state peaked around some group element, and then performing a complex shift.

The Casimir operator $\vec{J}\cdot\vec{J}$ plays the role of the complexifier. Therefore, the smoothening operator becomes:

$$e^{-\frac{\hat{C}}{2}} = e^{-t\frac{\vec{J}.\vec{J}}{2}}, \tag{2.20}$$

where $\vec{J}$ are the generators of $SU(2)$. The starting point for building coherent states is the usual delta function. In that case, the delta function is defined on the group $SU(2)$, thus,

$$\psi_{h_0}(g) = \delta(h_0^\dagger g), \tag{2.21}$$

where $g, h \in SU(2)$. Here, h plays the role of the "classical" variable and g of the general integration variable. Moreover, instead of the inverse h in the delta function, the $h^\dagger$ has been used. This makes no difference for $SU(2)$ since the conjugate transposed matrix equals the inverse one. However, h will be complexified later, and this detail will become important. Using the property of the delta function (Appendix B) on groups the state can be written as,

$$\psi_{h_0}(g) = \sum_j d_j \chi^j(h^\dagger g). \tag{2.22}$$

Where $d_j = 2j+1$ is the dimension of the representation and $\chi^j(h^\dagger g)$ is the character of the representation, namely the trace of the representation matrices, i.e.

$$\chi^j(h^\dagger g) = Tr[D^{(j)}(h^\dagger g)]. \tag{2.23}$$

As for the case of the free particle, now this delta has to be smoothened with the complexifier promoted to an operator,

$$\psi^t_{h_0}(g) = e^{-\frac{\hat{C}}{2}}\psi_{h_0}(g) = \mathcal{N}\sum_j d_j e^{-\frac{t}{2}(j+1)j}\chi^j(h_0^\dagger g). \tag{2.24}$$

The last step to have coherent states is to complexify the $SU(2)$ element h. The complexification of $SU(2)$ turns out to be $SL(2,\mathbb{C})$; it is thus sufficient to use the polar decomposition of the latter to write

$$SU(2) \ni \quad h \longrightarrow H = e^{t\frac{\vec{p}\cdot\vec{\sigma}}{2}} h \quad \in SL(2,\mathbb{C}). \tag{2.25}$$

Therefore the $SU(2)$ coherent state is

$$\psi^t_{h_0,p}(g) = \mathcal{N} \sum_j d_j e^{-\frac{t}{2}(j+1)j} \chi^j(h_0^\dagger e^{t\frac{\vec{p}\cdot\vec{\sigma}}{2}} g). \tag{2.26}$$

These states can be normalized by imposing the scalar product of the state with itself as equal to one. Consider the following relation between two characters,

$$\int dg \;\; \overline{\chi^j(h^\dagger g)} \chi^{j'}(h'^\dagger g) = \frac{\delta^{jj'}}{2j+1} \chi^j(h^\dagger h'). \tag{2.27}$$

The scalar product of two different coherent states centered on the same element h_0 is

$$\begin{aligned}
\left\langle \psi^t_{h_0,p} | \psi^t_{h_0,p'} \right\rangle &= \mathcal{N}\mathcal{N}' \sum_j \sum_{j'} d_j d_{j'} \int dg \;\; e^{-\frac{t}{2}(j+1)j} e^{-\frac{t}{2}(j'+1)j'} \overline{\chi^j(H^\dagger g)} \chi^j(H'^\dagger g), \\
&= \mathcal{N}\mathcal{N}' \sum_j \;\; d_j \;\; e^{-t(j+1)j} \chi^j(H^\dagger H'), \\
&= \mathcal{N}\mathcal{N}' \sum_j \;\; d_j \;\; e^{-t(j+1)j} \chi^j\left(e^{t\frac{p+p'}{2}\sigma_3} \right), \\
&= \mathcal{N}\mathcal{N}' \sum_j \;\; d_j \;\; e^{-t(j+1)j} \left(\sum_{n=-j}^{j} e^{t\frac{p+p'}{2} n} \right), \\
&= \mathcal{N}\mathcal{N}' \sum_j \;\; d_j \;\; e^{-t(j+1)j} \frac{\sinh(\frac{t(p+p')}{4}(2j+1))}{\sinh(\frac{t(p+p')}{4})}.
\end{aligned} \tag{2.28}$$

The result is a well-known feature of $SU(2)$; however, due to the complexification, instead of the $\sin(x)$, there is its analytical continuation $\sinh(x)$.

$$\left\langle \psi^t_{h_0,p} | \psi^t_{h_0,p} \right\rangle = \mathcal{N}^2 \sum_j \;\; d_j \;\; e^{-t(j+1)j} \frac{\sinh(\frac{tp}{2}(2j+1))}{\sinh(\frac{tp}{2})} \doteq 1. \tag{2.29}$$

Solving this sum exactly is nontrivial, but due to the exponential suppression deriving from the complexifier, truncating it achieves a good approximation.

The complete form for the coherent link of a spin network is

$$\psi^t_{h_0,p}(g) = \left(\sum_j \;\; d_j \;\; e^{-t(j+1)j} \frac{\sinh(\frac{tp}{2}(2j+1))}{\sinh(\frac{tp}{2})} \right)^{-\frac{1}{2}} \sum_j d_j e^{-\frac{t}{2}(j+1)j} \chi^j(h_0^\dagger e^{t\frac{\vec{p}\cdot\vec{\sigma}}{2}} g). \tag{2.30}$$

2.2.2 Coherent Spin Network

In the previous section, coherent states have been constructed using the Thiemann [20] complexifier method. The structure of these quantum states is always a Gaussian distribution plus a phase (up to normalization constants), both in momentum and coordinate spaces. It is time to build coherent spin networks and analyze their structure.

The simplest spin network in three dimensions is represented by a single tetrahedron.

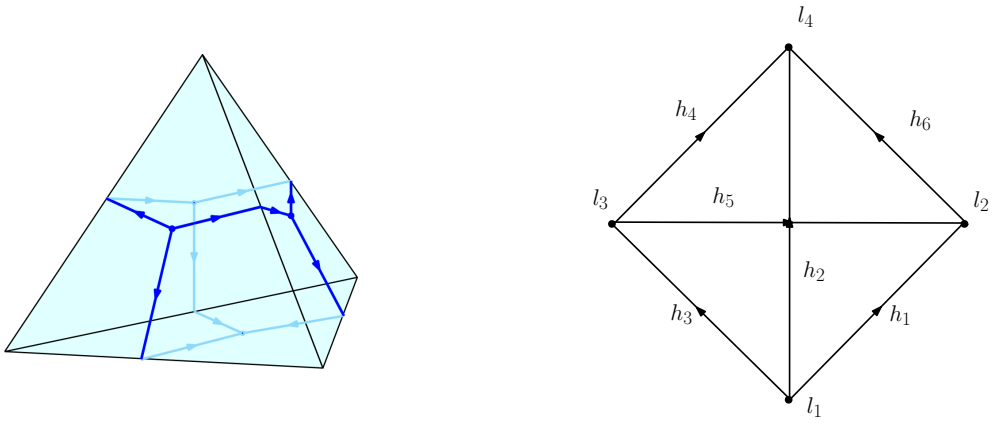

Figure 2.1: Simplest spin network in three dimensions. On the left is a pictorial representation of the spin network (blue graph) around a three-dimensional tetrahedra. The same spin network is labeled on the right with $SU(2)$ elements.

This section uses a simpler notation to label the elements of $SU(2)$, namely the group element associated with a single link is referred to as h_i. The group averaging is explicitly performed to project the states in $\mathcal{H}_\Gamma$.
The single link coherent state is,

$$\psi_h^t(g) = \mathcal{N} \sum_j (2j+1) e^{-\frac{t}{2} j(j+1)} \chi^j(h^\dagger g). \tag{2.31}$$

Remember that χ^j indicates the character of the representation, and here, with a slight abuse of notation, h refers also to the complexified $SU(2)$ element. Performing the group averaging consists of adding generic $SU(2)$ elements l_i to the nodes and then integrating them. Since the spin network has six links, six coherent states are combined. This means there is a product of six characters inside the four integrals (one per each l_i, and thus one per node). The characters turn out to have this form before the averaging

$$\chi^{j_a}(h_a^\dagger l_b^{-1} g_a l_c), \tag{2.32}$$

where l_b^{-1} is the element corresponding to the link's target and l_c is the one of the source node. Using the properties of the representation matrices, the latter can be split in

$$D^{j_a}_{m_a n_a}(h_a^\dagger) D^{j_a}_{n_a p_a}(l_b^{-1}) D^{j_a}_{p_a q_a}(g_a) D^{j_a}_{q_a m_a}(l_c). \tag{2.33}$$

Moreover each $D^{(j)}$ matrix of an inverse element can be written as

$$D^{j_a}_{n_a p_a}(l_b^{-1}) = (-1)^{j_a - p_a} \delta_{-p_a p'_a} D^{j_a}_{p'_a n'_a}(l_b) \delta_{-n_a n'_a} (-1)^{j_a - n_a}. \tag{2.34}$$

The non-gauge invariant states are projected into the invariant space $\mathcal{H}_\Gamma$ with the intertwiners. Isolating the integrals on the l_i elements, the intertwining structure automatically combines the coherent links. For the first node, which is a source of all of its links, the integration leads to

$$\int dl_1 \; D^{j_1}_{q_1 m_1}(l_1) D^{j_2}_{q_2 m_2}(l_1) D^{j_3}_{q_3 m_3}(l_1) = i^{q_1 q_2 q_3} \; i^{m_1 m_2 m_3} \; . \tag{2.35}$$

The same result appears for the fourth node, which is just a target of its links. Using the property (B.13),

$$\int dl_4 \; D^{j_4}_{p_4 n_4}(l_4) D^{j_2}_{p_2 n_2}(l_4) D^{j_6}_{p_6 n_6}(l_4) = i^{p_4 p_2 p_6} \; i^{n_4 n_5 n_6} \; . \tag{2.36}$$

The other two nodes undergo the same calculation, the ordering of the links becomes important since the intertwiner will gain a phase each time the node is a target instead of a source. Given the symmetry, these phases canceled out in the previous two nodes. Just for this first example, the intertwiners with one phase and two phases more are indicated respectively with $\tilde{i}$ and with $\tilde{\tilde{i}}$. In the next, this notation will be abandoned in order not to burden the formalism, indicating the intertwiners just with i. For the third node, the group averaging integrals take the form

$$\begin{aligned}
&\int dl_3 \; D^{j_3}_{n_3 p_3}(l_3^{-1}) D^{j_4}_{q_4 m_4}(l_3) D^{j_5}_{q_5 m_5}(l_3) =, \\
&= \int dl_3 \; (-1)^{j_3 - p_3} \delta_{-p_3 p'_3} D^{j_3}_{p'_3 n'_3}(l_3) \delta_{-n_3 n'_3} (-1)^{j_3 - n_3} (l_3) D^{j_4}_{q_4 m_4} D^{j_5}_{q_5 m_5}(l_3), \\
&= (-1)^{j_3 - p_3} (-1)^{j_3 - n_3} \delta_{-p_3 p'_3} \delta_{-n_3 n'_3} i^{p'_3 q_4 q_5} \; i^{n'_3 n_4 n_5}, \\
&= (-1)^{j_3 - p_3} (-1)^{j_3 - n_3} i^{-p_3 q_4 q_5} \; i^{-n_3 m_4 m_5}, \\
&\doteq \tilde{i}^{p_3 q_4 q_5} \tilde{i}^{n_3 m_4 m_5} \; .
\end{aligned} \tag{2.37}$$

The same is true for the last node, but this time with two phases,

$$\begin{aligned}
&\int dl_2 \; D^{j_1}_{n_1 p_1}(l_2^{-1}) D^{j_5}_{n_5 p_5}(l_2^{-1}) D^{j_6}_{q_6 m_6}(l_3) =, \\
&= (-1)^{j_1 - p_1} (-1)^{j_1 - n_1} (-1)^{j_5 - p_5} (-1)^{j_5 - n_5} i^{-p_1 - p_5 q_6} \; i^{-n_1 - n_5 m_6}, \\
&\doteq \tilde{\tilde{i}}^{p_1 p_5 q_6} \; \tilde{\tilde{i}}^{n_1 n_5 m_6} \; .
\end{aligned} \tag{2.38}$$

Calling Γ the oriented graph in Figure 2.2.2, the spin network state concerning only the g_i variables becomes

$$\begin{aligned}\psi^{j_l}_\Gamma(g_l) = (-1)^{j_1-p_1}(-1)^{j_3-p_3}(-1)^{j_5-p_5}\delta_{-p_1p_1'}\delta_{-p_3p_3'}\delta_{-p_5p_5'}\ i^{q_1q_2q_3}\ i^{p_4p_2p_6}\ i^{p_3'q_4q_5}\\ i^{p_1'p_5'q_6}\ D^{j_1}_{p_1q_1}(g_1)\ D^{j_2}_{p_2q_2}(g_2)\ D^{j_3}_{p_3q_3}(g_3)\ D^{j_4}_{p_4q_4}(g_4)\ D^{j_5}_{p_5q_5}(g_5)\ D^{j_6}_{p_6q_6}(g_6)\ .\end{aligned} \tag{2.39}$$

The structure is the same also for the group elements h. At the end, the final spin network state is given by

$$\psi^t_{\Gamma,h}(g) = \sum_{j_l}\left(\prod_{i=1}^{6}(2j_i+1)e^{-\frac{t}{2}j_i(j_i+1)}\right)\ \psi^{j_l}_\Gamma(g_l)\ \psi^{j_l}_\Gamma(h_l). \tag{2.40}$$

The interpretation of this result is exciting. Despite the mathematical complexity, it is exactly the structure of the wave packet used in quantum mechanics. Analyzing piece by piece, this result is very natural:

- The summation $\sum_{j_l}$ and the factor $(2j_l+1)$ are the equivalent of an integration with its measure. In the free particle case, this integration was performed immediately. In this case, it would require truncations or simplifications; however, it just lacks an analytical result, a common situation in physics.
- The term $e^{-\frac{t}{2}j_i(j_i+1)}$ is the Gaussian smoothing factor typical of the wave packets.
- The $\psi^{j_l}_\Gamma(g_l)$ is the basis of the gauge invariant Hilbert space of the spin network in the Schrödinger representation.
- The $\psi^{j_l}_\Gamma(h_l)$ term carries the information on the classical cell of the phase space in which the states are peaked.

This construction is simple and has a clear interpretation.

2.3 Twisted geometries parametrization of the holonomy

To conclude the kinematic part needed to settle the problem of the black-to-white hole transition, it is now essential to discuss the twisted geometries parametrization of the holonomy.
This reparametrization is fundamental, simplifying enormously the calculation concerning the dynamics. More precisely, dealing with the characters inside

$$\psi^t_{\Gamma,h}(g) = \sum_{j_l}\prod_{l}(2j_l+1)e^{-\frac{t}{2}j_l(j_l+1)}\chi^{j_l}(h^\dagger_{j_l}g_{j_l}), \tag{2.41}$$

is nontrivial. On the other hand, using the twisted geometries techniques makes it rather simple to compute this sum.

The goal of twisted geometry parametrization is to encode the information of the holonomies into the transport of spinors associated with the link. For details, see [21] [22] [23]. Spinors are elements of the vector space $\mathbb{C}^2$. A spinor and its conjugate transposed are denoted respectively with $|z\rangle$ and $\langle z|$. They are couples of two complex numbers $z^0, z^1 \in \mathbb{C}$,

$$|z\rangle := \begin{pmatrix} z^0 \\ z^1 \end{pmatrix}, \qquad \langle z| := \begin{pmatrix} \overline{z}^0, & \overline{z}^1 \end{pmatrix}. \tag{2.42}$$

Being elements of $\mathbb{C}^2$, they transform naturally under $SU(2)$ in the defining representation,

$$h : \mathbb{C}^2 \longrightarrow \mathbb{C}^2; \quad |z\rangle \longrightarrow h\,|z\rangle \;\; \forall h \in SU(2). \tag{2.43}$$

The spinorial space is endowed with a natural inner product given by:

$$\langle w|z\rangle := \overline{w}_0 z_0 + \overline{w}_1 z_1, \tag{2.44}$$

and a duality map $\mathcal{J} : \mathbb{C}^2 \longrightarrow \mathbb{C}^2$,

$$\mathcal{J}\,|z\rangle = |z] := \begin{pmatrix} -\overline{z}_1 \\ \overline{z}_0 \end{pmatrix}. \tag{2.45}$$

Without abandoning the elegant Dirac formalism in which $|z\rangle$ is called "ket", the analogous dual spinor $|z]$ will be called "sket". The map $\mathcal{J}$ is esplicitly realized using the anti-symmetric matrix ϵ, defined as,

$$\epsilon = \begin{pmatrix} 0 & -1 \\ 1 & 0 \end{pmatrix}, \tag{2.46}$$

and the above-cited map becomes:

$$|z\rangle \longrightarrow |z] := \epsilon\,|\overline{z}\rangle\,. \tag{2.47}$$

A fundamental property of spinors is that they naturally define a basis of $\mathbb{R}^3$ built from the matrix elements of Pauli matrices,

$$\langle z|\,\vec{\sigma}\,|z\rangle = -\vec{n}, \quad \text{and} \quad [z|\,\vec{\sigma}\,|z\rangle = i\vec{F} + \vec{n} \times \vec{F}. \tag{2.48}$$

For simplicity, unitary norm spinors are considered: $\langle z|z\rangle = 1$. In that way, the resulting $\mathbb{R}^3$ base is orthonormal. The relations (2.48) tell that each spinor identifies a normal vector $\vec{n}$ and a framed plane orthogonal to $\vec{n}$ whose orientation is given by $\vec{F}$ that is called frame vector.

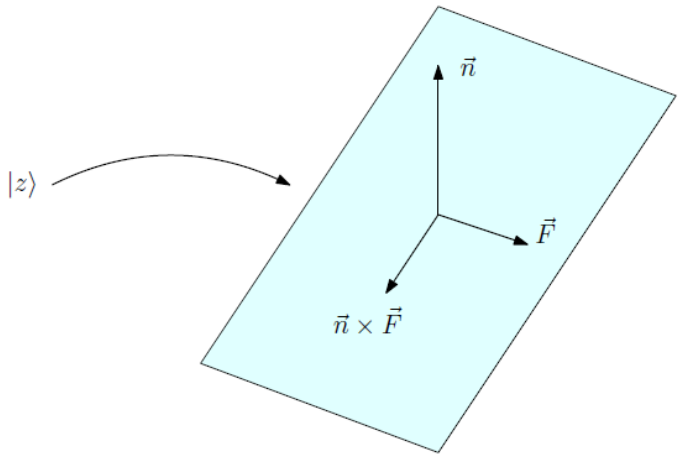

Figure 2.2: Each spinor $|z\rangle$ defines an orthogonal frame in $\mathbb{R}^3$. Image taken from [22]

These objects allow us to rewrite LQG in its spinorial representation.
Consider two spinors $|z\rangle$ and $|w\rangle$ representing the basis of two $\mathbb{C}^2$ spaces. The two spaces are interpreted as the source and the target of a general linear map $g \in GL(2,\mathbb{C})$, and using the projectors, a general group element can be decomposed in the following way,

$$g = a\,|w\rangle\langle z| + b\,|w]\langle z| + c\,|w\rangle[z| + d\,|w][z|\,. \tag{2.49}$$

Instead of group elements of $GL(2,\mathbb{C})$, consider now $g \in SU(2)$. Implementing the condition $g^\dagger = g^{-1}$ the previous expression becomes,

$$g = a\,|w\rangle\langle z| + b\,|w]\langle z| - \bar{b}\,|w\rangle[z| + \bar{a}\,|w][z|\,, \qquad \text{with} \quad |a|^2 + |b|^2 = 1. \tag{2.50}$$

There is the freedom to chose $b = 0$ and a such that $|a|^2 = 1$, in that way the general $g \in SU(2)$ transform in,

$$g = e^{i\frac{\phi_l}{2}}\,|w\rangle\langle z| + e^{-i\frac{\phi_l}{2}}\,|w][z|\,. \tag{2.51}$$

Vice-versa setting $a = 0$ and b s.t. $|b|^2 = 1$ it is possible to write an element of $SU(2)$ as

$$g = e^{i\frac{\phi_l}{2}}\,|w][z| - e^{-i\frac{\phi_l}{2}}\,|w\rangle[z|\,. \tag{2.52}$$

Here, two different spinors are used to parameterize an $SU(2)$ element. That is to represent a holonomy between two different spaces, the source and the target, allowing them to be expressed on different bases. However, the most general matrix of $SU(2)$ can

be written using a single spinor. Indeed, these objects have also the following properties [22],

$$|z\rangle\langle z| = \frac{\mathbb{I} - \vec{n}\cdot\vec{\sigma}}{2}, \qquad |z][z| = \frac{\mathbb{I} + \vec{n}\cdot\vec{\sigma}}{2}. \tag{2.53}$$

Considering the following parameterization of an element $g \in SU(2)$,

$$g = e^{i\frac{\phi}{2}} |z\rangle\langle z| + e^{-i\frac{\phi}{2}} |z][z|, \tag{2.54}$$

and using the previously mentioned properties:

$$\begin{aligned} g &= e^{i\frac{\phi}{2}} |z\rangle\langle z| + e^{-i\frac{\phi}{2}} |z][z|, \\ &= e^{i\frac{\phi}{2}} \frac{\mathbb{I} - \vec{n}\cdot\vec{\sigma}}{2} + e^{-i\frac{\phi}{2}} \frac{\mathbb{I} + \vec{n}\cdot\vec{\sigma}}{2}, \\ &= \mathbb{I}\cos\frac{\phi}{2} - i\vec{n}\cdot\vec{\sigma}\sin\frac{\phi}{2}, \\ &= e^{-i\frac{\phi}{2}\vec{n}\cdot\vec{\sigma}}. \end{aligned} \tag{2.55}$$

It is easy to notice that this is the usual $SU(2)$ representation in terms of the generators, a direction, and an angle.
Without going into much detail on this topic, which is covered exhaustively in [23], it is worth pointing out that there exists a map from the base of $L_2[SU(2)]$, denoted with $\{|j,m\rangle\}$ and the new one in terms of spinors, called $\{|jw\rangle\}$. Moreover, the space spanned by these base vectors is endowed with a Gaussian measure $d\mu(w)$.

The fundamental property of this representation is

$$\langle jw| D^{(j)}(g) |jw\rangle = \langle w| g |w\rangle^{2j}. \tag{2.56}$$

This is the essential difference when using the spinor representation of LQG. Whenever a trace of a general j-representation needs to be computed, it is possible to use the defining one and exponentiate the result to $2j$.

It will be shown how this construction can be applied to general coherent states; in particular, parametrization (2.52) will be used. The proper notation is also introduced here, abandoning the simplified version utilized in the former section. The holonomies are now written according to their source and target sapaces. When considering the parallel transport from node a to node b, the holonomy will be denoted with h_{ab}. The holonomies are, therefore, parametrized with two spinors: $|z_{ab}\rangle$ living at the source of the link and $|z_{ba}\rangle$ living at the target. Each boundary group element becomes

$$h_{ab} = e^{i\frac{\phi_{ab}}{2}} |z_{ba}]\langle z_{ab}| - e^{-i\frac{\phi_{ab}}{2}} |z_{ba}\rangle[z_{ab}|. \tag{2.57}$$

For simplicity, only the relevant parts of the states are considered, especially the ones concerning the character of the representation.
The goal is to compute $\chi^j(h_{ab}^\dagger\, g)$ in the base $\{|jw\rangle\}$, i.e.

$$\begin{aligned}\chi^j(h_{ab}^\dagger g) &= \int d\mu(w)\, \langle jw|\, D^{(j)}(h_{ab}^\dagger g)\, |jw\rangle\,, \\ &= \int d\mu(w)\, \langle w|\, h_{ab}^\dagger g\, |w\rangle^{2j}\,.\end{aligned} \tag{2.58}$$

Using the spinorial parametrization for h_{ab},

$$\begin{aligned}\langle w|\, h_{ab}^\dagger\; g\, |w\rangle &= \langle w|\left(e^{-i\frac{\phi_{ab}}{2}}\, |z_{ab}\rangle\, [z_{ba}| - e^{i\frac{\phi_{ab}}{2}}\, |z_{ab}]\, \langle z_{ba}|\right) g\, |w\rangle\,, \\ &= e^{-i\frac{\phi_{ab}}{2}}\, [z_{ba}|\, g\, |w\rangle\, \langle w|z_{ab}\rangle - e^{i\frac{\phi_{ab}}{2}}\, \langle z_{ba}|\, g\, |w\rangle\, \langle w|z_{ab}]\,.\end{aligned} \tag{2.59}$$

The second term can be neglected. This is because, even if not explicitly at the moment, the angle ϕ_{ab} will be complexified following the Thiemann method. The complexification consists of sending $\phi_{ab} \longrightarrow \phi_{ab} + it\eta$ where η represents the classical value of the area (length) where the coherent states are peaked. The semiclassical limit then is performed considering high values for the area (length) variable, i.e., $\eta \longrightarrow \infty$, and consequently, the second part of the former equation will be exponentially suppressed. It follows,

$$\langle w|\, h_{ab}^\dagger g\, |w\rangle \simeq e^{-i\frac{\phi_{ab}}{2}}\, [z_{ba}|\, g\, |w\rangle\, \langle w|z_{ab}\rangle\,. \tag{2.60}$$

Using the completeness of the basis $\{|w\rangle\}$ the character of the representation takes the form:

$$\begin{aligned}\chi^j(h_{ab}^\dagger g) &= \int d\mu(w)\left(e^{-i\frac{\phi_{ab}}{2}}\, [z_{ba}|\, g\, |w\rangle\, \langle w|z_{ab}\rangle\right)^{2j}, \\ &= e^{-i\phi_{ab}j}\, [z_{ba}|\, g\, |z_{ab}\rangle^{2j}\,, \\ &= e^{-i\phi_{ab}j} e^{2j\log[z_{ba}|g|z_{ab}\rangle}.\end{aligned} \tag{2.61}$$

The final coherent state in terms of the spinors becomes

$$\psi^t_{z_{ab},z_{ba}}(g) = \sum_{a<b}(2j_{ab}+1) e^{\frac{-t}{2}j_{ab}(j_{ab}+1)} e^{-i\phi_{ab}j_{ab}} e^{2j_{ab}\log[z_{ba}|g|z_{ab}\rangle}. \tag{2.62}$$

Keep in mind that this is not gauge invariant yet. However, the next section will clarify why it is still possible to work with it instead of the invariant one without changing the result.

Chapter 3

Semiclassical Dynamics

The semiclassical analysis is born from the necessity to link the quantum description with the classical one. Starting from the early development of quantum mechanics, it was necessary to settle this bridge. Niels Bohr, one of the founding fathers of QM, coined the *correspondence principle*, asking as a requirement that classical physics should be recovered in the limit of large quantum numbers. This work's construction of coherent states is attributable to this kind of computation.
Here, the focus is shifted to the semiclassical analysis of the dynamics. The semiclassical dynamics is what emerges from pure quantum mechanical computation when the limit $\hbar \to 0$ is taken. The motivation behind this limit is twofold. On the one hand, there is the correspondence with classical physics described above. On the other hand, there is a considerable simplification of the computations. This section will discuss and apply the saddle point approximation to the path integral calculation of the transition amplitude. In addition to the result of a general transition amplitude for the three-dimensional black-to-white hole model, an exciting feature of the coherent states in this approximation is also discussed.

3.1 Saddle point approximation

The saddle point approximation is a powerful tool widely used in physics to approximate integrals of the form

$$I = \int_a^b dx\ e^{Mf(x)}, \tag{3.1}$$

where the constant $M \gg 1$.
Let $f(x)$ be a twice-differentiable function, and suppose that there exists a maximum x_0. Using Taylor's theorem $f(x)$ can be expanded around x_0,

$$f(x) = f(x_0) + f'(x_0)(x - x_0) + \frac{1}{2}f''(x_0)(x - x_0)^2 + O((x - x_0)^3). \tag{3.2}$$

Being x_0 a stationary point, the first derivative vanishes; moreover, it is also a maximum. Therefore, the second derivative is negative due to the concavity of $f(x)$. The previous expression can be approximated with

$$f(x) \approx f(x_0) - \frac{1}{2}|f''(x_0)|(x - x_0)^2. \tag{3.3}$$

Plugging it back into the integral (3.1),

$$I = e^{Mf(x_0)} \int_a^b dx\ e^{-\frac{M}{2}|f''(x_0)|(x-x_0)^2} \tag{3.4}$$

If a and b were respectively $-\infty$ and $+\infty$, the result would have been straightforward since the remaining integral would have been an elementary Gaussian one. It is possible to show that the result is the same even if a and b are finite numbers. The only condition is $a < x_0 < b$ and to take the limit $M \to \infty$. Indeed, performing a change of the integration variable sending $M(x - x_0)^2 \to y^2$ the integral becomes,

$$I = \frac{e^{Mf(x_0)}}{\sqrt{M}} \int_{-\sqrt{M}|a-x_0|}^{\sqrt{M}(b-x_0)} dy\ e^{-\frac{1}{2}|f''(x_0)|y^2}. \tag{3.5}$$

Taking the limit $M \to +\infty$, the integral becomes Gaussian, and the final result is

$$I = \sqrt{\frac{2\pi}{M|f''(x_0)|}}\, e^{Mf(x_0)}. \tag{3.6}$$

This technique can be generalized to a more general form of integrand and for the multivariate case where $\mathbf{x}$ is a d-dimensional vector and $f(\mathbf{x})$ is a scalar function of $\mathbf{x}$. The result in this more general case is,

$$\int d\mathbf{x}\ h(\mathbf{x}) e^{Mf(\mathbf{x})} \approx \left(\frac{2\pi}{M}\right)^{d/2} \frac{h(\mathbf{x}_0) e^{Mf(\mathbf{x}_0)}}{|H_f(\mathbf{x}_0)|^{1/2}}, \qquad \text{where:} \quad M \to +\infty. \tag{3.7}$$

In the previous expression, H_f refers to the Hessian matrix computed at the critical point, and $|\cdot|$ is the determinant of the matrix. This approximation is extremely relevant in the context of quantum mechanics expressed in the path integral formulation [24]. As a matter of fact, the path integrals have the following form,

$$\mathcal{A} = \int \mathcal{D}[x] e^{\frac{i}{\hbar} S[x]}. \tag{3.8}$$

Remembering that the semiclassical limit is performed sending $\hbar \to 0$, the limit $M := \hbar^{-1} \to \infty$ is automatically defined. The result is

$$\mathcal{A} = \int_{x_0}^{x_1} \mathcal{D}[x] e^{iS[x]/\hbar} \approx \sqrt{\frac{i}{2\pi} \frac{\partial^2 S_H(x_c)}{\partial x_0 \partial x_1}}\, e^{iS_H(x_c)}. \tag{3.9}$$

There is a fundamental distinction to point out in this result. Inside the path integral is the action $S[x]$, a functional of the trajectories. In the result, $S_H(x_c)$ represents the Hamilton Principal function instead. In contrast, the Hamilton principal function, $S_H(x_c)$ is a function of the boundary data. The link between the two is the following: the Hamilton principal function is the action evaluated on the precise trajectory that dominates the path integral, namely in the classical path. This mathematical procedure has a very physical interpretation; by considering quantum mechanics in the semiclassical limit, the first-order result is the one classically expected. This is in perfect agreement with the correspondence principle.

3.2 Generic amplitude with coherent states

This section concerns a general feature of coherent states in the semiclassical limit. The resulting behavior of these states is fundamental and clarifies how their structure affects the final form of a general transition amplitude computed with saddle point techniques. Consider, not referring to a precise model, a completely generic action. In the current section, all the prefactors and multiplicative constants, as well as the Hessian matrices present in the amplitude, will be neglected. The focus is shifted to its exponential factors. Consider the coherent state of a free particle,

$$\psi^t_{q_j,p_j}(x_j) \propto e^{-\frac{1}{2\hbar t}(x_j-q_j)^2} e^{\frac{i}{\hbar}p_j(x_j-q_j)}. \tag{3.10}$$

The evolution of this state will be computed using a general action S. The final result in the semiclassical approximation will depend on a general Hamilton principal function, which will depend on the initial and final positions $S(x_1, x_2, E)$. Moreover, a fixed energy process is considered to prepare the stage for the black-to-white hole transition. With a slight abuse of notation, the action is also indicated here as $S(x_1, x_2, E)$. This is to simplify the notation in the next. The amplitude $\mathcal{A}$ is proportional to,

$$\begin{aligned}\mathcal{A} &\propto \int\int dx_1 dx_2 \left\langle \psi^t_{q_2,p_2} \right| e^{\frac{i}{\hbar}S(x_1,x_2,E)} \left| \psi^t_{q_1,p_1} \right\rangle, \\ &\propto \int\int dx_1 dx_2 \; e^{\frac{1}{\hbar}(-\frac{1}{2t}(x_1-q_1)^2+ip_1(x_1-q_1)+iS(x_1,x_2,E)-\frac{1}{2t}(x_2-q_2)^2-ip_2(x_2-q_2))}.\end{aligned} \tag{3.11}$$

Taking the limit $\hbar \to 0$ to pass into the semiclassical limit, the saddlepoint method's condition $M \to \infty$ is satisfied. The next step is to find the stationary point of the function at the exponent. Computing the first derivative and setting it to zero,

$$\begin{aligned} x_1^0 &= q_1 + it\left(p_1 + \frac{\partial S}{\partial x_1}\right), \\ x_2^0 &= q_2 - it\left(p_2 - \frac{\partial S}{\partial x_2}\right). \end{aligned} \tag{3.12}$$

These mathematically translate into the conditions:

$$x_1 = q_1, \quad x_2 = q_2, \quad p_1 = -\frac{\partial S}{\partial x_1} \quad \text{and} \quad p_2 = \frac{\partial S}{\partial x_2}. \tag{3.13}$$

This result is expected, as the derivatives of the Hamilton principal function with respect to the coordinates give the classical momentum. That means that the coherent states are peaked on the classical values. Instead of imposing these conditions directly, it is more interesting to Taylor expand the amplitude around these stationary points. The current form of the amplitude is,

$$A \propto e^{\frac{t}{2}(p_1+\frac{\partial S}{\partial x_1})^2} e^{\frac{t}{2}(p_2-\frac{\partial S}{\partial x_2})^2} e^{-p_1 t(p_1+\frac{\partial S}{\partial x_1})} e^{-p_2 t(p_2-\frac{\partial S}{\partial x_2})} e^{iS(x_1^0,x_2^0,E)}. \tag{3.14}$$

Now, a Taylor expansion in S is performed,

$$\begin{aligned} S(x_1^0, x_2^0, E) &= S(q_1 + it(p_1 + \partial S/\partial x_1), q_2 - it(p_2 - \partial S/\partial x_2), E), \\ &\approx S(q_1, q_2, E) + it(p_1 + \partial S/\partial x_1)\frac{\partial S}{\partial x_1} - it(p_2 - \partial S/\partial x_2)\frac{\partial S}{\partial x_2}. \end{aligned} \tag{3.15}$$

Plugging this inside the full expression for the amplitude leads to the interesting result:

$$A \propto e^{-\frac{t}{2\hbar}(p_1+\partial S/\partial x_1)^2} e^{-\frac{t}{2\hbar}(p_2-\partial S/\partial x_2)^2} e^{\frac{i}{\hbar}S(q_1,q_2,E)}. \tag{3.16}$$

This shows that coherent states produce a Gaussian suppression on the momenta. Moreover, the dynamic is governed by a classical trajectory. Grouping the momenta into a generic one p, the amplitude computed with the coherent states becomes:

$$\mathcal{A} = \left\langle A|\psi_{q,p}^t\right\rangle \propto e^{-\frac{t}{2\hbar}(p-p_{cl})^2} e^{\frac{i}{\hbar}S_{cl}}. \tag{3.17}$$

Discussing this structure piece by piece is interesting and of fundamental importance. This result is composed of two parts:

- The exponential of the Hamilton principal function $e^{\frac{i}{\hbar}S_{cl}}$ indicates what is, in the semiclassical analysis, the most significant contribution to the amplitude: the classical path.
- Inside the other exponential $e^{-\frac{t}{2\hbar}(p-p_{cl})^2}$, p represents the label of the coherent state and p_{cl} stays for the classical momentum. This term forces the momentum where the state is peaked to be equal to the one determined by the classical trajectory.

It is worth noting one detail of this fundamental result. Imagine neglecting the dynamics, which mathematically translates into setting in (3.17) $S = 0$. Since the classical momentum in the Hamilton formalism is the derivative of S it would also lead to $p_{cl} = 0$.

This amplitude, which without dynamics is just a kinematical property of the states, becomes

$$\mathcal{A}_{S=0} \propto e^{-\frac{t}{2\hbar}p^2}. \tag{3.18}$$

This is crucial in analyzing the major misconception of the black-to-white hole transition calculation in the LQG literature. This suppression has not to be confused with the one typical of tunneling phenomena; the trend with the squared momentum p^2 is a feature of coherent states.

3.3 Spin foam amplitude in saddle point

It is now the time to dive into the computation of the amplitude in detail. In section 1.4, we defined the form of the amplitude for the Ponzano-Regge spin foam model. The amplitude is

$$\mathcal{A}_\Delta = \mathcal{N} \prod_f (2j_f + 1) \prod_v \begin{Bmatrix} j_1 & j_2 & j_3 \\ j_4 & j_5 & j_6 \end{Bmatrix}_v . \tag{3.19}$$

This section focuses on computing the single vertex amplitude, combining this calculation with the structure of coherent states analyzed in section 2.2.2 and with the techniques developed in 3.1.

3.3.1 Vertex amplitude in terms of spinors

This section aims to compute the vertex amplitude's form when the spin network states are parameterized in terms of the spinors as described in section 2.3. The single spin foam vertex can be studied through its boundary spin network, as seen in section 1.4. Accordingly to (2.62), the coherent states, with the twisted geometry parametrization, have the form

$$\psi^t_{z_{ab}, z_{ba}}(g) = \sum_{a<b} (2j_{ab} + 1) e^{\frac{-t}{2} j_{ab}(j_{ab}+1)} e^{-i\phi_{ab} j_{ab}} e^{2j_{ab} \log[z_{ba}|g|z_{ab}\rangle}. \tag{3.20}$$

An important note has to be made. The attentive reader may object that these coherent states are the non-invariant ones (2.31) and not the (2.40). They would be right in saying this. However, this is not a problem since the amplitude with which the states are contracted is gauge invariant. Contracting the states (2.31) with a gauge invariant object automatically projects the result into the invariant space.

To compute the vertex amplitude A_v, the equation that imposes local flatness into the simplices of the triangulation must be solved. That is, performing the integral over the

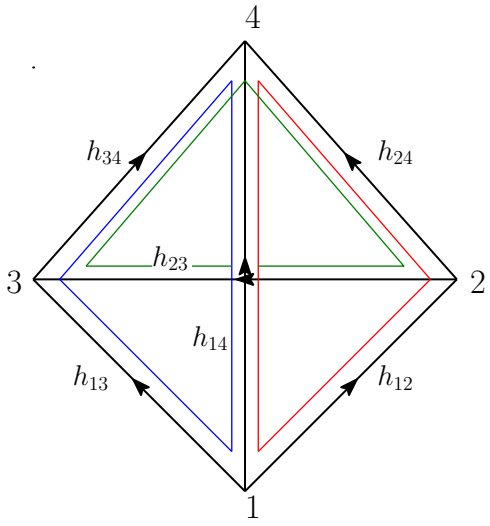

Figure 3.1: Boundary spin-network of a vertex. In red (δ_1), blue (δ_2) and green (δ_3) are depicted three fundamental cycles.

group elements and imposing it with the fundamental cycles (Figure 3.1),

$$A_v \propto \int \left(\prod_{a<b} dg_{ab}\ \psi^t_{z_{ab},z_{ba}}(g) \right) \delta_1(g_{24}\ g_{12}\ g_{14}^{-1}) \delta_2(g_{34}\ g_{13}\ g_{14}^{-1}) \delta_3(g_{34} g_{23} g_{24}^{-1}). \tag{3.21}$$

In total, there are six integrations, one for each wedge. The three delta functions "consume" three out of six. There are three other integrations to be solved using saddle point techniques. However, adding a fourth dummy integration is useful to symmetrize the system to always have the structure $g_b^{-1} g_a$. Indeed, the final form ready to be computed in saddle point is

$$A_v \propto \sum_{a<b} (2j_{ab}+1) e^{\frac{-t}{2} j_{ab}(j_{ab}+1)} e^{-i\phi_{ab} j_{ab}} \int \prod_{a<b} dg_{ab}\ e^{2j_{ab} \log[z_{ba}| g_b^{-1} g_a |z_{ab}\rangle}, \tag{3.22}$$

where $a, b = 1, .., 4$. At this stage, the analysis is restricted to the function at the exponent, i.e. the action,

$$S = \sum_{a<b} 2j_{ab} \log \left[z_{ba} \right| g_b^{-1} g_a \left| z_{ab} \right\rangle . \tag{3.23}$$

The critical point equation with respect to the group elements g_a has to be solved. This procedure is not as trivial as in the case of functional analysis since the derivatives are computed inside a non-abelian structure. Attention must be paid to the ordering and how the derivative acts on functions of $SU(2)$. In particular, deriving an abstract group element does not make sense; it is necessary to remember that a g_a is represented

through the exponential map. The exponential map contains factors that simplify and the generators of $SU(2)$: the Pauli matrices $\vec{\sigma}$. The derivative corresponds thus to an insertion of $\vec{\sigma}$. Consider the element g_1 as an example. The equation to be solved is,

$$\frac{\delta S}{\delta g_1} = \sum_{b>1} 2j_{1b} \frac{[z_{b1}| g_b^{-1} g_1 \vec{\sigma} |z_{1b}\rangle}{[z_{b1}| g_b^{-1} g_1 |z_{1b}\rangle} = 0. \tag{3.24}$$

Inserting now the resolution of the identity $\mathbb{I} = |z_{1b}\rangle \langle z_{1b}| + |z_{1b}] [z_{1b}|$ between the g's and the $\vec{\sigma}$, it gets transformed in,

$$\begin{aligned}
0 = \frac{\delta S}{\delta g_1} &= \sum_{b>1} 2j_{1b} \frac{[z_{b1}| g_b^{-1} g_1 (|z_{1b}\rangle \langle z_{1b}| + |z_{1b}] [z_{1b}|) \vec{\sigma} |z_{1b}\rangle}{[z_{b1}| g_b^{-1} g_1 |z_{1b}\rangle}, \\
&= \sum_{b>1} 2j_{1b} \frac{[z_{b1}| g_b^{-1} g_1 |z_{1b}\rangle \langle z_{1b}| \vec{\sigma} |z_{1b}\rangle}{[z_{b1}| g_b^{-1} g_1 |z_{1b}\rangle} + \sum_{b>1} 2j_{1b} \frac{[z_{b1}| g_b^{-1} g_1 |z_{1b}] [z_{1b}| \vec{\sigma} |z_{1b}\rangle}{[z_{b1}| g_b^{-1} g_1 |z_{1b}\rangle}, \\
&= \sum_{b>1} 2j_{1b} \langle z_{1b}| \vec{\sigma} |z_{1b}\rangle + \sum_{b>1} 2j_{1b} \frac{[z_{b1}| g_b^{-1} g_1 |z_{1b}]}{[z_{b1}| g_b^{-1} g_1 |z_{1b}\rangle} [z_{1b}| \vec{\sigma} |z_{1b}\rangle , \\
&= \sum_{b<1} \; -2 \; j_{1b} \vec{n}_{1b} + 2 \; j_{1b} c_{1b} (i\vec{F}_{1b} + \vec{n}_{1b} \times \vec{F}_{1b}).
\end{aligned} \tag{3.25}$$

The correspondences between spinors and framed reference frames has been used, i.e:

$$\langle z_{ab}| \vec{\sigma} |z_{ab}\rangle = -\vec{n}_{ab}, \qquad [z_{ab}| \vec{\sigma} |z_{ab}\rangle = i\vec{F}_{ab} + \vec{n}_{ab} \times \vec{F}_{ab}. \tag{3.26}$$

In general, there are two kinds of equations:

- If $a < b$

$$j_{ab} \langle z_{ab}| \vec{\sigma} |z_{ab}\rangle + j_{ab} \; c_{ab} [z_{ab}| \vec{\sigma} |z_{ab}\rangle = 0, \tag{3.27}$$

  where the complex coefficient c_{ab} has been defined as:

$$c_{ab} = \frac{[z_{ba}| g_b^{-1} g_a |z_{ab}]}{[z_{ba}| g_b^{-1} g_a |z_{ab}\rangle}. \tag{3.28}$$

- If $a > b$,

$$-j_{ab} [z_{ab}| \vec{\sigma} |z_{ab}] + j_{ab} \; c_{ba} [z_{ab}| \vec{\sigma} |z_{ab}\rangle = 0, \tag{3.29}$$

  where the coefficients c_{ba}, using the properties of spinors, are defined as:

$$c_{ba} = \frac{[z_{ab}| g_a^{-1} g_b |z_{ba}]}{[z_{ab}| g_a^{-1} g_b |z_{ba}\rangle} = -\frac{\langle z_{ba}| g_b^{-1} g_a |z_{ab}\rangle}{[z_{ba}| g_b^{-1} g_a |z_{ab}\rangle}. \tag{3.30}$$

It is possible to write the general compact form of the variation with respect to the element g_a:

$$\frac{\delta S}{\delta g_a} = 0 \quad \longrightarrow \quad -\sum_{b\neq a} j_{ab}\vec{n}_{ab} \; + \; \sum_{b\neq a} j_{ab}c_{ab}(i\vec{F}_{ab} + \vec{n}_{ab} \times \vec{F}_{ab}) = 0. \tag{3.31}$$

It is now assumed that the only possible solution to this equation is to have together:

$$\sum_{b\neq a} j_{ab}\vec{n}_{ab} = 0, \tag{3.32}$$

$$c_{ab} = 0, \tag{3.33}$$

both of them $\forall a, b$.

These two contain different information on the system. This information has to be extracted by solving both of the equations. It is convenient to start from the closure condition (3.32) and consider the variation of g_1 again as an example.

$$\begin{aligned} \frac{\delta S}{\delta g_1} = 0 &\longrightarrow j_{12} \langle z_{12}| \vec{\sigma} |z_{12}\rangle + j_{14} \langle z_{14}| \vec{\sigma} |z_{14}\rangle + j_{13} \langle z_{13}| \vec{\sigma} |z_{13}\rangle = 0, \\ &\longrightarrow -j_{12}\vec{n}_{12} - j_{13}\vec{n}_{13} - j_{14}\vec{n}_{14} = 0, \end{aligned} \tag{3.34}$$

Contracting the whole expression with the three normal vectors, and after some algebra, a system of three equations with three unknowns is obtained,

$$\begin{cases} \Delta_{432} = j_{14}S_{24} + j_{13}S_{23}, \\ \Delta_{243} = j_{12}S_{23} + j_{14}S_{34}, \\ \Delta_{234} = j_{13}S_{34} + j_{12}S_{24}. \end{cases} \tag{3.35}$$

In order not to make the notation too cruel, the variables represent respectively,

$$\Delta_{abc} := \frac{1}{2}(j_{1a} + j_{1b} - j_{1c}), \quad \text{and} \quad S_{ab} := |\langle z_{1a}|z_{1b}\rangle|^2. \tag{3.36}$$

The values of the three S_{ab} can be found by solving this system. Considering S_{34}, for example, the norm of the spinors is completely defined by the lengths j_{ab},

$$S_{34} = |\langle z_{13}|z_{14}\rangle|^2 = \frac{j_{12}^2 - (j_{13} - j_{14})^2}{4j_{13}j_{14}}. \tag{3.37}$$

This result can be generalized. Remember that in three dimensions, each node of the spin network identifies a triangle, and each link is dual to a length of the latter.

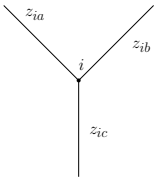

Therefore considering that in each three-valent node (i) three spinors (z_{ia}, z_{ib}, z_{ic}) meet, the norm of the spinors should have the precise form:

$$|\langle z_{ia}|z_{ib}\rangle|^2 = \frac{j_{ic}^2 - (j_{ia} - j_{ib})^2}{4j_{ia}j_{ib}}. \tag{3.38}$$

This ensures that the triangle satisfies the triangle inequalities and effectively closes. This purely geometric information is encoded directly inside the triangles' closures.

It is time to analyze what is hidden inside (3.33). Recalling the form of the coefficients c_{ab} and c_{ba},

$$\begin{aligned} c_{ab} &= \frac{[z_{ba}|\, g_b^{-1} g_a\, |z_{ab}]}{[z_{ba}|\, g_b^{-1} g_a\, |z_{ab}\rangle}, \\ c_{ba} &= -\frac{\langle z_{ba}|\, g_b^{-1} g_a\, |z_{ab}\rangle}{[z_{ba}|\, g_b^{-1} g_a\, |z_{ba}\rangle}. \end{aligned} \tag{3.39}$$

Finding a solution to these equations means selecting the right form of the elements $g_b^{-1}g_a$. These are two different variables. However, it is easier to work considering them as a single $SU(2)$ element g_{ba}; this, in terms of parallel transports, translates into working with wedges. As studied in section 2.3 spinors can parametrize elements of $SU(2)$. The most general one in terms of two spinors z_{ab} and z_{ba} is,

$$g_b^{-1}g_a = a\,|z_{ba}\rangle\,\langle z_{ab}| + b\,|z_{ba}]\,\langle z_{ab}| - b^\star\,|z_{ba}\rangle\,[z_{ab}| + a^\star\,|z_{ba}]\,[z_{ab}|\,, \tag{3.40}$$

where a and b are complex coefficients satisfying $|a|^2+|b|^2 = 1$. Plugging this form inside the equations $c_{ab} = 0$ and $c_{ba} = 0$ lead to $a = 0$ and $a^\star = 0$, therefore,

$$g_b^{-1}g_a = b\,|z_{ba}]\,\langle z_{ab}| - b^\star\,|z_{ba}\rangle\,[z_{ab}|\,, \tag{3.41}$$

with $|b|^2 = 1$. This coefficient turns out to be just a phase. The final form of the wedge holonomy becomes,

$$g_b^{-1}g_a = e^{i\frac{w_{ab}}{2}}\,|z_{ba}]\,\langle z_{ab}| - e^{-i\frac{w_{ab}}{2}}\,|z_{ba}\rangle\,[z_{ab}|\,. \tag{3.42}$$

It is easy to find the set of equations that this parametrization defines just by contracting it with the proper spinor, namely,

$$\begin{cases} g_b^{-1}g_a\,|z_{ab}\rangle = e^{i\frac{w_{ab}}{2}}\,|z_{ba}]\,, \\ g_b^{-1}g_a\,|z_{ab}] = -e^{-i\frac{w_{ab}}{2}}\,|z_{ba}]\,. \end{cases} \tag{3.43}$$

Together with the equation (3.38), these form the set of equations that must be solved. All of the information contained in the first part of the saddle point analysis has been extracted. The remaining part is effectively to *solve* the integrals.

The local flatness demanded by the very definition of the model has to be imposed. Again, the simplest way of doing this is through the fundamental cycles. Isolating the wedge holonomy from the local flatness condition

$$\mathbb{I} = g_{ab} g_{ca} g_{bc}^{-1} \longrightarrow g_{ab}^{-1} = g_{ca} g_{bc}. \tag{3.44}$$

This is a matrix equation. However, it is easier to work with scalar equations, choosing particular matrix elements,

$$\begin{cases} [z_{ac}|\, g_{ab}^{-1}\, |z_{bc}\rangle = [z_{av}|\, g_{ca} g_{bc}\, |z_{bc}\rangle\,, \\ \langle z_{ac}|\, g_{ab}^{-1}\, |z_{bc}] = \langle z_{ac}|\, g_{ac} g_{bc}\, |z_{bc}]\,. \end{cases} \tag{3.45}$$

In order to isolate the angle w_{ab}, the explicit form (3.42) can be inserted, resulting in

$$\begin{cases} e^{-i\frac{w_{ab}}{2}}\, [z_{ac}|z_{ab}\rangle\, [z_{ba}|z_{bc}\rangle - e^{i\frac{w_{ab}}{2}}\, [z_{ac}|z_{ab}]\, \langle z_{ba}|z_{bc}\rangle = e^{i\frac{(w_{ca}+w_{bc})}{2}}\, \langle z_{ca}|z_{cb}]\,, \\ e^{-i\frac{w_{ab}}{2}}\, \langle z_{ac}|z_{ab}\rangle\, [z_{ba}|z_{bc}] - e^{i\frac{w_{ab}}{2}}\, \langle z_{ac}|z_{ab}]\, \langle z_{ba}|z_{bc}] = e^{-i\frac{(w_{ca}+w_{bc})}{2}}\, [z_{ca}|z_{cb}\rangle\,. \end{cases} \tag{3.46}$$

Then, taking the term-by-term multiplication of these two equations,

$$\begin{aligned} & e^{iw_{ab}}\, \langle z_{ac}|z_{ab}]\, \langle z_{ba}|z_{bc}]\, [z_{ac}|z_{ab}]\, \langle z_{ba}|z_{bc}\rangle + e^{-iw_{ab}}\, \langle z_{ac}|z_{ab}\rangle\, [z_{ba}|z_{bc}]\, [z_{ac}|z_{ab}\rangle\, [z_{ba}|z_{bc}\rangle + \\ & - [z_{ac}|z_{ab}]\, \langle z_{ba}|z_{bc}\rangle\, \langle z_{ac}|z_{ab}\rangle\, [z_{ba}|z_{bc}] - [z_{ac}|z_{ab}\rangle\, [z_{ba}|z_{bc}\rangle\, \langle z_{ac}|z_{ab}]\, \langle z_{ba}|z_{bc}] \\ & = \langle z_{ca}|z_{cb}]\, [z_{ca}|z_{cb}\rangle\,. \end{aligned} \tag{3.47}$$

Notice that the first two terms are one the complex conjugate of the other; It is thus possible to write them as a norm plus a common phase. Manipulating the remaining part of the equation using the properties of spinors, the angle w_{ab} can be isolated,

$$\cos(w_{ab} + \xi_{ab}^c) = \frac{-\,|\,[z_{ca}|z_{cb}\rangle\,|^2 + |\,\langle z_{ba}|z_{bc}\rangle\,|^2 |\,\langle z_{ac}|z_{ab}\rangle\,|^2 + |\,[z_{ac}|z_{ab}\rangle\,|^2 |\,[z_{ba}|z_{bc}\rangle\,|^2}{2|\,\langle z_{ac}|z_{ab}\rangle\, [z_{ba}|z_{bc}]\, [z_{ac}|z_{ab}\rangle\, [z_{ba}|z_{bc}\rangle\,|}, \tag{3.48}$$

where it has been introduced the so-called *twist angle* ξ_{ab}^c. This angle depends explicitly on the phase of spinors and represents the misalignment of the frames,

$$\xi_{ab}^c = \arg\left(\frac{[z_{ac}|z_{ab}\rangle\, \langle z_{ab}|z_{ac}\rangle}{\langle z_{bc}|z_{ba}\rangle\, [z_{ba}|z_{bc}\rangle} \right). \tag{3.49}$$

Recalling that,

$$\begin{gathered} |\,\langle z_{ab}|z_{ac}\rangle\,|^2 = \frac{1+\cos\phi_{bc}^a}{2}\,, \qquad |\,[z_{ab}|z_{ac}\rangle\,|^2 = \frac{1-\cos\phi_{bc}^a}{2}\,, \\ 2|\,[z_{ab}|z_{ac}]\, \langle z_{ab}|z_{ac}\rangle\,| = 2\sin\phi_{bc}^a\,, \end{gathered} \tag{3.50}$$

the equation (3.48) is completely expressed in terms of angles. The crucial part is that up to now, the phase w_{ab} was totally arbitrary. Still, by virtue of (3.48) united with (3.38), the angle is fully determined by the lengths of the triangles.

$$\cos(w_{ab} + \xi^c_{ab}) = \frac{\cos\phi^c_{ab} + \cos\phi^a_{bc}\cos\phi^b_{ac}}{\sin\phi^a_{bc}\sin\phi^b_{ac}}. \tag{3.51}$$

To find the equivalent equations for w_{ca} and w_{bc}, it is sufficient to repeat the calculation isolating g_{ca} and g_{bc} in (3.44). Now, using the *spherical cosine laws*, the right-hand side of (3.51) can be written as the cosine of a single three-dimensional angle $\hat{\theta^c_{ab}}$. The spherical cosine laws relate precisely three angles of dimension N with one single angle of dimension $N+1$. Therefore,

$$\cos(w_{ab} + \xi^c_{ab}) = \cos(\hat{\theta^c_{ab}}). \tag{3.52}$$

Time should be spent on the notation being used. As depicted in figure 3.2, the angles of the type ϕ^a_{bc} refer to the external plane angle sitting on the triangle a formed with the other two triangles b and c.

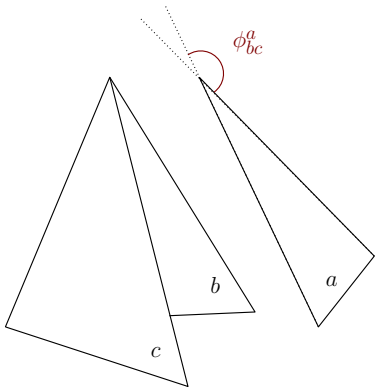

Figure 3.2: With ϕ^a_{bc} the external plane angle on the triangle a, and formed with the other two triangles b and c is unambiguously identified.

With $\hat{\theta^c_{ab}}$, written with the hat to stress the difference again, it is indicated as the three-dimensional external angle. The index on the top refers to the triangle opposite the considered edge. The two low indices, as before, specify the other triangles.

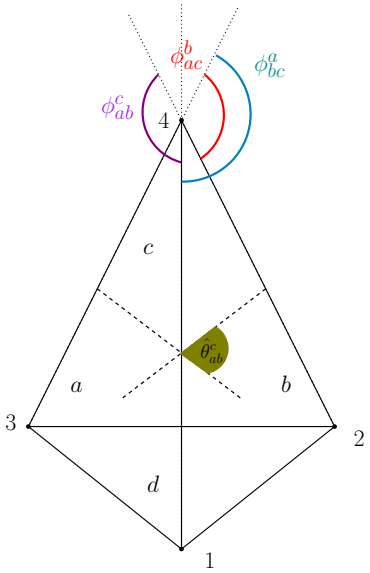

Figure 3.3: Visual representation of the Spherical Cosine Laws. Starting from three plane angle, in the figure ϕ^a_{bc},ϕ^b_{ac},ϕ^c_{ba} it is possible to reconstruct the three dimensional one $\hat{\theta}^c_{ab}$.

The following step will be to prove that by choosing a proper gauge for the orientation of the plane frames, it is always possible to reduce to the case in which ξ^c_{ab} the *twist angle* is zero.
Using that gauge in which the twist angle is equal to zero (extension to generical ξ^c_{ab} is a bit more laborious but possible), the following equality holds,

$$\cos(w_{ab}) = \cos(\hat{\theta^c_{ab}}) \implies w_{ab} = \epsilon\hat{\theta^c_{ab}}, \quad \text{where} \quad \epsilon = \pm 1. \tag{3.53}$$

This is exactly the desired condition on angles. Indeed w_{ab} at first was an arbitrary angle derived from the parameterizations of the SU(2) group; now, however, this angle has a direct connection with the lengths of the triangles. In fact, it is important to remember that $\hat{\theta^c_{ab}} = \hat{\theta}^c_{ab}(j_{ab})$. Putting on-shell the equations in this context means precisely having angles determined by the system's geometry. Finding how the action is transformed once evaluated on these extremal trajectories is immediate. Actually, it is sufficient to plug the following form of the group elements into the action,

$$g_b^{-1} g_a = e^{i\frac{\epsilon\hat{\theta^c_{ab}}(j_{ab})}{2}} |z_{ba}] \langle z_{ab}| - e^{-i\frac{\epsilon\hat{\theta^c_{ab}}(j_{ab})}{2}} |z_{ba}\rangle [z_{ab}| \,. \tag{3.54}$$

The action had the form,

$$S = \sum_{a<b} 2j_{ab} \log [z_{ba}| \, g_b^{-1} g_a \, |z_{ab}\rangle \,, \tag{3.55}$$

and therefore it becames,

$$\begin{aligned} S &= \sum_{a<b} 2j_{ab} \log \left[z_{ba}\right| \left(e^{i\frac{\epsilon \hat{\theta}^c_{ab}(j_{ab})}{2}} \left|z_{ba}\right] \left\langle z_{ab}\right| - e^{-i\frac{\epsilon \hat{\theta}^c_{ab}(j_{ab})}{2}} \left|z_{ba}\right\rangle \left[z_{ab}\right| \right) \left|z_{ab}\right\rangle , \\ &= i\ \epsilon\ \sum_{a<b} j_{ab} \hat{\theta}^c_{ab}(j_{ab}), \quad \text{where } \epsilon = \pm 1. \end{aligned} \tag{3.56}$$

This is the Regge action. The desired result has been obtained. To complete this first saddle point analysis, the Hessian matrix coming from this procedure remains to be discussed. The ϵ is a direct consequence of the structure of GR expressed in terms of tetrads instead of being expressed in the metric formalism. This also occurs in many other situations in quantum mechanics; the same behavior can be seen in free particle action. Since the framework is the path integral formulation of the quantum theory, both possible signs must be considered, which coincide with two opposite configurations of our tetrahedron. Roughly speaking, it is as considering the evolution of space and of "anti-space".

After the saddle point on the group element, the form of the transition amplitude is the following,

$$A_v \simeq \sum_{\epsilon=\pm 1} \sum_{j_{ab}} \prod_{ab} \mathcal{N}(j_{ab})(2j_{ab}+1) e^{\frac{-t}{2} j_{ab}(j_{ab}+1)} e^{-i\phi_{ab} j_{ab}} e^{i\epsilon j_{ab}\theta(j_{ab})}. \tag{3.57}$$

The normalization constant in this notation, depending on j_{ab}, is for reminding that inside it, the Hessian matrix is also incorporated.

3.3.2 Twist angle = 0

A gauge exists in which the twist angle is identically zero; Orient the frame vectors along the side of the triangles. The expression of the twist angle can be rewritten using the properties of spinors,

$$\begin{aligned} \xi^c_{ab} &= \arg\left(\frac{\left[z_{ac}|z_{ab}\right\rangle \left\langle z_{ab}|z_{ac}\right\rangle}{\left\langle z_{bc}|z_{ba}\right\rangle \left[z_{ba}|z_{bc}\right\rangle} \right), \\ &= \arg\left(\frac{\vec{n}_{ac} \cdot \left\langle z_{ab}\right| \vec{\sigma} \left|z_{ab}\right]}{\vec{n}_{bc} \cdot \left[z_{ba}\right| \vec{\sigma} \left|z_{ba}\right\rangle} \right), \\ &= \arg\left(-\frac{\vec{n}_{ac} \cdot \vec{F}_{ab}}{\vec{n}_{bc} \cdot \vec{F}_{ba}} \right). \end{aligned} \tag{3.58}$$

The discussion is about angles. Therefore, ξ, which is the argument of a real number, can be of two types. Consider a real number A. This can be positive or negative; thus:

(i) $A = A\ e^{i0} \implies \xi^c_{ab} = 0,$

(ii) $-A = A\ e^{i\pi} \implies \xi^c_{ab} = \pi.$

The following geometrical construction is handy to prove that this angle is always zero.

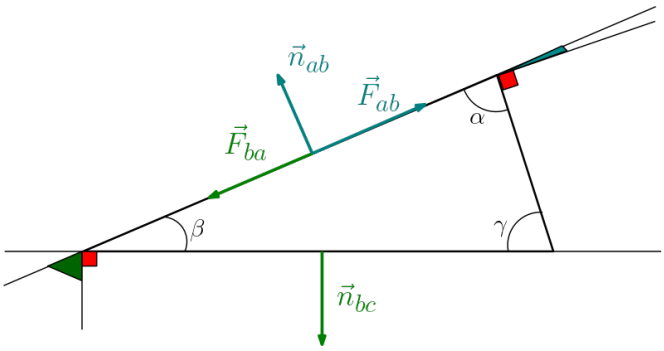

The numerator is represented by the cosine of the angle denoted in blue, i.e.

$$\vec{F}_{ab} \cdot \vec{n}_{ac} = \cos\left(\frac{\pi}{2} - \alpha\right), \tag{3.59}$$

and this number is positive iff $0 \leq \alpha \leq \frac{\pi}{2}$. The denominator in the picture is in green and has the form,

$$\vec{F}_{ba} \cdot \vec{n}_{bc} = \cos\left(\frac{\pi}{2} - \beta\right), \tag{3.60}$$

and the condition for this to be positive is $0 \leq \beta \leq \frac{\pi}{2}$. Consequently, the ratio between the two scalar products is negative if one of the two angles is obtuse and the other is acute. However, looking at the structure in three dimensions is illuminating.

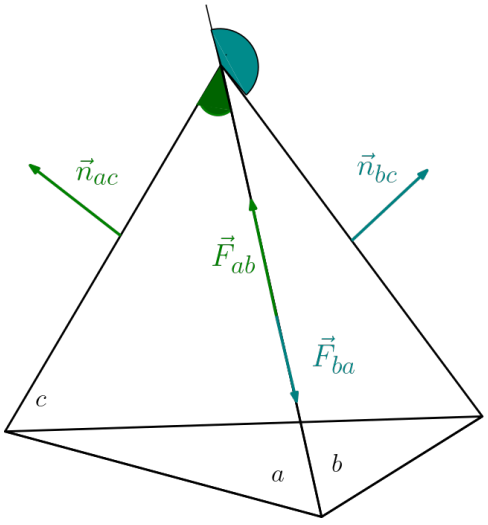

The green angle is acute, so the scalar product between the normal and the frame vector is greater than zero. However, contracting the second normal vector $\vec{n}_{bc}$ with $\vec{F}_{ba}$, which is $-\vec{F}_{ab}$, then it means considering the external angle. If the green angle had been obtuse, the blue one would have been acute as a consequence. This translates into the fact that

$$-\frac{\vec{n}_{ac}\cdot\vec{F}_{ab}}{\vec{n}_{bc}\cdot\vec{F}_{ba}}>0. \tag{3.61}$$

Consequently, being the twist angle the argument of a positive number, it vanishes.

Complexification of the variables

The time has come to complexify the variables. At this point, the saddle point approximation must be applied a second time, and the complexification needs to be performed. This is because the j_0 parameter of the complexification will play the role of the large parameter M of the method described in section 3.1. The complexification is performed wisely,

$$\phi_{ab}\longrightarrow\phi_{ab}=\phi_{ab}+it\left(j_0+\frac{1}{2}\right). \tag{3.62}$$

The $1/2$ obtains the Gaussian factor typical of coherent states. With the addition of some phase factors that can be reabsorbed inside the normalization constant, the amplitude takes the form

$$A_v\simeq\sum_{\epsilon=\pm1}\sum_{j_{ab}}\prod_{ab}\mathcal{N}(j_{ab})(2j_{ab}+1)e^{-\frac{t}{2}(j_{ab}-j_0)^2}e^{-i\phi_{ab}j_{ab}}e^{i\epsilon j_{ab}\theta(j_{ab})}. \tag{3.63}$$

Lastly, inside $\mathcal{N}$ there are numerical factors and the determinant of the Hessian matrix from the previous analysis. However, the Hessian $H_g(j_{ab})$ still depends on the lengths; for that reason, it is indicated as $\mathcal{N}(j_{ab})$. Next, the pure numerical factor will be divided from the terms depending on j_{ab}. For practical reasons, it is also renamed the function $\epsilon j_{ab}\theta(j_{ab}):=\Omega(j_{ab})$; this latter has the property to be a homogeneous function of degree one. Furthermore, it is added another phase $e^{i\phi_{ab}j_0}$ reabsorbing it inside $\mathcal{N}(j_{ab})$. The addition of this phase term is significant and comes from considering the symplectic structure already discussed in constructing the free particle's coherent states. The new, equivalent form of the amplitude is,

$$A_v\simeq\sum_{\epsilon=\pm1}\sum_{j_{ab}}\prod_{ab}\mathcal{N}(j_{ab})(2j_{ab}+1)e^{-\frac{t}{2}(j_{ab}-j_0)^2}e^{-i\phi_{ab}(j_{ab}-j_0)}e^{i\Omega(j_{ab})}. \tag{3.64}$$

3.3.3 Summation Saddle Point

The goal is to compute the summation using the saddle point approximation. This time, it is necessary to use a slightly modified technique. To get a guideline on the problem,

the modified saddle point is first applied to the following toy integral,

$$I = \int d\vec{x}\ h(\vec{x})\ e^{-\frac{1}{2}(\vec{x}-\vec{\mu})^2} e^{-i\vec{p}\cdot(\vec{x}-\vec{\mu})} e^{i\Omega(\vec{x})}. \tag{3.65}$$

In this integral, what will play the role of the parameter $M \gg 1$ is $\vec{\mu}$; thus, the first step is to isolate it. Remembering that it is a vector, it will be written as $\vec{\mu} = \mu\hat{\mu}$ where μ is a n-tuple of numbers where n is the dimension of the vector space and $\hat{\mu}$ is the vector of unit directions. Remember the homogeneity properties of $\Omega(\vec{x})$. The integral can be recast as

$$I = \int d\vec{x}\ h(\vec{x})\ e^{\mu[-\frac{\mu}{2}(\frac{\vec{x}}{\mu}-\hat{\mu})^2 - i\vec{p}\cdot(\frac{\vec{x}}{\mu}-\hat{\mu}) + \frac{i}{\mu}\Omega(\vec{x})]}. \tag{3.66}$$

Now it is performed a change of integration variable, defining $\vec{\xi} := \frac{\vec{x}}{\mu}$ the integral becomes,

$$I = \int d\vec{\xi}\ \mu\ h(\mu\vec{\xi})\ e^{\mu[-\frac{\mu}{2}(\vec{\xi}-\hat{\mu})^2 - i\vec{p}\cdot(\vec{\xi}-\hat{\mu}) + \frac{i}{\mu}\Omega(\mu\vec{\xi})]}. \tag{3.67}$$

Focusing on the term at the exponent, this is exactly the equivalent, but in n-dimensions, to the function $f(x)$ in (3.1), i.e.

$$F(\vec{\xi}) = -\frac{\mu}{2}(\vec{\xi}-\hat{\mu})^2 - i\vec{p}\cdot(\vec{\xi}-\hat{\mu}) + i\Omega(\vec{\xi}). \tag{3.68}$$

In the last term, it has been used the homogeneity property of $\Omega(\vec{\xi}) = \frac{1}{\mu}\Omega(\mu\vec{\xi})$. As usual, the maximum of this function has to be found. To find the critical point is made an ansatz on its form, and then solved for the unknown function $\vec{C}$,

$$\vec{\xi_0} = \hat{\mu} + \frac{\vec{C}}{\mu}. \tag{3.69}$$

By considering $F'(\vec{\xi_0}) = 0$, it is possible to find:

$$\vec{\xi_0} = \hat{\mu} + i\frac{(\vec{p} + \Omega'(\hat{\mu}))}{\mu}. \tag{3.70}$$

The time has come to use the classical procedures for the saddle point approximation, expanding the $F(\vec{\xi})$ function. At the end, calling $M(\mu)$ the matrix $\mathbb{I} + i\Omega''(\vec{\mu})$, the final result of this toy model integral is,

$$I \approx \left(\frac{2\pi}{\det(M(\vec{\mu}))}\right)^{\frac{n}{2}} h(\vec{\mu}) e^{-\frac{1}{2}(\vec{p}+\Omega'(\vec{\mu}))^2 + i\Omega(\vec{\mu})}. \tag{3.71}$$

This saddle point behaves similarly to the usual one once the large parameter M is well isolated. It can be applied to the summation, expecting a result similar to that with

the integration but with corrections due to the discretization of the sum. Returning to (3.64), the role of the large parameter $\vec{\mu}$ is played by the length j_0, which is written as l to not burden the notation too much. The form of the amplitude is

$$A_v \simeq \sum_{\epsilon=\pm 1} \sum_{j_{ab}} \prod_{ab} \mathcal{N}(j_{ab})(2j_{ab}+1) e^{l_{ab}(-\frac{l_{ab}}{2}(\frac{j_{ab}}{l_{ab}}-\hat{l}_{ab})^2 - i\phi_{ab}(\frac{j_{ab}}{l_{ab}}-\hat{l}_{ab}) + i\frac{\Omega(j_{ab})}{l_{ab}})}. \tag{3.72}$$

This is a (huge) high-dimensional summation, and the notation $\hat{l_{ab}}$ means that in each sum, are collected the relative maxima. This is the equivalent of the versors $\hat{\mu}$ in the toy integral above. Moreover, j_{ab}/l_{ab} is the ratio between the variable j_{ab} and the relative maximum l_{ab} of the considered link.

Defining the new set of variables $j^{\xi}_{ab} = \frac{j_{ab}}{l_{ab}}$, and rescaling the sum,

$$A_v \simeq \sum_{\epsilon=\pm 1} \sum_{j^{\xi}_{ab}} \prod_{ab} \mathcal{N}(j^{\xi}_{ab} l_{ab})(2j^{\xi}_{ab} l_{ab}+1) e^{l_{ab}(-\frac{l_{ab}}{2}(j^{\xi}_{ab}-\hat{l}_{ab})^2 - i\phi_{ab}(j^{\xi}_{ab}-\hat{l}_{ab}) + i\Omega(j^{\xi}_{ab}))}. \tag{3.73}$$

The same form of the ansatz used in the toy integral becomes,

$$j^{\xi_0}_{ab} = \hat{l}_{ab} - \frac{i}{l_{ab}}(\phi_{ab} - \partial_a \Omega(l_{ab})), \tag{3.74}$$

where $\partial_a \Omega(l_{ab})$ is the gradient of Ω. As usual, the function at the exponent has to be evaluated at the maximum. The conditions are,

$$\begin{aligned} F(j^{\xi_0}_{ab}) &= -\frac{1}{2\gamma_{ab}}(\phi_{ab} - \partial_a \Omega(l_{ab}))^2 + \frac{i}{\gamma_{ab}}\Omega(l_{ab}), \\ \partial_a \partial^b F(j^{\xi_0}_{ab}) &= -l_{ab}(\mathbb{I} - \partial_a \partial^b \Omega(l_{ab})), \end{aligned} \tag{3.75}$$

It is important to remember that all these calculations consider both Ω homogeneity and a truncated Taylor expansion to first order in $1/l_{ab}$. Plugging everything back again, after some algebraic passage, the result is,

$$\begin{aligned} A_v \simeq \sum_{\epsilon=\pm 1} \prod_{ab} \mathcal{N}(l_{ab})(2l_{ab}+1) e^{-\frac{1}{2}(\phi_{ab} - \partial_a \Omega(l_{ab}))^2} e^{i\Omega(l_{ab})} \\ \times \sum_{j_{ab}} e^{-\frac{1}{2}(j_{ab}-l_{ab})^T (\mathbb{I} - i\partial_a \partial^b \Omega(l_{ab}))(j_{ab}-l_{ab})}, \end{aligned} \tag{3.76}$$

where the $(j_{ab} - l_{ab})^T$ indicates the transposed vector of $(j_{ab} - l_{ab})$. Performing the change of variables $J_{ab} = j_{ab} - l_{ab}$ in the last term, and making explicit the extremes of the summation (once rescaled),

$$\sum_{J_{ab}=-l_{ab}}^{+\infty} e^{-\frac{1}{2}\ J^T_{ab}(\mathbb{I} - i\partial_a \partial^b \Omega(l_{ab}))J_{ab}} \tag{3.77}$$

Extending the sum from $-\infty$ to $+\infty$ is still a good approximation. Indeed, the added terms are very strongly and exponentially suppressed. Performing this extension, the above sum fits the definition of the *Riemann–Siegel theta function*, which is the multi-dimensional generalization of the *Jacobi theta function*. The final result is:

$$A_v \simeq \prod_{ab} \mathcal{N}(l_{ab})(2l_{ab}+1)e^{-\frac{1}{2}(\phi_{ab}-\partial_a\Omega(l_{ab}))^2}e^{i\Omega(l_{ab})} \;\; \Theta(0|\frac{i}{2\pi}(\mathbb{I}-i\partial_a\partial^b\Omega(l_{ab}))\;. \tag{3.78}$$

Discrete Gaussian distribution and Jacobi θ-functions

A brief analysis of the $\Theta(0|\frac{i}{2\pi}(\mathbb{I}-i\partial_a\partial^b\Omega(l_{ab}))$ function is needed.
The Riemann theta function $\Theta(z|\tau)$ is typically defined for a vector of complex variables $z\in\mathbb{C}^g$ and a symmetric, positive-definite matrix τ with positive imaginary part in $\mathbb{C}^{g\times g}$. Its definition is:

$$\Theta(z|\tau)=\sum_{n\in\mathcal{Z}^g} e^{2\pi i(\frac{1}{2}n^T\tau n+n^Tz)}. \tag{3.79}$$

Note that considering $z=0$ and a one-dimensional space, i.e., $g=1$ this function transforms exactly in the 3-Jacobi Theta function,

$$\Theta(0|\tau) \quad\longrightarrow\quad \theta_3(0|\tau)=\sum_{n\in\mathcal{Z}} e^{\pi i n^2\tau}, \tag{3.80}$$

where again $\tau=\frac{i}{2\pi}(\mathbb{I}-i\partial_b\partial^a l_{ab}\theta(l_{ab}))$. It has been proved [25] that it is possible to parametrize a discrete Gaussian distribution as follows,

$$J(q)U(q,p)=\sum_{n=-\infty}^{\infty} q^{\frac{(n-p)^2}{2}}. \tag{3.81}$$

Here,

$$J(q)=\sqrt{\frac{2\pi}{\ln(q^{-1})}}, \tag{3.82}$$

and there is a bound for $U(q,p)$,

$$|U(q,p)-1|\leq\frac{2\exp(-2\pi^2/\ln(1/q))}{1-\exp(-6\pi^2/\ln(1/q))}\;. \tag{3.83}$$

If the RHS of the previous inequality is sufficiently low, this result indicates that it is possible to approximate a Gaussian summation with the Gaussian integral. Geometrically, the difference between a Gaussian integral and a sum is that the second has an oscillating term that depends on the discretization. Suppose the steps of the discretization are sufficiently small in terms of the width of the distribution. In that case, the oscillating term is negligible, and the result is approximately the one of the integration.

In the case under study, in one dimension, (3.80) can be recast in the following form,

$$J(q_\tau)U(q_\tau,0) = \sum_n q_\tau^{\frac{n^2}{2}} \quad \text{where } q = e^{2\pi i\tau} = e^{-(1-i\partial^2 l_{ab}\theta(l_{ab}))} \ . \tag{3.84}$$

The result is,

$$J(q_\tau) = \sqrt{\frac{2\pi}{(1-i\partial^2 l_{ab}\theta(l_{ab}))}} \ . \tag{3.85}$$

To estimate the bound, it is sufficient to notice that the second derivative of the Regge action (the Hessian in the multidimensional case) from dimensional analysis scales as length to the minus one (l^{-1}). Taking the semiclassical limit then will suppress that part and $|U(q_\tau,0)-1| \leq 5\cdot 10^{-9}$.

In the following, these results will be considered valid also in the multidimensional case, so the sum (3.77) will be approximated with

$$I = \int d^6 j \ e^{-\frac{1}{2}\ j^T\ (\mathbb{I}-i\partial_a\partial^b l_{ab}\theta(l_{ab})))\ j} = \left(\frac{(2\pi)^6}{\det(\mathbb{I}-i\partial_a\partial^b l_{ab}\theta(l_{ab}))}\right)^{\frac{1}{2}} . \tag{3.86}$$

The consideration on the suppression of the Hessian term still holds, and it is possible to prove it using particular variables called area-angle variables [26].

Chapter 4

Black to White Hole spin foam transition in Euclidean 3D gravity

The time has come to apply all of the previous results to the study of the 3D model of the black to white hole transition. The motivation for all of this started with the work of Carlo Rovelli and Hal Haggard. In [1], a classical GR spacetime is constructed where the transition between the black hole spacetime and the white hole is possible. This is called the fireworks spacetime and is regular everywhere except for a small quantum region in which GR is violated. The four-dimensional calculation of the transition amplitude has been performed deeply in [3]. This section aims to make a three-dimensional analog of the model, compute the amplitude of the process again, and compare the result with the 4D case.

Using the tools of Loop Quantum Gravity discussed in the previous chapters, the system will be analyzed and the problem will be set up in the simplest possible fashion. Moreover, General relativity in three dimensions does not have any local degree of freedom, which makes the 3D computation disentangled by many details on how the calculation is performed. Indeed, that translates into the spin foam formalism, with the final result independent of the number of vertex used in the bulk. The construction is thus kept in the easiest form possible with just one vertex in the spin foam.
Additionally, thanks to a fundamental recent breakthrough in the comprehension of tunneling processes [27], ample attention will be focused on tunneling between geometries.

4.1 Definition of the model

In [1], C.Rovelli and H.Haggard studied the black to white hole transition from a semi-classical point of view. They found a spacetime that describes this process satisfies Einstein's classical equation everywhere except in a small region. The LQG community

has studied this spacetime extensively.

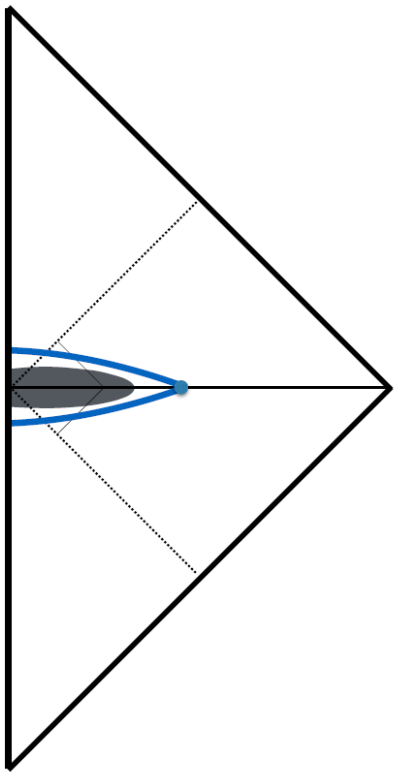

Figure 4.1: Firework spacetime's Penrose diagram. Image taken from [2].

The grey region in the figure represents the quantum zone violating Einstein's equations. LQG offers tools to study this process. Indeed, it is possible to enclose this quantum region into two spacelike hypersurfaces (blue in the figure) and codify the quantum behavior of space into the spin networks. The probability amplitude for this process can be computed with the spin foams. Fabio D'Ambrosio has done the most detailed study on the four-dimensional transition in [3, 28]. In that work, the three-dimensional hypersurfaces were two spheres glued by their boundary. A matching of the intrinsic metric in the intersection point between the blue lines in the figure was imposed, and a discontinuity in the extrinsic curvature (more precisely, a flip in its sign). The two spheres were triangulated using four isosceles tetrahedra each. The evolution was chosen to be the simplest possible, i.e. a spin foam with just two vertices.

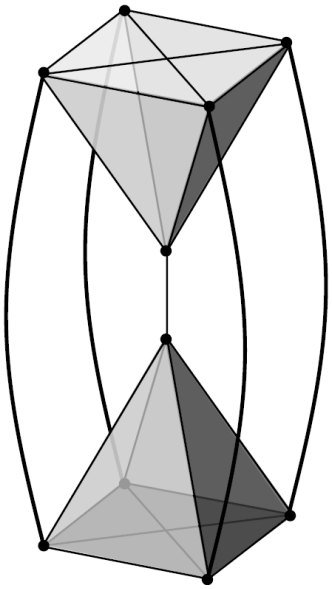

Figure 4.2: Two boundary spheres triangulated with four tetrahedra each. The spin foam represents the simplest possible evolution, with just two bulk vertices. Image taken from [3].

In [3] they computed the transition amplitude for the process in this very symmetric situation and after a series of approximations and detailed mathematical procedures, they found a result of the magnitude,

$$A \propto \exp\left[\frac{-\gamma^2 \Delta_l^2}{4t}\right]. \tag{4.1}$$

The main issue with their calculation is the lack of control over the many approximations necessary to complete the calculation. We investigate their problem by performing an analog spin foam calculation in a simplified setting. For this reason, it is chosen 3D Euclidean spin foam theory. Instead of two spheres, two disks will be triangulated, and the transition between them will be studied. The obtained result, surprisingly, will slightly differ from [3].

4.1.1 Parametrization of the 3D geometry

The goal is to study the transition between two disks. The model [1] requires a matching in the intrinsic curvature of the surfaces and a discontinuity in the extrinsic curvature. Here, the configuration of these surfaces is chosen to be the simplest possible. One of the disks, let's say the bottom one, is triangulated by a single flat triangle. In this way, all of the geometry is specified by its lengths and has no extrinsic curvature. The other

is instead triangulated by three triangles. This upper disk's triangulation is symmetric and will be described in the next. The spin network resulting from this configuration is simple, with only four three-valent nodes.
The evolution described by the spin foam has been maintained, too, in the simplest possible form. The spin foam has just one node, which corresponds to a triangulation of the bulk three-dimensional space (the region enclosed by the two boundary surfaces) with just one tetrahedron. This choice in three dimensions is also supported by the lack of local degrees of freedom, which makes the result independent of the details of the evolution.

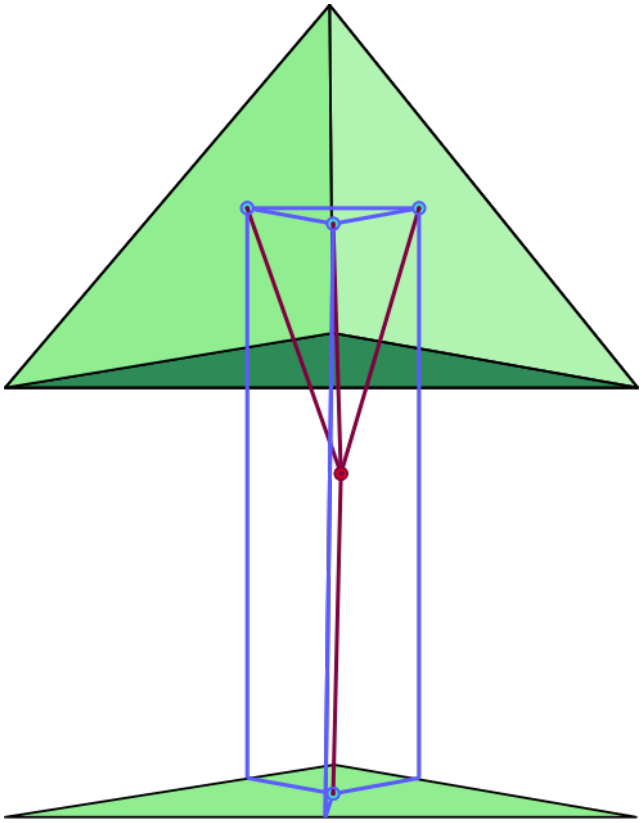

Figure 4.3: In green, the triangulation of the two disks. In blue is the correspondent spin network. In red, the spin foam describes the evolution with just one vertex, representing the quantum version of the gluing of the base triangle to the top three, forming a single tetrahedron.

The base triangle is isosceles with the side length equal to λ. The side lengths of the other three triangles are expressed in terms of λ through a proportionality constant η, namely $\eta\lambda$. In that way, the scale of the problem is all encoded into a single parameter (λ) and the extrinsic curvature, namely the angles, into another (η). This configuration

is very symmetric and allows a study of the relevant quantities.
The three-dimensional angles will be denoted with θ, while the two-dimensional with ϕ. In particular, the external 3D dihedral angle of the base will be called $\bar{\theta}_b$ and the one (equal for each side due to the symmetry) codifying the parallel transport from one side triangle to the other will be denoted with θ_s.

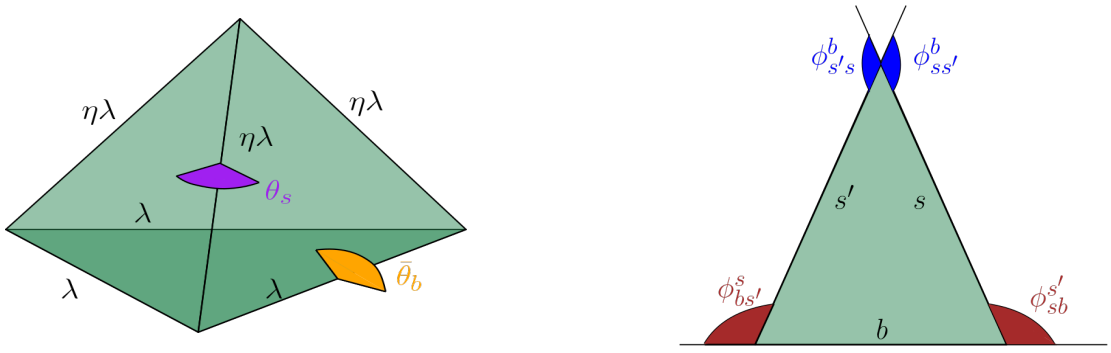

Figure 4.4: Left, parameterization of all system lengths and three-dimensional angles θ_s, $\bar{\theta}_b$. On the right, a single upper triangle with the relative notation of two-dimensional angles ϕ^i_{jk}.

Resuming the notation:

- $\lambda \longrightarrow$ Base side length, $\eta\lambda \longrightarrow$ Isosceles side lengths.
- $\theta_s \longrightarrow$ Side dihedral angles (3D), $\theta_b \longrightarrow$ Base dihedral angle (3D).
- $\phi^{s'}_{sb}, \phi^s_{s'b} \longrightarrow$ Base 2D angles, $\phi^b_{ss'}, \phi^b_{s's} \longrightarrow$ Side 2D angles.

All of these informations have to be codified inside the spinors used to write the amplitude. The relation that links the norm of the spinors and the lengths is (3.38), i.e.

$$|\langle z_{ia}|z_{ib}\rangle|^2 = \frac{j_{ic}^2 - (j_{ia} - j_{ib})^2}{4 j_{ia} j_{ib}}. \tag{4.2}$$

There are three different combinations,

$$\begin{cases} |\langle z_s|z_b\rangle|^2 = \dfrac{2\eta - 1}{4\eta}, \\ |\langle z_b|z_b\rangle|^2 = \dfrac{1}{4}, \\ |\langle z_s|z_{s'}\rangle|^2 = \dfrac{1}{4\eta^2}. \end{cases} \tag{4.3}$$

There is a correspondence between the norm of the spinors and the two-dimensional angles; see [22][21]. Indeed, it is possible to express,

$$|\langle z_{ab}|z_{ac}\rangle|^2 = \frac{1+\cos\phi^a_{bc}}{2}. \tag{4.4}$$

With this relation it is possible to compute the angles $\phi^s_{s'b}, \phi^{s'}_{sb}, \phi^b_{s's}$. The connection between angles and lengths is,

$$\begin{cases} \cos\phi^{s'}_{sb} = \cos\phi^s_{s'b} = -\dfrac{1}{2\eta}, \\ \cos\phi^b_{ss'} = \dfrac{1}{2\eta^2} - 1. \end{cases} \tag{4.5}$$

With the information on the 2D angles, it is possible to determine the three-dimensional dihedral angles using the spherical cosine laws (3.51). Before doing this, it is important to focus on the conditions of existence of these angles. It is necessary to solve the equation for both angles, ensuring that the condition $-1 < \cos\phi < 1$ is met.

- $\exists \quad \cos\phi^{s'}_{sb}, \cos\phi^s_{s'b} \quad \Longrightarrow \quad \eta < -\frac{1}{2} \ \wedge \ \eta > \frac{1}{2}$.
- $\exists \quad \cos\phi^b_{ss'} \quad \Longrightarrow \quad \eta < -\frac{1}{2} \wedge \ \eta > \frac{1}{2}$.

Since the length of a side is always nonnegative, the solutions with $\eta > 0$ are chosen. This condition represents the existing condition for the boundary state. Therefore,

$$\eta > \frac{1}{2}, \tag{4.6}$$

must be always satisfied.

Having specified the parametrization and the 2D angles in terms of the lengths, it is now possible to compute explicitly the three-dimensional angles using (3.51),

$$\begin{cases} \cos\theta_s = \dfrac{1-2\eta^2}{4\eta^2-1} \quad \Longrightarrow \quad \theta_s = \arccos\left(\dfrac{1-2\eta^2}{4\eta^2-1}\right), \\ \cos\bar{\theta}_b = -\dfrac{1}{\sqrt{3(4\eta^2-1)}} \quad \Longrightarrow \quad \bar{\theta}_b = \arccos\left(\dfrac{-1}{\sqrt{3(4\eta^2-1)}}\right). \end{cases} \tag{4.7}$$

The notation $\bar{\theta}_b$ has been used because the definition of this angle is more subtle due to the minus sign inside the $\arccos(x)$. When the argument of that function is negative the property $\arccos(-x) = \pi - \arccos(x)$ can be used. Therefore, we define also,

$$\theta_b = \pi - \bar{\theta}_b = \arccos\left(\frac{1}{\sqrt{3(4\eta^2-1)}}\right), \tag{4.8}$$

this difference will become relevant in section 4.3.
The existence condition, solving $-1 < \cos\theta < 1$, reduces to

$$\eta > \frac{1}{\sqrt{3}}. \tag{4.9}$$

The next section will analyze the validity of these conditions when considering tunneling processes. Just a brief anticipation, as already mentioned, the condition (4.6) cannot be broken, while the values of θ_i will be continued analytically into regions where (4.9) is broken.

Focusing on the exponentials of the amplitude containing the angle variables, i.e., on $\exp[iS]\exp[-1/2(\phi_i - \theta_i)^2]$, become explicitly

$$\begin{aligned} A_v = \sum_{\epsilon\pm 1}\prod_{ab} N(l_{ab}) \Bigg(& e^{-\frac{3}{2}\left(\phi_s - \epsilon \arccos\left(\frac{1-2\eta^2}{4\eta^2-1}\right)\right)^2} e^{-\frac{3}{2}\left(\phi_b - \epsilon \arccos\left(\frac{-1}{\sqrt{3(4\eta^2-1)}}\right)\right)^2} \\ & \cdot e^{i\epsilon\left(3\eta\lambda \arccos\left(\frac{1-2\eta^2}{4\eta^2-1}\right) + 3\lambda \arccos\left(\frac{-1}{\sqrt{3(4\eta^2-1)}}\right)\right)}\Bigg). \end{aligned} \tag{4.10}$$

4.1.2 Hessian Matrix - Saddle point of the SU(2) integration

The time has now come to analyze the Hessian matrix resulting from the saddle point calculation of integrations on SU(2) group elements. This is easier now because the triangles are explicitly parametrized; thus, the determinant has a particular form. The starting action form is:

$$S = \sum_{a<b} 2j_{ab} \log\left[z_{ba}\right| g_b^{-1} g_a \left|z_{ab}\right\rangle, \tag{4.11}$$

where $a, b = 1, 2, 3, 4$. The second derivatives of this object for group elements have to be computed, paying attention to the correct insertion of Pauli matrices derived from the structure of $SU(2)$ generators. There are two cases: the second derivative with respect to the same group element and the mixed derivatives. Let's start from the first, whose general structure is the following,

$$\frac{\delta^2 S}{\delta g_a \delta g_a} = \sum_{b\neq a} \frac{1}{2} j_{ab} \left(\left(\frac{\left[z_{ba}\right| g_b^{-1} g_a \vec{\sigma} \left|z_{ab}\right\rangle}{\left[z_{ba}\right| g_b^{-1} g_a \left|z_{ab}\right\rangle} \right)^2 - \frac{\left[z_{ba}\right| g_b^{-1} g_a \vec{\sigma}\vec{\sigma} \left|z_{ab}\right\rangle}{\left[z_{ba}\right| g_b^{-1} g_a \left|z_{ab}\right\rangle} \right). \tag{4.12}$$

Putting the equations on-shell and using the property of Pauli matrices $\sigma_j \sigma_k = \delta_{jk}\mathbb{I} + i\epsilon_{jkl}\sigma^l$, together with the closure conditions,

$$\frac{\delta^2 S}{\delta g_a \delta g_a} = -\frac{1}{2} \sum_{b\neq a} j_{ab} (\delta_{jk}\mathbb{I} - n_{ab}^j n_{ab}^k). \tag{4.13}$$

The other terms are the off-diagonal ones and after some calculations, have the following form,

$$\frac{\delta^2 S}{\delta g_a \delta g_b} = \frac{1}{2}\, j_{ab}\; e^{-i\theta_{ab}} (i\vec{F}_{ab} + \vec{n}_{ab} \times \vec{F}_{ab}) \otimes (i\vec{F}_{ba} + \vec{n}_{ba} \times \vec{F}_{ba}) \tag{4.14}$$

This one is for the choice $\epsilon = +1$; in the case with the opposite sign, the only difference is in the term $e^{i\theta_{ab}}$, and the determinant of the two Hessian matrices are one the complex conjugate of the other.
The construction of this Hessian matrix was done by using a planar gauge, that is, by choosing a particular orientation of the frame vector; this, being a gauge choice, does not affect the result but simplifies the calculation enormously. Below is a figure showing this particular choice.

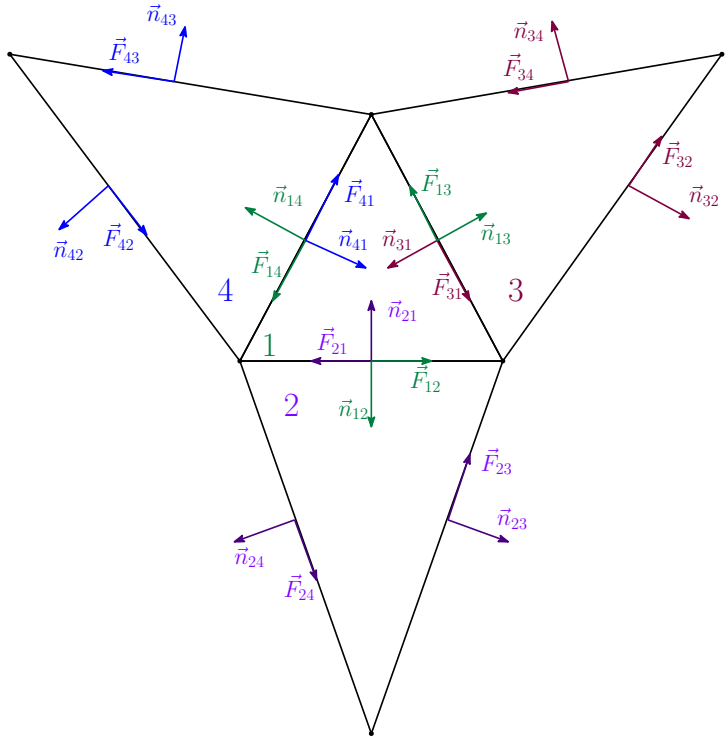

Figure 4.5: Planar triangles gauge. Different colors represent the normals and the frame vectors chosen for each length.

We performed the calculation of the Hessian and its determinant using Mathematica since an explicit generic formula is not available. This matrix results in 12x12 because the saddle point approximation was done on four integrals over the group. However, one of the four integrals is redundant; therefore calculating the determinant results in zero. This is consistent with the previously described construction in which a dummy integration was added to symmetrize the problem. The correct result is obtained excluding one of

the four group elements by removing the relative rows and columns from the Hessian matrix. The two Hessian determinants are called H^+ and H^-, one the complex conjugate of the other. In compact notation,

$$-\det H_g^{\pm} = \frac{3\sqrt{3}\ \lambda^9}{2048\ \eta^3}(2\eta+1)^3\sqrt{(4\eta^2-1)^3(3\eta^2-1)}\ \ e^{i\Upsilon^{\pm}}. \tag{4.15}$$

Some geometrical structures of the problem are hidden inside this expression. Indeed, it is possible to rewrite the determinant in terms of a volume, and of the areas:

$$-\det H_g^{\pm} = \frac{9(2\eta+1)^3}{2\lambda^2\eta^3}\ V\ A_b\ A_s^3\ \ e^{i\Upsilon^{\pm}}. \tag{4.16}$$

The argument of this complex number is a little bit more tangled,

$$\Upsilon^{\pm} = \mp\,\mathrm{arccot}\left(\frac{2(\eta+1)\ \sqrt{3\eta^2-1}\ (7+4\eta\ (4\eta\ (6\eta^2+3\eta-2)-1))}{(6\eta^2+2\eta-1)\ (4\eta\ (4\eta\ (3\eta+2)-5)-13)}\right). \tag{4.17}$$

Just for completeness, the expressions of these quantities are:

$$\begin{aligned} V &= \frac{\lambda^3}{12}\sqrt{3\eta^2-1}, \\ A_s &= \frac{\lambda^2}{4}\sqrt{4\eta^2-1}, \\ A_b &= \lambda^2\frac{\sqrt{3}}{4}. \end{aligned} \tag{4.18}$$

These are geometrical properties of the system. V is the volume of the tetrahedron forming when the four triangles glue together. A_s is the area of each side triangle triangulating the upper disk and A_b is the area of the base triangle.

4.2 Tunneling of quantum geometries

Tunneling processes are the type of phenomena sought for the black to white hole transition. A way to characterize tunneling trajectories for geometries has been elegantly found in [27]. The particle through the barrier is the simplest example in quantum mechanics, and it helps us understand the mechanisms of a tunneling process.

Consider a point particle of mass m and a potential barrier of height V_0 and width L. The process is a fixed energy E_0. Classically, there are no compatible trajectories for each set of initial and final boundary conditions at an energy E smaller than V_0. In quantum mechanics, instead, there is an exponentially dumped probability that the

particle tunnels from one side to the other. The kinetic energy E_k of the particle in the barrier region is,

$$E_k = \frac{p^2}{2m} = E_0 - V_0. \tag{4.19}$$

There are therefore two cases $E_0 - V_0 > 0$ and $E_0 - V_0 < 0$. Remember that the process is studied in the semiclassical regime, i.e. $\hbar \to 0$.

(i) $(E_0 - V_0) > 0$

When this condition is satisfied, the particle energy is above the barrier. Classically, a trajectory compatible with the boundary data exists. The path integral, and thus, the transition amplitude is naturally dominated in this region by the classical trajectory, which is the one for which the action is stationary.

$$A \propto e^{\frac{i}{\hbar} L \sqrt{\frac{m}{2}(E_0 - V_0)}}. \tag{4.20}$$

(ii) $(E_0 - V_0) < 0$

In that case, the situation changes. The boundary data, when the particle's energy is below the value of the potential barrier, are not compatible with a classical evolution. However, the path integral is still dominated by a classical trajectory, but when some of the variables get analytically continued into values that are not admissible in the classical phase space. Considering the kinetic energy as before,

$$E_k = (E_0 - V_0) = \frac{p^2}{2m} < 0, \tag{4.21}$$

it becomes negative. For this to happen, a complex value for momentum is needed. Therefore,

$$p \longrightarrow p = i\sqrt{2m|E_0 - V_0|}. \tag{4.22}$$

Clearly, the new configuration of variables is not anymore inside the phase space of the classical theory, but is inside a complexified phase space that contains the analytic continuation of the variables into the complex plane.

Computing the transition amplitude in the semiclassical approximation,

$$A \propto e^{-\frac{1}{\hbar} L \sqrt{\frac{m}{2}|E_0 - V_0|}}. \tag{4.23}$$

The classical trajectory dominates again the transition amplitude but with complex momenta.

Thus, there is a way to characterize the tunneling processes. These are processes in which the momenta is analytically continued into the complex plane. Moreover, some quantities become classically ill-defined. In this case, for example, the kinetic energy becomes negative.

It is time to analyze the same process but in the case of geometries. For details, see [27]. In that work, Pietro Donà, Hal Haggard, and Francesca Vidotto considered the evolution, dictated by the Regge action (4.24), of a surface discretized by two triangles sharing one edge into a surface discretized by two triangles sharing another edge. These two surfaces share the boundary; in this way, the only variable lengths are l_{12} and l_{34} in Figure 4.6. The latter completely characterizes the two surfaces. Fixing these two corresponds with choosing boundary data, and they also characterize the tunneling processes.

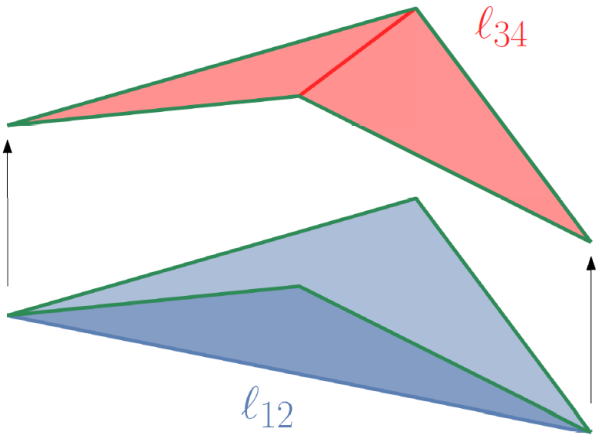

Figure 4.6: Canonical evolution from the bottom blue to the top red surface. The green perimeter is fixed; the only variables are the lengths l_{12} and l_{34}.

The Regge action guides the evolution,

$$S_R[l_{ab}] = \sum_{ab} \phi_{ab}(l_{ab}) l_{ab}. \tag{4.24}$$

The evolution governed by (4.24) acts by gluing the four triangles in a single tetrahedron. In this case, the parameter that plays the role of the free particle's kinetic energy is the tetrahedron's squared volume. The squared volume of a tetrahedron can be computed directly from its lengths through the Cayley-Menger determinant,

$$V^2(l_{ab}) = \frac{1}{144}\begin{vmatrix} 0 & 1 & 1 & 1 & 1 \\ 1 & 0 & l_{12}^2 & l_{13}^2 & l_{23}^2 \\ 1 & l_{12}^2 & 0 & l_{14}^2 & l_{24}^2 \\ 1 & l_{13}^2 & l_{14}^2 & 0 & l_{34}^2 \\ 1 & l_{13}^2 & l_{14}^2 & l_{34}^2 & 0. \end{vmatrix} \tag{4.25}$$

Suppose the volume squared of the resulting tetrahedron is $V^2 > 0$. In that case, it is a Euclidean one (meaning that it can be embedded in a three-dimensional space endowed with an Euclidean metric) and the evolution classical. Instead, in the case $V^2 < 0$, the evolution has to be considered classically forbidden, passing through a Lorentzian tetrahedron. These are the trajectories associated with tunneling phenomena.
It is possible to find a whole set of boundary data (l_{12}, l_{34}, with perimeter lengths fixed) that represent admissible triangles for the triangulation, i.e., the triangular inequalities are satisfied, but in turn, a Lorentzian tetrahedron is formed. As a concrete example, in [27] the authors took a fixed perimeter with $l_{13} = l_{23} = 10$ and $l_{14} = l_{24} = 15$ and plotting the configuration space for l_{12} and l_{34}.

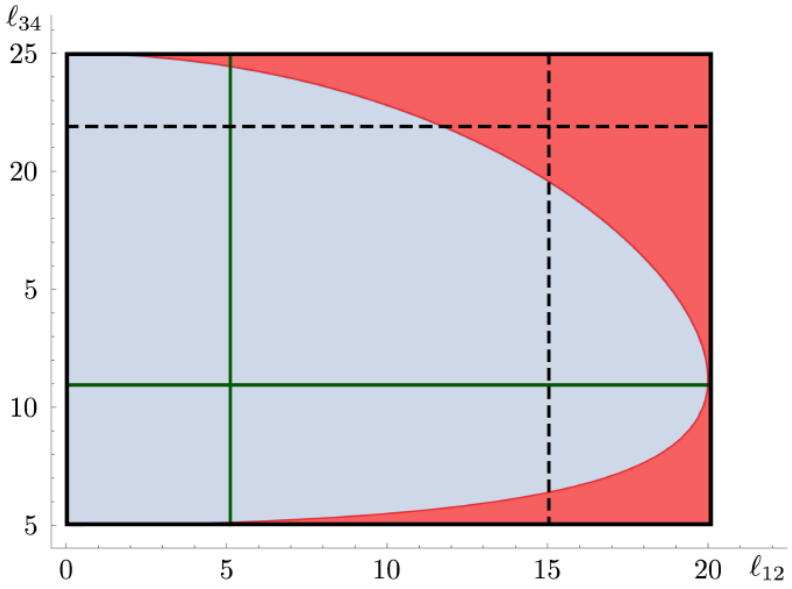

Figure 4.7: Configuration space of the initial and final surfaces. This is spanned by the variables l_{12} and l_{34} for fixed lengths $l_{13} = l_{23} = 10$ and $l_{14} = l_{24} = 15$. In blue, the configurations are compatible with a classical evolution; therefore, $V^2(l_{ab}) > 0$. In red, the tunneling region where the boundary states are not compatible with a classically allowed trajectory, $V^2(l_{ab}) < 0$. Image taken from [27].

The red zone represents the configurations in which the volume squared of the tetrahedron becomes negative. This is possible if the angles get analytically continued into

complex values, so as in the case of the free particle where the momenta get complexified, here are the dihedral angles that get continued into the complex plane,

$$\phi_{ab} \longrightarrow \tilde{\phi}_{ab} = i\phi_{ab}. \tag{4.26}$$

Computing the transition amplitude in the semiclassical limit, as described in the Ponzano-Regge model, results in,

$$A \simeq \frac{1}{2\sqrt{12V(l_{ab})}} \exp\left(iS_R[l_{ab}] + i\frac{\pi}{4} \right) + c.c. \ , \tag{4.27}$$

where $S_R[l_{ab}]$ is the Regge action computed on a solution of the equation of motion. However, selecting boundary data that are not compatible with a classical evolution, the dihedral angles are analytically continued to complex values and, therefore,

$$A \simeq \frac{1}{2\sqrt{12|V(l_{ab})|}} \exp(-\tilde{S}_R[l_{ab}]), \tag{4.28}$$

where the phase of $\pi/4$ has been reabsorbed by the i factor coming from the volume at the denominator. Surprisingly, this amplitude is nonvanishing and formally presents the typical exponential dumping of tunneling phenomena.

This is a method for characterizing the tunneling trajectories and understanding what happens to variables when the boundary data are incompatible with a classical evolution. In the next section, this will be applied to the transition amplitude (4.10) and its effects on the structure of the coherent states analized.

4.3 Disk to Disk transition

Given the model studied in [1][2], tunneling trajectories (in the spirit of [27]) must be considered for the transition. In the previous section, the tunneling processes between geometries were characterized as processes in which the momenta were analytically continued into the complex plane. In this context, the angle variables have to be analytically

continued. The final complete form of the transition amplitude is

$$
\begin{aligned}
A_v = \sum_{\epsilon=\pm 1} \prod_{ab} ((2\pi)^{\frac{15}{2}} & \frac{1}{\sqrt{-\det(H_g^{\pm})}} \frac{1}{\sqrt{\det(\mathbb{I} - i\epsilon \partial_a \partial^b l_{ab} \theta(l_{ab}))}} (2l_{ab}+1)) \\
& \cdot \exp\left[-\frac{3}{2} \left(\phi_s - \epsilon \arccos\left(\frac{1-2\eta^2}{4\eta^2-1} \right) \right)^2 \right] \\
& \cdot \exp\left[-\frac{3}{2} \left(\phi_b - \epsilon \arccos\left(\frac{-1}{\sqrt{3(4\eta^2-1)}} \right) \right)^2 \right] \\
& \cdot \exp\left[i\epsilon \left(3\eta\lambda \arccos\left(\frac{1-2\eta^2}{4\eta^2-1} \right) + 3\lambda \arccos\left(\frac{-1}{\sqrt{3(4\eta^2-1)}} \right) \right) \right].
\end{aligned}
\tag{4.29}
$$

The angles $\theta_s = \arccos(\frac{1-2\eta^2}{4\eta^2-1})$ and $\bar{\theta}_b = \arccos(\frac{-1}{\sqrt{3(4\eta^2-1)}})$ are the conjugate momenta.

Combining the information contained in (4.6) and (4.9), the tunneling region corresponds to the range,

$$
\frac{1}{2} < \eta < \frac{1}{\sqrt{3}}, \tag{4.30}
$$

for the proportionality parameter η. The parametrization chosen allows encoding the information on the angles in this single parameter.
Since these angles are expressed in terms of $\arccos(x)$, complexifying them means performing the continuation of this function. This translates in substituting,

$$
\arccos(x) \quad \longrightarrow \quad \pm i \operatorname{arccosh}(x). \tag{4.31}
$$

However, there is a fundamental remark. For the continuation to make sense, it must not lead to exponential divergences. This constrains the sign of the complex unity i and depends also on the other terms in the amplitude. To clarify this point, we can study the particle's case against the barrier again. This time, by adding the structure of the coherent states and the forward-backward propagation ($\epsilon \pm 1$) to make a formal similarity with the amplitude (4.29).

Consider the form (3.17), in which are taken into account both the directions of propagation,

$$
\mathcal{A} = N \sum_{\epsilon=\pm 1} e^{-\frac{1}{2\hbar}(p-\epsilon p_{cl})^2} e^{\frac{i}{2\hbar}\epsilon L p_{cl}}, \quad \text{where} \quad p_{cl} = \sqrt{2m(E_0 - V_0)}. \tag{4.32}
$$

The first term is a Gaussian that forces the momentum in which the coherent states are peaked to be classical. The second is the complex exponential of the Hamilton principal function, i.e. the dynamics. For $(E_0 - V_0) < 0$, the momenta must be continued

analytically in the tunneling region [29]. The only way to do this without crashing into divergences is:

- For $\epsilon = +1$: $p_{cl} = \sqrt{2m|E_0 - V_0|} \longrightarrow i\sqrt{2m|E_0 - V_0|}$,
- For $\epsilon = -1$: $p_{cl} = \sqrt{2m|E_0 - V_0|} \longrightarrow -i\sqrt{2m|E_0 - V_0|}$.

The tunneling amplitude becomes,

$$\mathcal{A}_{tun} = Ne^{-\frac{1}{2\hbar}(p-ip_{cl})^2} e^{-\frac{L}{2\hbar}p_{cl}}. \tag{4.33}$$

The form of this amplitude is crucial. The first important consideration is that the forward ($\epsilon = +1$) propagation and the backward ($\epsilon = -1$) collapse into the same term. Moreover, the form of the various terms changes not only the mathematical structure but also the physical interpretation. The first term is still a Gaussian, but note that expanding the exponent,

$$e^{-\frac{1}{2\hbar}(p-ip_{cl})^2} = e^{-\frac{1}{2\hbar}p^2} e^{\frac{1}{2\hbar}p_{cl}^2} e^{i\frac{pp_c}{\hbar}}, \tag{4.34}$$

then the structure of the coherent states breaks down. The link between the classical momentum and the label of the coherent states enters just inside a phase. Taking the modulus squared of the amplitude to compute probabilities, this phase cancels. The other two exponents are unrelated and can be reabsorbed inside the normalization constant. In (4.33), the Gaussian factor forces the momentum of the coherent states to peak on the analytically continued one. However, by definition, the coherent states have to be peaked on a classical phase space cell, but the complexified variables no longer belong to this space. This also happens to the disk-to-disk tunneling amplitude; therefore the conclusion is that the coherent state structure does not work anymore.

This is a fundamental result. The new understanding is that coherent states are not suitable for studying processes that are not allowed classically. This derives from their very definition, which is strictly related to the classical phase space.

The other term,

$$e^{-\frac{L}{2\hbar}p_{cl}} = e^{-\frac{L}{2\hbar}\sqrt{2m|E_0-V_0|}}, \tag{4.35}$$

is the usual exponential of the analytically continued Hamilton principal function. Squaring the amplitude absorbing the irrelevant terms inside the normalization constant, the usual form of the transmission coefficient in the saddle-point approximation is obtained:

$$T = N^2 e^{-\frac{L}{\hbar}\sqrt{2m|E_0-V_0|}}. \tag{4.36}$$

The case of the disk-to-disk transition is completely equivalent. The functions to be continued are θ_s and $\bar{\theta}_b$. A small detail is what was discussed in section 4.1.1. The

argument of the $\arccos(x)$ function of $\bar{\theta}_b$ is negative. The already mentioned property $\arccos(-x) = \pi - \arccos(x)$ is now important. The real part π indeed remains the same after the analytic continuation. Namely,

$$\bar{\theta}_b = \arccos\left(\frac{-1}{\sqrt{3(4\eta^2-1)}}\right) \longrightarrow \pi \pm i\,\mathrm{arccosh}\left(\frac{1}{\sqrt{3(4\eta^2-1)}}\right). \tag{4.37}$$

Therefore, for the sake of simplicity in this chapter, it was previously defined the "bare" variable θ_b.

The only non-exponentially enhanced amplitude relies on the analytic continuation of the angles:

- For $\epsilon = +1$:

$$\begin{cases} \theta_s = \arccos\left(\dfrac{1-2\eta^2}{4\eta^2-1}\right) \longrightarrow i\,\mathrm{arccosh}\left(\dfrac{1-2\eta^2}{4\eta^2-1}\right), \\ \theta_b = \arccos\left(\dfrac{1}{\sqrt{3(4\eta^2-1)}}\right) \longrightarrow -i\,\mathrm{arccosh}\left(\dfrac{1}{\sqrt{3(4\eta^2-1)}}\right). \end{cases} \tag{4.38}$$

- For $\epsilon = -1$:

$$\begin{cases} \theta_s = \arccos\left(\dfrac{1-2\eta^2}{4\eta^2-1}\right) \longrightarrow -i\,\mathrm{arccosh}\left(\dfrac{1-2\eta^2}{4\eta^2-1}\right), \\ \theta_b = \arccos\left(\dfrac{1}{\sqrt{3(4\eta^2-1)}}\right) \longrightarrow +i\,\mathrm{arccosh}\left(\dfrac{1}{\sqrt{3(4\eta^2-1)}}\right). \end{cases} \tag{4.39}$$

This collapses the two configurations $\epsilon = \pm 1$ into the same one, except for some irrelevant factors absorbable in the normalization constant. Grouping also every multiplicative term in (4.29) into the normalization constant N, the tunneling amplitude becomes,

$$\begin{aligned} \mathcal{A}_{tun} = N \exp&\left[-\frac{3}{2}\left(\phi_s - i\,\mathrm{arccosh}\left(\frac{1-2\eta^2}{4\eta^2-1}\right)\right)^2\right] \\ &\cdot \exp\left[-\frac{3}{2}\left(\phi_b - i\,\mathrm{arccosh}\left(\frac{1}{\sqrt{3(4\eta^2-1)}}\right)\right)^2\right] \\ &\cdot \exp\left[-3\lambda\left(\eta\,\mathrm{arccosh}\left(\frac{1-2\eta^2}{4\eta^2-1}\right) + \mathrm{arccosh}\left(\frac{1}{\sqrt{3(4\eta^2-1)}}\right)\right)\right]. \end{aligned} \tag{4.40}$$

This tunneling amplitude is one of the major results of this work.

In analogy with the particle through the barrier, the transmission coefficient is straightforwardly found by squaring the amplitude. The transmission coefficient for the disk-to-disk transition is:

$$\boxed{T = N^2 \ \exp\left[-3\lambda\left(\eta \,\mathrm{arccosh}\left(\frac{1-2\eta^2}{4\eta^2-1}\right) + \mathrm{arccosh}\left(\frac{1}{\sqrt{3(4\eta^2-1)}}\right)\right)\right].} \tag{4.41}$$

The transmission coefficient for the black-to-white hole transition in three dimensions represents the actual result of this work. This is the first model with an analytical form of the transition amplitude with all approximations under control. Written in a truly compact version:

$$T \propto \exp[-\Lambda\Phi], \tag{4.42}$$

where Λ refers to the scale of the problem and Φ to the extrinsic curvature.
It is possible to notice a different trend from the original works. In fact, this time, the transmission coefficient turns out to be proportional to the scale of the problem, in the specific context, the perimeter of the disks, times the extrinsic curvature. On the other hand, in [3], the trend scaled with an exponential of the squared angles.

4.3.1 Discussion and further developments

With a transmission amplitude, it is generally possible to calculate observables. In this context, the problem is more intricate. The difficulties involved in calculating observables in this context are twofold. The first is a feature of the three-dimensional model, and the second is a technicality to be addressed in the general context of Loop Quantum Gravity.

The first difficulty is a lack of asymptotics in this three-dimensional model. This is because the three-dimensional model lacks specific metrics, present instead in General Relativity in four dimensions, to refer to. In the original works [3] [1] [2], the first step in the calculation was precisely to write a classical metric and then encode the information in the discretized version. Three-dimensional metrics can indeed be written in this context; however, these cannot be tied to any physical world. For these reasons, the analysis in this paper stops with result (4.41). The mathematical techniques used formally turn out to be the same in four dimensions, so it is part of future developments to create a metric that actually has physical meaning.
Nevertheless, the result obtained turns out to be of crucial importance. With a fully controlled transition amplitude in four dimensions it will be possible to calculate observables such as the abundance of black holes and white holes (or superpositions of the two) and to compare it with the abundance of dark matter.

The second technicality is more general and must be studied in depth for future developments. The modulus of the transition amplitude usually directly returns the process's probability. However, this is true only when the amplitude is normalized. Normalization requires knowledge of all the process's outcomes, which is absent in this context. What can be done is to work with conditional probabilities to construct a system that is known from the point of view of possible outcomes. To explain what is intended, one can think of the roll of a die. Assuming for true that rolled a die, either 2 or 4 came out (this is the condition), what is the probability that 2 came out? The answer is 50%. However, the probability of 2 coming out on a generic roll is 1/6. The model can then be refined by expanding the possibilities. Given a toss in which the possible outcomes are 2, 4 or 3, what is the probability that 2 will come out? In this case, it will be 33%. By refining the condition of the problem to the maximum, the true likelihood of the process is obtained. Given a roll of the dice in which all numbers from 1 to 6 can come up, what is the probability of getting 2? 1/6, which is the correct result.
In the context of the black-to-white hole transition, this conditional probability can be implemented and combined with an analog of Gamow's model for alpha decays. Imagine a conditioned process; given the transition, the outcome can be a classical transition or a tunneling one,

$$\begin{aligned} A_{cl} &\propto \frac{e^{iS}}{\sqrt{V}}\,, \\ A_{tun} &\propto \frac{e^{-\tilde{S}}}{\sqrt{\tilde{V}}}\,. \end{aligned} \tag{4.43}$$

Here, S is the action, and $\tilde{S}$ is the analytically continued one. With V, it indicates the volume of the Euclidean tetrahedron, and with $\tilde{V}$, the Lorentzian tetrahedron's volume modulus. The probability is given by the modulus squared of these amplitudes:

$$\begin{aligned} |A_{cl}|^2 \quad &\dashrightarrow \quad P_{cl} \propto \frac{1}{V}\,, \\ |A_{tun}|^2 \quad &\dashrightarrow \quad P_{tun} \propto \frac{1}{|\tilde{V}|}\, e^{-2\tilde{S}}. \end{aligned} \tag{4.44}$$

These are the conditional probabilities and it is possible to "impose" the normalization:

$$\begin{aligned} &C\left(\frac{1}{V} + \frac{1}{|\tilde{V}|}\, e^{-2\tilde{S}}\right) = 1, \\ &C = \frac{V\tilde{V}}{\tilde{V} + Ve^{-2\tilde{S}}}\,. \end{aligned} \tag{4.45}$$

Defining the ratio of the volumes $v = V/\tilde{V}$, the probabilities become,

$$P_{cl} = \frac{1}{1 + v\ e^{-2\tilde{S}}}\ , \qquad P_{tun} = \frac{v\ e^{-2\tilde{S}}}{1 + v\ e^{-2\tilde{S}}}\ . \tag{4.46}$$

Clearly by constuction $P_{cl} + P_{tun} = 1$. Now, it is possible to define a probability p and it can be considered a sequence of "attempts" for the transition. This is a full analogy with the Gamow model for particle decay in which the α tries a certain number of times to escape from the nucleus. The number of "attempts" of the transition can be computed with:

$$p = P_{tun} \sum_{n=0}^{N} (P_{cl})^n. \tag{4.47}$$

Considering a classical metric, it is, in principle, possible to define and tie a time scale to the process and translate this information into a transition time. Characterizing the transition time for the black-to-white hole transition is one of the most interesting developments in calculus.

Chapter 5

Conclusion

In this work, the theory of Loop Quantum Gravity (LQG), a fruitful and interesting attempt at a quantum gravity theory, has been briefly introduced. LQG, by combining the basic concepts of General Relativity with the mathematical structure typical of Quantum Mechanics, stands as a powerful tool and emerges as a genuinely quantum theory of geometry.

The interest of the quantum gravity community is strongly directed toward purely quantum processes. This is in the hope of finding observable traces that are not, inevitably, minuscule corrections to classical phenomena. One of the prototypical phenomena of this kind is quantum tunneling. Among the most famous problems in the context of Loop Quantum Gravity, there is the transition between black and white holes. Interest in this topic started from the first studies [1], and [2]. In the latter, a classical metric satisfying classical Einstein equations everywhere except in a small quantum region was found. This discovery opened the doors to many interesting possibilities, the most exciting being the resolution of the black hole singularities of General Relativity (GR). It transformed black holes from the ultimate limit of everything to something bouncing and making a transition into theoretically well-known objects, the white holes. From that moment, extensive research was conducted to calculate the quantum transition amplitude of the process.

The first and most extensive study of the black-to-white hole transition in four Lorentzian dimensions is in [3]. However, this calculation is technically very difficult and requires many approximations, sometimes uncontrolled. Because of this, the results obtained are not transparent and are very difficult to interpret. To circumvent this problem, we propose an analog calculation in the drastically simpler setting of the three-dimensional Euclidean spin foam quantum gravity. We stress and know that the physical interpretation of our calculation cannot be extended immediately to the real world. The reduction by one dimension has important implications. The very nature of General Relativity is

completely different in 3D, becoming a topological theory, effectively incompatible with the presence of black holes. However, this does not turn out to be a limitation of this work. Instead, we propose it as a toy model to be followed as a guideline for future calculations concerning the physical world. Loop Quantum Gravity defines quantum transitions between hypersurfaces. Most of the math and the techniques involved in the 3D calculation also apply to the physically more interesting models. Moreover, all steps were constructed with a view to future developments in four dimensions, creating a formal model to be followed. The simplification of the problem allowed us to shed light on some critical technical issues and to provide a clearer interpretation of the existing results. In addition, it has been possible for the first time (albeit in a simpler model) to carry out a complete calculation of the spinfoam transition amplitude with all approximations under control.

In this thesis work, we derived two main results. The first result consists of understanding the role of the amplitude boundary states. The traditional calculation is done using coherent boundary states. The role of coherent states was studied in detail, and their limitations have been identified. Indeed, it has been shown how, in the study of purely quantum tunneling transitions, they no longer succeed in placing constraints on variables when the phase space is expanded even to complex values of certain quantities. A basic example was that of the free particle (3.2), and then this structure was also reflected in the transition amplitude of the disk-to-disk process (4.40). This result made it possible not only to identify the specific features of these states but also to identify the misinterpretation in the result (4.1). What had been interpreted in the original work as the exponential suppression typical of tunneling effects turns out to be an artifact of the coherent boundary states. This was probably due to two main causes. The first is the inherent difficulty of the calculation. To overcome this complication, the chosen configuration truncated away the dynamic part of the transition amplitude, thus falling into the case (3.18). The second was the lack of a dictated understanding of tunneling processes between geometries, only recently obtained in [27]. Thus, the original result still turns out to be correct, but not the trace of tunneling between geometries.
The second important achievement is calculating the transition amplitude (4.29) and transmission coefficient themselves (4.41). These, in fact, are the first complete calculations for this type of amplitude, with precise control over the approximations used. Moreover, the assumptions associated with this result are small and consist mainly of the specific symmetry of the problem, which is not stringent and is used for simplicity and to maintain the analogy with [3]. The transmission coefficient for the disk-to-disk transition manifests tunneling processes' typical exponential suppression characteristic, with a linear trend in the problem scale and extrinsic curvature $T \propto \exp[-\Lambda\Phi]$. Despite the important result, a critical issue common to all these calculations remains the difficulty of probabilistic interpretation of the transmission coefficient due to the lack of knowledge of the normalization constant. However, at the end of this work, a path of

reasoning has been reported that effectively circumvents this difficulty by resorting to conditional probability. The quantities (4.46) indeed turn out to be truly interpretable as probabilities, being normalized to one. This pragmatic approach to studying conditional probabilities is limited only by the number of processes being considered. The more possibilities considered, the closer the probability values are to those calculated with a normalized amplitude. This result is thus not only the calculation of the amplitude but also a cue to circumvent the difficulties associated with its use.

In conclusion, this work marks a significant step in understanding tunneling between quantum geometries. The three-dimensional model provides a guideline for a new four-dimensional process calculation and offers the potential to revolutionize our understanding of quantum gravity. With a 4D form of the transmission amplitude, which is also analytical and controlled, we could calculate physical transition amplitudes in quantum gravity. This could lead to groundbreaking studies on the abundance of (Planck scales) black holes and white holes or linear combinations of the two that have been suggested as a possible dark matter candidate [30]. Such studies could provide detailed theoretical predictions about the formation process of these objects, offering a unique comparison with dark matter abundance data. Moreover, by paying close attention to mathematical details such as the structure of states and semiclassical calculus, this work offers exciting insights into applying the theory to the early universe. As we eagerly await future developments in this work, which will provide predictions comparable to those of the physical world, we can already see the potential of this thesis as another significant step forward in the understanding of quantum gravity. The anticipation for what lies ahead is great, and we look forward to the new insights and discoveries that will further enrich our understanding of the universe.

Appendix A

Connection with GR

This appendix is dedicated to the link between Loop Quantum Gravity and General Relativity. It is also close to the historical path that LQG followed. In this chapter, many concepts are not explained in detail to avoid being too specific. However, the literature on the classical GR part is huge, and for what concerns the LQG, we remand to [9], and to the very detailed introduction [31].

In General Relativity (1915), the gravitational field is described by a symmetric tensor field $g_{\mu\nu}(x)$, which can be interpreted as the metric of a pseudo-Riemaniann manifold. The equation of motion for the metric can be derived from an action principle. The action of gravity (without cosmological constant for simplicity) is the famous Einstein-Hilbert action,

$$S_{EH}[g] = \frac{1}{16\pi G}\int d^4x\sqrt{-g}R, \tag{A.1}$$

where g is the determinant of the metric and R is the Ricci scalar. Adding also a matter-energy action to S_{EH} and varying with respect to the metric led to Einstein's field equations,

$$R_{\mu\nu} - \frac{1}{2}g_{\mu\nu}R = 8\pi G\ T_{\mu\nu}. \tag{A.2}$$

Despite its great success, this formulation cannot be fundamental. Indeed, it is not possible to couple the fermions with gravity. We must use the *tetrads* $e^I_\mu(x)$ instead of the metric tensor $g_{\mu\nu}(x)$. Geometrically, a tetrad $e^I_\mu(x)$ is a map from the tangent space at x to the Minkowski space, capturing the idea that in each point, there exists a local inertial reference frame. The relation with the metric is

$$g_{\mu\nu}(x) = e^I_\mu(x)e^J_\nu(x)\eta_{IJ}. \tag{A.3}$$

The EH action can be written replacing the metric with its expression in terms of tetrads $S_{EH}[g] \to S_{EH}[g[e]]$.

The tetrad formalism gain an additional local Lorentz $SO(3,1)$ gauge invariance under the transformation

$$e^I_\mu(x) \longrightarrow \Lambda^I_J(x) e^J_\mu(x). \tag{A.4}$$

This invariance allows to treat gravity similarly to the usual Yang-Mills gauge theories. We can introduce, therefore, a connection related to this symmetry: the Lorentz connection ω^{IJ}_μ. This is an object living in the algebra of the Lorentz group and satisfying

$$\omega^{IJ}_\mu = -\omega^{JI}_\mu. \tag{A.5}$$

These objects also allow getting entirely rid of any reference to the coordinates, using the form notation,

$$e^I = e^I_\mu dx^\mu, \qquad \omega^{IJ} = \omega^{IJ}_\mu dx^\mu. \tag{A.6}$$

The tetrads define an extension of Riemann geometry called the Cartan geometry (Riemann geometry admitting also torsion). The first and the second structure Cartan equations are

$$\begin{cases} F^I_J = d\omega^I_J + \omega^I_K \wedge \omega^K_J, \\ de^I + w^I_J \wedge e^J = 0. \end{cases} \tag{A.7}$$

The first one defines the curvature tensor, and the second sets the torsion equal to zero (correctly in GR). The unique torsionless solution $\omega[e]$ is called *spin-connection*. The curvature of the spin-connection is directly related to the Riemann tensor,

$$F^{IJ} = e^I_\mu e^J_\nu R^{\mu\nu}{}_{\rho\lambda} dx^\rho \wedge dx^\lambda. \tag{A.8}$$

Using this the Einstein-Hilbert action becomes

$$S_{EH}[e] = \int e \wedge e \wedge F^\star, \quad \text{where} \quad F^\star = \frac{1}{2}\epsilon_{IJKL} F^{KL}. \tag{A.9}$$

One important note about this formalism is that working with the Einstein-Hilbert action in the metric and the tetrad formalism is not entirely equivalent. Applying the time reversal symmetry to the tetrad version of the action flips the sign (as usual in non-relativistic physics) while the other is invariant. This is reflected in the quantum theory of having contribution in the Feynman integral with two signs,

$$e^{-\frac{i}{\hbar}S_{EH}} + e^{+\frac{i}{\hbar}S_{EH}}, \tag{A.10}$$

that is precisely the structure of the amplitude in the previous sections.

Lifting the connection to an independent variable, we can write the *Palatini* action

$$S[e,\omega] = \int e \wedge e \wedge F[w]^\star, \tag{A.11}$$

that is polynomial, and its variation $\delta\omega$ forces the connection to be the spin-connection (without torsion), and δe gives the tetrad version of Einstein's equations. As usual in quantum field theory, we seek out other terms with the same symmetries that can be added to the action. There is another one, and we couple it at the action through a constant $1/\gamma$, where γ is the famous *Barbero-Imirzi constant*,

$$S[e,w] = \int e \wedge e \wedge F^{\star} + \frac{1}{\gamma}\int e \wedge e \wedge F. \tag{A.12}$$

This new action is called the *Holst action*. The new term does not affect the equation of motion, recovering; therefore, again, General Relativity.
This action can be reorganized in the suggestive form of a constrained BF theory. Rewriting the action as

$$S[e,w] = \int (\star\, e \wedge e + \frac{1}{\gamma} e \wedge e) \wedge F, \tag{A.13}$$

the theory can be seen as [32],

$$\begin{cases} S[e,\omega] = \int B \wedge F, & \text{BF theory,} \\ B = (\star\, e \wedge e + \dfrac{1}{\gamma} e \wedge e), & \text{Constraint.} \end{cases} \tag{A.14}$$

One more core concept is needed to introduce Loop Quantum Gravity from the classical theory: the ADM decomposition. This is fundamental for LQG; however, as a famous procedure, we will explain it without formal proof or derivation. The literature on this topic is huge, and for a brief reminder, we suggest again [31].
The ADM (Arnowit, Deser, Misner) decomposition is the elegant procedure applied to General Relativity to recast the theory in Hamiltonian formalism. The main problem before the discovery of this technique was the covariant nature of GR. Indeed, a Hamiltonian theory requires a preferred time variable t for quantities to evolve (the Hamiltonian itself represents the generator of time translations). The compliance with gravity is the fundamental nonexistence of this preferred variable.
The decomposition breaks the four-dimensional manifold into a 3+1 manifold using variables adapted for the Hamiltonian formalism. This is possible by introducing a preferred and fictitious time variable t and then imposing conditions that make this 3+1 separation completely arbitrary, restoring the covariant nature of gravity.

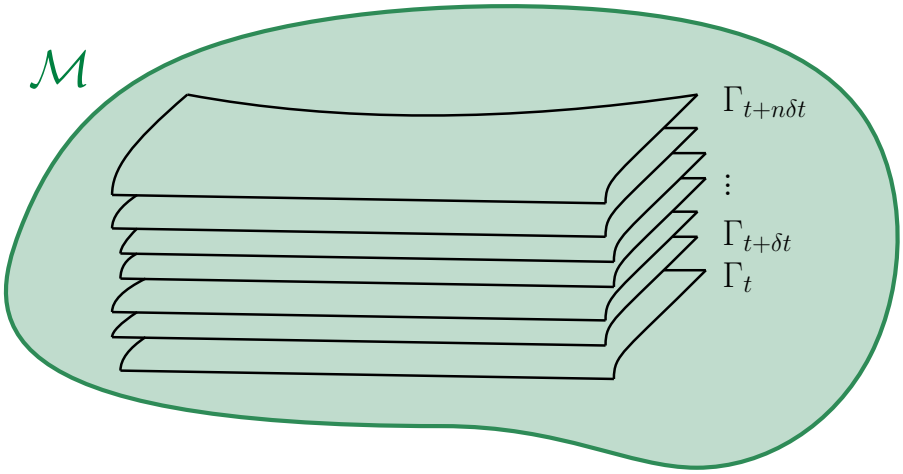

Figure A.1: Pictorial representation of the foliation of a manifold $\mathcal{M}$. The Γ_t represents the spacelike leaves.

The decomposition takes a four-dimensional manifold $\mathcal{M}$ and defines a real-valued scalar field τ whose gradient $\nabla\tau$ is time-like everywhere. Considering all the three-dimensional spacelike hypersurfaces with different constant values of this vector field, there is a natural foliation of $\mathcal{M}$. The next step is to project all the tensor quantities of $\mathcal{M}$ on the leaves, and in that way, the system can be described as the evolution of these quantities along the vector field defined by $\nabla\tau$.
The ADM decomposition identifies the degrees of freedom of the gravitational field: the three metric q_{ab} of the space-like hypersurface and its conjugate momenta π^{ab} defined as

$$\pi^{ab} = \sqrt{q}(k^{ab} - kq^{ab}), \tag{A.15}$$

where q is the determinant of the metric and k^{ab} represents the extrinsic curvature of the three-surface.

Combining the ADM decomposition with the tetrad formalism, settles all of the ingredients to define the LQG variables.
It is possible to write the tetrad field for the ADM decomposition and to rewrite the conjugate variables in the new formalism,

$$q_{ab} = e^i_a(x)e^j_b(x)\delta_{ij}, \quad \text{and} \quad k_{ab} = k^i_a e^i_b, \tag{A.16}$$

where $i, j = 1...3$ and e^i_a is called *triad* and is the spatial part of the tetrad and k^i_a is the triad version of the extrinsic curvature (that can be written in terms of the connection as $k^i_a = \omega^{0i}_a$).

The crucial change of variables is the definition of the *densitized triad* and the *Ashtekar-Barbero connection*:

$$\begin{cases} E^a_i = ee^a_i = \dfrac{1}{2}\epsilon_{ijk}\epsilon^{abc}e^j_b e^k_c, \\ A^i_a = \dfrac{1}{2}\epsilon^i_{jk}\omega^{jk}_a + \gamma\omega^{0i}_a. \end{cases} \tag{A.17}$$

These two variables transform respectively as an $SU(2)$ vector and an $SU(2)$ connection and are conjugate variables. This $SU(2)$ symmetry is inherited by the local Lorentz freedom of the tetrad that, once projected on the slice, remains with rotational symmetry. This is the local freedom to orient a frame of reference.
In the end, it is needed a regularization of these two variables taking care of their tensor nature. More precisely, E^a_i is a 2-form and thus naturally integrated on a surface,

$$E_i(S) = \int_S n_a E^a_i d^2\sigma \tag{A.18}$$

where n_a is the normal to the surface. The quantity $E_i(S)$ is the flux of E across S.
The connection on the other hand is a 1-form, naturally integrated along a path γ (parametrized with $s \in [0,1]$),

$$A^i_a \longrightarrow \int_\gamma A \equiv \int_0^1 ds A^i_a(x(s))\frac{dx^a(s)}{ds}\tau_i, \tag{A.19}$$

where τ_i is a generator of $SU(2)$. From this, taking the path integral exponential, we obtain the *holonomy*,

$$h_\gamma = \mathcal{P}\exp\left(\int_\gamma A\right). \tag{A.20}$$

These two variables $(h_\gamma, E_i(S))$ form the *holonomy-flux algebra*. When these variables get promoted to operators we obtain precisely the holonomies $\hat{h}_l$ and the derivative operator (1.8) with correct units $\hat{E}^i{}_l = 8\pi\hbar G\hat{L}^i{}_l$. The quantization of this algebra gives precisely (1.11).

Appendix B

SU(2) Math

B.0.1 Intertwiners

The intertwiners are projection operators on the invariant subspace of the tensor product of different Hilbert spaces. Consider two spins j_1 and j_2 living in different Hilbert spaces $\mathcal{H}^{j_1}$ and $\mathcal{H}^{j_2}$. The tensor product among them can be decomposed as,

$$\mathcal{H}^{j_1} \otimes \mathcal{H}^{j_2} = \bigoplus_{j_3=|j_1-j_2|}^{|j_1+j_2|} \mathcal{H}^{j_3}, \tag{B.1}$$

that follows from the Clebsch-Gordan conditions, namely $|j_1 - j_2| \leq j_3 \leq |j_1 + j_2|$. When the latter is satisfied, and the sum of the spins is even, an invariant subspace $\mathcal{H}^0 \in \mathcal{H}^{j_1} \otimes \mathcal{H}^{j_2} \otimes \mathcal{H}^{j_3}$ exists. Projectors are thus needed for this invariant subspace. These are the intertwiners $i^{m_1 m_2 m_3}$, satisfying,

$$D^{j_1 m_1}_{n_1}(h) D^{j_2 m_2}_{n_2}(h) D^{j_3 m_3}_{n_3}(h) i^{n_1 n_2 n_3} = i^{m_1 m_2 m_3}. \tag{B.2}$$

They are also called Wigner $(3j)$-symbols,

$$\begin{pmatrix} j_1 & j_2 & j_3 \\ m_1 & m_2 & m_3 \end{pmatrix} = i^{m_1 m_2 m_3}. \tag{B.3}$$

In 3D $\mathrm{Inv}(\mathcal{H}_{j_1} \otimes \mathcal{H}_{j_2} \otimes \mathcal{H}_{j_3})$ has dimension one. There exists, therefore, a unique $(3j)$-symbol.
In the 4D case, $\mathcal{H}^0$ contains a finite-dimensional set of intertwiners for each one. The $\mathrm{Inv}(\mathcal{H}^{j_1} \otimes \mathcal{H}^{j_2} \otimes \mathcal{H}^{j_3} \otimes \mathcal{H}^{j_4})$ contains linearly independent invariant tensors,

$$i_k^{m_1 m_2 m_3 m_4} = \begin{pmatrix} j_1 & j_2 & k \\ m_1 & m_2 & m \end{pmatrix} g_{mn} \begin{pmatrix} k & j_3 & j_4 \\ n & m_3 & m_4 \end{pmatrix}, \tag{B.4}$$

for any k satisfying the Clebsh-Gordan conditions both in j_1, j_2 and j_3, j_4, i.e.

$$\max[|j_1 - j_2|, |j_3 - j_4|] \geq k \leq \min[j_1 + j_2, j_3 + j_4]. \tag{B.5}$$

For more details, see [4][9].

B.0.2 Properties $D^j_{mn}(g)$

In this section, some useful properties of intertwiners and Wigner matrices used in spin-network calculations are reported.
Start by evaluating a Wigner matrix on an inverse element of the group. It is very immediate, from the structure of SU(2), that:

$$D^j_{nm}(g^{-1}) = \overline{D^j_{mn}(g)}. \tag{B.6}$$

However, less intuitive is the following equality:

$$\begin{aligned} D^j_{mn}(g^{-1}) &= (-1)^{n-m} D^j_{-n-m}(g), \\ &= (-1)^{n-m} D^j_{-n-m}(g)(-1)^{2(j-n)}, \\ &= (-1)^{j-n} D^j_{-n-m}(g)(-1)^{j-m}, \\ &= (-1)^{j-n}\delta_{-nn'} D^j_{n'm'}(g)(-1)^{j-m}\delta_{-mm'}, \\ &= D^j(\epsilon_{AB}) D^j_{n'm'} D^j(\epsilon_{AB}). \end{aligned} \tag{B.7}$$

This also imposes a condition in the very definition of intertwiners. It is required to keep track of these phases. However, in 3D, the intertwiner is indeed unique up to phases. Since the theory is $SU(2)$ gauge invariant, the notion of intertwiner appears naturally. Indeed any gauge invariant state is in the triple tensor product of representation is proportional to the state:

$$|i\rangle = \sum_{m_1 m_2 m_3} \begin{pmatrix} j_1 & j_2 & j_3 \\ m_1 & m_2 & m_3 \end{pmatrix} |j_1, m_1\rangle \otimes |j_2, m_2\rangle \otimes |j_3, m_3\rangle \,. \tag{B.8}$$

The intertwiners are invariants under gauge transformations and satisfy the condition:

$$D^{j_1}_{m_1 n_1}(g) D^{j_2}_{m_2 n_2}(g) D^{j_3}_{m_3 n_3}(g) i^{m_1 m_2 m_3} = i^{n_1 n_2 n_3}. \tag{B.9}$$

The intertwiners are the result of group averaging, namely a procedure that is used to build automatically gauge invariant states, and integrating the three Wigner matrices:

$$\int dg D^{j_1}_{m_1 n_1}(g) D^{j_2}_{m_2 n_2}(g) D^{j_3}_{m_3 n_3}(g) = i^{m_1 m_2 m_3}\ i^{n_1 n_2 n_3}. \tag{B.10}$$

Every time a graph is analyzed attention to the ordering of the links has to be paid. Performing the group averaging, given a matrix $D^j_{mn}(h_0)$ and a general group element $l \in SU(2)$, then:

$$\begin{aligned} D^j_{mn}(h_0\ l) &\qquad \text{if the node is a source,} \\ D^j_{mn}(l^{-1}\ h_0) &\qquad \text{if the node is a target.} \end{aligned} \tag{B.11}$$

The combination of this with (B.7) translates into a condition on intertwiners.

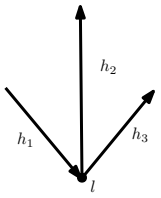

When a graph has all of the link that are sources of a node the intertwiner is simply given by $i^{m_1 m_2 m_3}$. But in the case of a mixed node, as the one in the picture aside, the intertwiner takes a phase every time a link enters in the node. For example, for the depicted one the intertwiner would be:

$$\tilde{i}^{m_1,m_2,m_3} = (-1)^{j_1 - m1} \delta_{-m_1 m'} i^{m' m_2 m_3}. \tag{B.12}$$

If all of the links are entering the node the intertwiner has the property that:

$$\begin{aligned} \tilde{i}^{m_1,m_2,m_3} &= (-1)^{j_1 - m1} \delta_{-m_1 m'} (-1)^{j_2 - m2} \delta_{-m_2 m''} (-1)^{j_3 - m3} \delta_{-m_3 m'''} i^{m' m'' m'''} \\ &= i^{m_1 m_2 m_3}. \end{aligned} \tag{B.13}$$

Bibliography

[1] H. M. Haggard and C. Rovelli, "Black hole fireworks: quantum-gravity effects outside the horizon spark black to white hole tunneling," arXiv:1407.0989.

[2] M. Christodoulou, C. Rovelli, S. Speziale, and I. Vilensky, "Realistic Observable in Background-Free Quantum Gravity: the Planck-Star Tunnelling-Time," arXiv:1605.05268.

[3] F. D'Ambrosio, "Semi-Classical Holomorphic Transition Amplitudes in Covariant Loop Quantum Gravity," arXiv:2001.04651.

[4] C. Rovelli and F. Vidotto, *Covariant Loop Quantum Gravity - An Elementary Introduction to Quantum Gravity and Spinfoam Theory*. Cambridge University Press, 2014.

[5] C. Rovelli, "Loop Quantum Gravity," LivingRev.Rel.1:1,1998 (1997) arXiv:gr-qc/9710008.

[6] C. Rovelli, "Notes for a brief history of quantum gravity," arXiv:gr-qc/0006061.

[7] R. Oeckl, "A positive formalism for quantum theory in the general boundary formulation," Found. Phys. 43 (2013) 1206-1232 (2012) arXiv:1212.5571.

[8] A. Ashtekar and J. Lewandowski, "Projective techniques and functional integration for gauge theories," J. Math. Phys. **36** (1995) 2170–2191, arXiv:gr-qc/9411046.

[9] C. Rovelli, *Quantum Gravity*. Cambridge University Press, 2004.

[10] P. Frisoni, "Introduction to Loop Quantum Gravity: Rovelli's lectures on LQG," arXiv:2305.12215.

[11] C. Rovelli and L. Smolin, "Discreteness of area and volume in quantum gravity," Nucl.Phys. B442 (1995) 593-622; Erratum-ibid. B456 (1995) 753 (1994) arXiv:gr-qc/9411005.

[12] R. De Pietri and C. Rovelli, "Geometry eigenvalues and scalar product from recoupling theory in loop quantum gravity," Phys. Rev. D **54** (1996) 2664–2690, arXiv:gr-qc/9602023.

[13] W. Wieland, "Fock representation of gravitational boundary modes and the discreteness of the area spectrum," Annales Henri Poincare **18** (2017), no. 11, 3695–3717, arXiv:1706.00479.

[14] A. Perez, "Introduction to Loop Quantum Gravity and Spin Foams," Lectures presented at the II International Conference of Fundamental Interactions, Pedra Azul, Brazil (2005) arXiv:gr-qc/0409061.

[15] J. Engle, E. Livine, R. Pereira, and C. Rovelli, "LQG vertex with finite Immirzi parameter," Nucl.Phys.B799:136-149,2008 (2007) arXiv:0711.0146.

[16] P. Dona and P. Frisoni, "How-To compute EPRL spin foam amplitudes," Universe 2022, 8(4), 208 (2022) arXiv:2202.04360.

[17] H. Haggard, *Asymptotic Analysis of Spin Networks with Applications to Quantum Gravity*. http://bohr.physics.berkeley.edu/hal/pubs/ Thesis/, 2011.

[18] T. Regge, "General Relativity without Coordinates," Nuovo Cim. 19 (1961) 558-571 (1961).

[19] T. Thieman, "Complexifier Coherent States for Quantum General Relativity," Class. Quantum Grav. 23 2063 (2002) arXiv:gr-qc/0206037.

[20] T. Thiemann, *Modern Canonical Quantum General Relativity*. Cambridge University Press, 2007.

[21] A. Calcinari, L. Freidel, E. Livine, and S. Speziale, "Twisted Geometries Coherent States for Loop Quantum Gravity," (2022) arXiv:2009.01125.

[22] P. Donà, "Geometry from local flatness in Lorentzian spin foam theories," Phys.Rev.D 107 (2023) 6, 066011 (2023) arXiv:2211.04743.

[23] E. R. Livine and J. Tambornino, "Spinor Representation for Loop Quantum Gravity," J. Math. Phys. 53, 012503 (2012) (2012) arXiv:1105.3385.

[24] H. Kleinert, *Path integrals in quantum mechanics, statistics, polymer physics, and financial markets (5th edition)-2009*. World Scientific Publishing Company, 2009.

[25] P. J. Szablowski, "Discrete Normal Distribution and Its Relationship with Jacobi Theta Functions," Statistics and Probability Letters, Vol. 52, No. 3, 2001, pp. 289-299. (2001).

[26] B. Dittrich and S. Speziale, "Area-angle variables for general relativity," NewJ.Phys.10:083006,2008 (2008) arXiv:0802.0864.

[27] P. Dona, H. M. Haggard, C. Rovelli, and F. Vidotto, "Tunneling of quantum geometries in spinfoams," Phys. Rev. D 109, 106016 (2024) arXiv:2402.09038.

[28] M. Christodoulou, F. D'Ambrosio, and C. Theofilis, "Geometry Transition in Spinfoams," 2, 2023. arXiv:2302.12622.

[29] E. R. Livine and J. Tambornino, "Asymptotics of lowest unitary SL(2,C) invariants on graphs," Phys. Rev. D 102, 086016 (2020) (2020) arXiv:2007.09089.

[30] A. Perez, C. Rovelli, and M. Christodoulou, "Detecting Gravitationally Interacting Dark Matter with Quantum Interference," arXiv:2309.08238.

[31] P. Doná and S. Speziale, "Introductory lectures to loop quantum gravity," (2010) arXiv:1007.0402.

[32] J. C. Baez, "4-Dimensional BF Theory as a Topological Quantum Field Theory," Lett.Math.Phys. 38 (1996) 129-143 (1996) arXiv:q-alg/9507006.